

In vivo analysis of the role of FADD
in the regulation of intestinal epithelial homeostasis

Inaugural-Dissertation

zur

Erlangung des Doktorgrades
der Mathematisch-Naturwissenschaftlichen Fakultät
der Universität zu Köln

vorgelegt von

Patrick-Simon Welz

aus Lübeck

Köln, 2012

Berichterstatte: Prof. Dr. Manolis Pasparakis
Prof. Dr. Jonathan C. Howard

Tag der mündlichen Prüfung: 04.04.2012

Diese Arbeit ist meiner Mutter Claudia Barbara Welz gewidmet.

Zusammenfassung

Die Einleitung von Zelltod kann ein wichtiger Bestandteil einer Immunreaktion gegen infizierte oder anderweitig beschädigte Zellen sein. FADD ist ein Adapterprotein, welches verschiedene der Immunreaktion zugehörige Signalwege mit der Einleitung von apoptotischem Zelltod verbindet. FADD abhängige Signalwege wurden hauptsächlich in Immunzellen studiert, während die *in vivo* Rolle von FADD in epithelialem Gewebe, welches sich an der Grenze zu einer großen Anzahl von Stressfaktoren von außerhalb des Organismus befindet, weitestgehend unbekannt ist. Das einzellschichtige intestinale Epithel bildet eine Barriere, die die Bakterien im Darmlumen von den Immunzellen in der Darmschleimhaut des Darmtraktes trennt. Die Integrität dieser Barriere ist von essentieller Bedeutung für die intestinale Homöostase, was die Regulierung des Zelltods von intestinalen Epithelzellen (IEZ) zu einer wichtigen Angelegenheit macht.

In dieser Doktorarbeit wurde die Rolle von FADD im intestinalen Epithel untersucht. Wir konnten zeigen, dass FADD essentiell für die intestinale Homöostase ist, indem RIP3 abhängige Nekrose in IEZ verhindert wird. Mäuse, denen FADD speziell in den IEZ fehlt (FADD^{IEZ-KO} Mäuse), entwickelten spontan eine schwere Kolitis sowie eine Dünndarmentzündung. Die Nekrose von IEZ im Dickdarm von FADD^{IEZ-KO} Mäusen wurde unterbunden durch die Deletion von RIP3 oder durch die Expression von mutiertem CYLD, welchem die Deubiquitinierungsaktivität fehlt. Wie im Dickdarm, so war auch die Nekrose von IEZ im Dünndarm abhängig von RIP3. Wie auch immer, die Deubiquitinierungsaktivität von CYLD war nicht notwendig für das Auftreten von Nekrose in den IEZ im Dünndarm, was impliziert, dass verschiedene Signalwege die Nekrose in den IEZ des Dickdarms und des Dünndarms vermitteln. Die Entwicklung der Kolitis war abhängig von der Expression von TNF und MyD88 vermittelten Signalen, die durch die Darmbakterien induziert wurden. Entgegengesetzt dazu war die Entwicklung der Entzündung im Dünndarm der FADD^{IEZ-KO} Mäuse unabhängig von TNF, den Darmbakterien und MyD88 abhängigen Signalen. Folglich sind verschiedene Mechanismen verantwortlich für die Entwicklung der Entzündung des Dickdarms und des Dünndarms von FADD^{IEZ-KO} Mäusen.

Die in dieser Doktorarbeit gezeigten Ergebnisse demonstrieren, dass FADD nicht nur ein potentieller Mediator von apoptotischem Zelltod im intestinalen Epithel ist, sondern dass es auch essentiell für das Überleben der IEZ unter homöostatischen Bedingungen ist, indem RIP3 abhängige Nekrose verhindert wird.

Abstract

The initiation of cell death can be an integral part of the immune response to infected or otherwise damaged cells. FADD is an adaptor protein connecting various immune response related signalling pathways to the induction of apoptotic cell death. FADD dependent signalling has mainly been studied in immune cells, while the *in vivo* role of FADD in epithelial tissues, which are at the border to various stress factors from outside the organism, is largely unknown. The intestinal epithelium is a single cell layer that forms a barrier, separating the luminal microbiota from the mucosal immune cells in the gastro-intestinal tract. The integrity of this barrier is essential for intestinal homeostasis, making the regulation of intestinal epithelial cell (IEC) death in response to infections or other stress-factors an important issue.

In this thesis, the role of FADD in the intestinal epithelium was studied. We found that FADD is essential for intestinal homeostasis by preventing excessive RIP3 dependent IEC necrosis. Mice lacking FADD specifically in the intestinal epithelium (FADD^{IEC-KO} mice) developed severe spontaneous colitis and enteritis. IEC necrosis in the colon of FADD^{IEC-KO} mice was abrogated by deletion of RIP3 or by the expression of a CYLD mutant lacking the deubiquitinase activity. Like in the colon, necrosis of FADD deficient IECs in the small intestinal epithelium was also depending on RIP3. However, the deubiquitinating activity of CYLD was not required for small intestinal IEC necrosis to occur, suggesting different pathways to mediate IEC necrosis in the colon and small intestine of FADD^{IEC-KO} mice. Development of colitis was partially depending on the expression of TNF and MyD88 mediated signalling induced by the microbiota. On the contrary, enteritis development in FADD^{IEC-KO} mice was independent of TNF, the commensal bacteria and MyD88 dependent signalling. Thus, different mechanisms are responsible for the development of inflammation in the colon and small intestine of FADD^{IEC-KO} mice.

The results presented in this thesis demonstrate that FADD is not only a potential mediator of apoptotic cell death in the intestinal epithelium, but it is also essential for IEC survival under homeostatic conditions by preventing RIP3 dependent IEC necrosis.

Contents

Abbreviations	6
1. Introduction	9
1.1. Regulated cell death	9
1.2. Immunity and cell death	9
1.2.1. FADD	10
1.2.2. Immunity and extrinsically induced apoptosis	12
1.2.2.1. TNF-induced extrinsic apoptosis	12
1.2.2.2. FASL-induced apoptosis	14
1.2.2.3. TRAIL-induced apoptosis	15
1.2.3. Cell autonomous immunity and apoptosis	16
1.2.4. Immunity and regulated necrosis	16
1.3. The gastrointestinal tract	20
1.3.1. The intestinal epithelium	21
1.3.2. Immunity, epithelial cell death and inflammation in the intestinal tract	23
1.4. Cre/LoxP conditional gene targeting	26
1.5. Project description	26
2. Material and Methods	28
2.1. Material	28
2.1.1. Chemicals	28
2.1.2. Material for mouse work	28
2.1.3. Material for histology	28
2.1.4. Material for biochemistry	29
2.1.5. Molecular biology reagents and equipment	29
2.1.6. Laboratory equipment	29
2.1.7. Cell culture	30
2.1.8. Software	30
2.1.9. Buffers and solutions	30
2.1.9.1. Washing buffers	30
2.1.9.2. Buffers and solutions for immunostainings	31
2.1.9.3. Preparation of protein extracts	31
2.1.9.4. Buffers and solutions for Western Blot analysis	31
2.1.9.5. Buffers and solution for DNA extraction, genotyping PCRs and Southern Blot	33
2.2. Methods	35
2.2.1. Animal handling and mouse experiments	35

2.2.1.1.	Mouse maintenance	35
2.2.1.2.	Generation of conditional and knock-out mice	35
2.2.1.3.	Endoscopy.....	35
2.2.1.4.	Antibiotic treatment, generation of germ-free mice and conventionalisation	36
2.2.1.5.	Sacrifice of mice	36
2.2.1.6.	Tissue preparation	37
2.2.2.	Histology	37
2.2.2.1.	Preparation of intestinal tissue for histological analysis.....	37
2.2.2.2.	Haematoxylin and Eosin staining of intestinal tissue sections	37
2.2.2.3.	Immunostainings.....	38
2.2.2.4.	Electron microscopy	39
2.2.3.	Biochemistry	39
2.2.3.1.	IEC isolation from colon and small intestine.....	39
2.2.3.2.	Preparation of IEC protein extracts	40
2.2.3.3.	Assessment of protein concentration by Bradford assay.....	40
2.2.3.4.	Western Blot analysis	40
2.2.4.	Molecular Biology.....	42
2.2.4.1.	Preparation of genomic DNA	42
2.2.4.2.	Southern Blot.....	42
2.2.4.3.	Genotyping PCRs.....	43
2.2.4.4.	Agarose gel electrophoresis	45
2.2.4.5.	Extraction of RNA	45
2.2.4.6.	cDNA synthesis	45
2.2.4.7.	Quantitative real time PCR	46
2.2.5.	Cell Biology	48
2.2.5.1.	Culture of mouse embryonic fibroblasts (MEFs).....	48
2.2.5.2.	Cell death assay with MEFs.....	48
2.2.6.	Statistics.....	48
3.	Results	49
3.1.	Deletion of FADD in IECs results in chronic spontaneous colitis and enteritis.....	49
3.1.1.	Generation of mice deficient for FADD only in the intestinal epithelium	49
3.1.2.	FADD ^{IEC-KO} mice develop spontaneous chronic colitis	49
3.1.3.	FADD ^{IEC-KO} mice develop spontaneous chronic enteritis and have reduced numbers of Paneth cells.....	54
3.2.	FADD deficient IECs are sensitised towards cell death with necrotic features	57
3.2.1.	FADD ^{IEC-KO} mice show increased colonic epithelial cell death.....	57
3.2.2.	FADD ^{IEC-KO} mice show increased epithelial cell death in the small intestine.....	58

3.3.	Development of colitis in FADD ^{IEC-KO} mice depends on RIP3-dependent regulated necrosis	59
3.3.1.	IEC death in the colon and development of colitis in FADD ^{IEC-KO} mice is RIP3 dependent	59
3.3.2.	Cell death and inflammation in the colon of FADD ^{IEC-KO} mice depends on CYLD	61
3.3.3.	Cell death and inflammation in the colon of FADD ^{IEC-KO} mice depends partially on TNF	63
3.4.	Role of the microbiota in the development of colitis in FADD ^{IEC-KO} mice	64
3.4.1.	The development of chronic colitis but not the increased cell death in FADD ^{IEC-KO} mice depends on MyD88.....	64
3.4.2.	The development of chronic colitis in FADD ^{IEC-KO} mice depends on microbiota induced signals	66
3.5.	Development of enteritis in FADD ^{IEC-KO} mice depends on RIP3-dependent regulated necrosis	69
3.5.1.	IEC death in the small intestine and development of enteritis in FADD ^{IEC-KO} mice is RIP3 dependent	69
3.5.2.	Cell death and inflammation in the small intestine of FADD ^{IEC-KO} mice is independent of CYLD	71
3.5.3.	Cell death and inflammation in the small intestine of FADD ^{IEC-KO} mice is not induced by TNF	73
3.6.	Role of the microbiota in the development of enteritis in FADD ^{IEC-KO} mice	75
3.6.1.	Enteritis and IEC death in FADD ^{IEC-KO} mice does not depend on MyD88.....	75
3.6.2.	Enteritis and IEC death does not depend on the presence of the microbiota.....	77
3.6.3.	Differential regulation of cell death and inflammation in the colon and small intestine of FADD ^{IEC-KO} mice	79
4.	Discussion	81
4.1.	FADD protects IECs from RIP3 dependent necrosis	81
4.2.	Regulation of RIP3 dependent IEC necrosis by FADD and CYLD	82
4.3.	Possible inducers of RIP3 dependent regulated necrosis in IECs and their physiological impact.....	83
4.3.1.	Extrinsically induced necroptosis in IECs	84
4.3.2.	Cell autonomous immunity as a possible trigger for RIP3 dependent IEC necrosis	86
4.3.3.	Paneth cell death and endoplasmic reticulum (ER) stress	87
4.3.4.	Other possible inducers of RIP3 dependent regulated necrosis	88
4.4.	RIP3 dependent IEC necrosis and inflammation	89
4.4.1.	Development of colitis in FADD ^{IEC-KO} mice.....	89
4.4.2.	Development of enteritis in FADD ^{IEC-KO} mice	91
5.	Concluding Remarks	93
	Bibliography	94
	Acknowledgements	107

Teilpublikation	108
Erklärung	125
Curriculum Vitae	126

Abbreviations

Ang4	- Angiogenin, ribonuclease A family, member 4 (Protein)
Atg5	- autophagy-related 5
Atg12	- autophagy-related 12
BCL-2	- B-cell lymphoma 2
c-FLIP	- cellular FLICE-like inhibitory protein
CMV	- Cytomegalovirus
CYLD	- Cylindromatosis (Protein)
DAMP	- danger-associated molecular pattern
DD	- Death Domain
Defa20	- Defensin, alpha, 20 (Protein)
Defa-rs1	- Defensin, alpha, related sequence 1 (Protein)
DISC	- Death-Inducing Signalling Complex
DR	- Death Receptor
DRL	- Death Receptor Ligand
DSS	- dextran sodium sulphate
e.g.	- for example
ER	- endoplasmic reticulum
<i>Fadd</i>	- Fas (TNFRSF6)-associated via death domain (Gene)
FADD	- Fas (TNFRSF6)-associated via death domain (Protein)
<i>Fas</i>	- TNF receptor superfamily member 6 (Gene)
FAS	- TNF receptor superfamily member 6 (Protein)
<i>Fasl</i>	- TNF superfamily, member 6 (Gene)
FASL	- TNF superfamily, member 6 (Protein)
H&E	- Haematoxylin and Eosin
HCS	- Histological Colitis Score
HMGB1	- high-mobility group protein B1
HOIL-1L	- heme-oxidized IRP2 ubiquitin ligase 1 homolog
HOIP	- HOIL-1-interacting protein
HRP	- horseradish peroxidase
HS	- Histological Small Intestinal Score
IBD	- inflammatory bowel disease
IECs	- intestinal epithelial cells

IHC	- immunohistochemical
IKK	- Inhibitor of kappaB kinase
IRAK1	- interleukin-1 receptor-associated kinase 1
IRE1	- Inositol-requiring enzyme-1
IRF3	- interferon regulatory factor 3
JNK	- c-Jun N-terminal kinase
LT α	- Lymphotoxin α
LUBAC	- linear ubiquitin chain assembly complex
Lyz1	- Lysozyme 1 (Protein)
MAPK	- mitogen-activated protein kinases
MBD4	- methyl-CpG binding domain protein 4
MEFs	- mouse embryonic Fibroblasts
MEICS	- murine endoscopic index of colitis severity
MOMP	- mitochondrial outer membrane permeabilization
<i>Myd88</i>	- Myeloid differentiation primary response gene 88 (Gene)
MyD88	- Myeloid differentiation primary response gene 88 (Protein)
NCCD	- Nomenclature Committee on Cell Death
NEMO	- NF-kappa-B essential modulator
neo	- neomycin
NF- κ B	- nuclear factor kappa B
PAMP	- pathogen-associated molecular pattern
PCD	- programmed cell death
PRR	- pattern recognition receptor
qRT-PCR	- quantitative real time PCR
RCD	- regulated cell death
RHIM	- Receptor-Interacting Protein Homotypic Interaction Motif
RIP1	- Receptor (TNFRSF)-interacting serine-threonine kinase 1 (Protein)
RIP3	- Receptor (TNFRSF)-interacting serine-threonine kinase 3 (Protein)
<i>Ripk3</i>	- Receptor (TNFRSF)-interacting serine-threonine kinase 3 (Gene)
ROS	- reactive oxygen species
SHARPIN	- SHANK-associated RH domain interacting protein
TAB1	- TAK1-binding protein 1
TAB2	- TAK1-binding protein 2
TAK1	- TGF-beta-activated kinase 1
<i>Tnf</i>	- Tumour necrosis factor (Gene)

TNF	- Tumour necrosis factor (Protein)
<i>Tnfr1</i>	- tumour necrosis factor receptor superfamily, member 1a (Gene)
TNFR1	- tumour necrosis factor receptor superfamily, member 1a (Protein)
TLR	- Toll-like receptor
TLR3	- Toll-like receptor 3
TLR4	- Toll-like receptor 4
TRADD	- TNFRSF1A-associated via death domain
TRAF2	- TNF receptor-associated factor 2
TRAF5	- TNF receptor-associated factor 5
TRAIL	- tumour necrosis factor (ligand) superfamily, member 10
TRAIL1	- tumour necrosis factor receptor superfamily, member 10a
TRAIL2	- tumour necrosis factor receptor superfamily, member 10b
TRIF	- TIR domain-containing adaptor inducing interferon-beta
UPR	- unfolded protein response
XBP1	- X-box-binding protein 1
XIAP	- X-linked inhibitor of apoptosis

1.Introduction

1.1. Regulated cell death

Regulated cell death (RCD) in multicellular organisms occurs on the one hand during development and in the maintenance of tissue homeostasis and on the other hand as a mechanism for the removal of stressed, damaged or infected cells as well as in the termination of immune responses by inducing death of activated immune cells. While RCD involved in developmental processes or in the regulation of turnover procedures and tissue homeostasis, also commonly described as programmed cell death (PCD), evolved in multicellular organisms, early stress induced RCD-like mechanisms evolved already in unicellular organisms like bacteria (Ameisen, 2004).

Three main forms of cell death have been described and categorized, mainly according to morphological criterias: cell death type I or apoptotic cell death, cell death type II or autophagic cell death and cell death type III or necrotic cell death, which was for a long time being regarded as a solely non-regulated accidental form of cell death. Recently, the Nomenclature Committee on cell death (NCCD) proposed to use new definitions based on molecular features of the different RCD pathways (Galluzzi et al., 2011), which will be referred to in this work. According to the NCCD, regulated cell death is defined as a process initiated and executed by a “dedicated molecular machinery and can therefore be inhibited by pharmacological and/or genetic interventions”.

1.2. Immunity and cell death

In response to an infection the immune system reacts by activating pathways that promote cell survival as well as pathways that promote cell death. The primary response is focussed on the defence against the infection by activation of proinflammatory pathways, the recruitment of immune cells and production of antimicrobial factors. If the infection cannot be cleared, cell death can be induced to remove the infected cells (Lamkanfi and Dixit, 2010). Such cell death can be triggered extrinsically by certain cytokines, the death receptor ligands (DRLs), or as a cell autonomous response induced by pattern recognition receptors (PRRs). Fas (TNFRSF6)-associated via death domain (FADD) is a signal transducer involved in both, extrinsically induced cell death and PRR triggered cell death. Therefore, FADD

is an important mediator of cell death triggered by the immune response (Locksley et al., 2001; Wilson et al., 2009).

1.2.1. FADD

FADD was discovered in 1995 by two groups (Boldin et al., 1995; Chinnaiyan et al., 1995). The FADD protein contains two known domains: a Death Domain (DD), and a Death Effector Domain (DED). The DD of FADD is necessary for binding to other DD containing proteins, like the death receptors, receptor (TNFRSF)-interacting serine-threonine kinase 1 (RIP1) or TNFRSF1A-associated via death domain (TRADD). The DED is also involved in protein-protein interactions, for example in the recruitment of procaspase 8 or in humans additionally procaspase 10 (Boldin et al., 1995; Chaudhary et al., 1997; Chinnaiyan et al., 1995; Hsu et al., 1996; Muzio et al., 1996; Schneider et al., 1997). By recruiting procaspase 8, FADD serves as a signalling transducer which can connect various upstream signalling pathways to the induction of cell death. Subsequent cleavage of the catalytically inactive procaspase 8 leads to the active isoform of the cysteine aspartate specific protease Caspase 8, which can induce apoptosis by activating downstream molecules involved in the execution of cell death. Cell death pathways depending on FADD as well as those being regulated by FADD are described in the following chapters.

Beside of its role as a signal transducer towards cell death as part of the immune response, FADD has also been associated with other signalling pathways. FADD deficient T cells die upon mitogenic activation, which led to the speculation that FADD has a role in T cell proliferation and cell cycle progression (Newton et al., 1998; Zhang et al., 2001). In addition, mitogen activated FADD deficient T cells have a hyperautophagic appearance and FADD has been found to interact with an autophagy-related 5 - autophagy-related 12 (Atg5-Atg12) complex (Bell et al., 2008), implicating FADD in the autophagic machinery. FADD has also been suggested to interact with Atg5 in interferon- γ stimulated HeLa cells (Pyo et al., 2005), further promoting a potential role of FADD in autophagy.

An involvement of FADD in IL-1 β induced signalling by binding to interleukin-1 receptor-associated kinase 1 (IRAK1) and myeloid differentiation primary response gene 88 (MyD88) has been reported. This interaction was proposed to lead to the

inhibition of further downstream signalling to NF- κ B and expression of inflammatory cytokines (Bannerman et al., 2002; Zhande et al., 2007).

FADD is not only located in the cytoplasm, but also in the nucleus (Gomez-Angelats and Cidlowski, 2003). One potential nuclear role of FADD is the interaction with the DNA mismatch repair machinery. FADD has been shown to interact with DNA mismatch repair enzyme methyl-CpG binding domain protein 4 (MBD4) (Screaton et al., 2003). The function of this interaction between FADD and MBD4 has not been resolved yet, but DNA damage induced MBD4 dependent signalling can lead to apoptosis, potentially involving FADD.

Additionally, FADD has been found in microvesicles after adenosine receptor controlled secretion (Tourneur et al., 2008). However, the potential function of this process has not been identified yet.

FADD deficiency in mice leads to embryonic lethality at embryonic day 11.5, suggesting FADD dependent signalling to be important for development (Yeh et al., 1998; Zhang et al., 1998). FADD deficient mice exhibit cardiac failure and abdominal haemorrhage, implicating a role for FADD in those tissues. However, cell type specific roles of FADD have not been studied into great detail yet.

Although loss of FADD expression has been linked to tumourigenesis in certain cases (Tourneur et al., 2004; Tourneur et al., 2003), surprisingly little is known about the potential involvement of FADD in human diseases. Mutations resulting in decreased FADD protein levels were found to be linked to the autoimmune lymphoproliferative syndrome (ALPS), hepatopathy, encephalopathy, and cardiac malformations (Bolze et al., 2010). FADD mutations have only rarely been found in colon or stomach cancers (Soung et al., 2004). Overexpression of FADD has been reported to be involved in certain cancers (Gibcus et al., 2007), and the phosphorylation status of FADD has been linked to prostate cancer (Matsumura et al., 2009; Shimada et al., 2005). However, up to now, despite its important role in cellular signalling, direct linkages between FADD and human diseases seem to be rare.

1.2.2. Immunity and extrinsically induced apoptosis

Apoptotic cell death can be induced extrinsically during an immune response by the DRLs, which are cytokines of the tumour necrosis factor (TNF) ligand superfamily. DRLs can be expressed by different types of immune- and non-immune cells and are either secreted or presented at the surface of these cells. The DRLs act through their cognate receptor of the TNF receptor (TNFR) superfamily. These receptors, the death receptors (DRs), all contain a DD in their cytoplasmic part. DRLs binding to the extracellular domain of DRs induce formation of a receptor-bound complex via the intracellular DD, by recruiting certain DD containing signal transducers. Apoptosis triggered by DRLs and their cognate DR is defined as “extrinsic apoptosis” (Galluzzi et al., 2011). Beside of being able to induce death, DRs can trigger as diverse functions as the expression of proinflammatory cytokines or prosurvival factors as well as proliferative signals (Wilson et al., 2009).

DRL/DR signalling modules known to be able to induce extrinsic apoptosis are tumour necrosis factor (TNF) and Lymphotoxin α (LT α) binding to Tnfrsf1a (tumour necrosis factor receptor superfamily, member 1a) (TNFR1), FAS Ligand (TNF superfamily, member 6) (FASL) binding to FAS (TNF receptor superfamily member 6) as well as TNFSF10 (tumour necrosis factor (ligand) superfamily, member 10) (TRAIL) binding to TNFRSF10A (tumour necrosis factor receptor superfamily, member 10a) (TRAILR1) or TNFRSF10B (tumour necrosis factor receptor superfamily, member 10b) (TRAILR2) (Schutze et al., 2008). The DRL/DR signalling pathways are highly conserved between humans and mice, beside of the mouse TRAILR, which is a single ortholog of the human TRAILR1 and TRAILR2.

1.2.2.1. TNF-induced extrinsic apoptosis

Upon activation by TNF or LT α , trimeric TNFR1 recruits the signalling adaptor TRADD via its DD. TRADD serves as a signalling scaffold for the assembly of the receptor bound complex I (Ermolaeva et al., 2008), which further contains RIP1, TNF receptor-associated factor 2 (TRAF2) or TNF receptor-associated factor 5 (TRAF5) (Tada et al., 2001) and the ubiquitin ligases cIAP1 and cIAP2 (Shu et al., 1996). The receptor bound complex can activate signalling to nuclear factor kappa B (NF- κ B) through the I κ B kinase (IKK) complex, to p38 mitogen-activated protein kinases (MAPK) and to c-Jun N-terminal kinase (JNK). Different forms of ubiquitination on several proteins within this receptor-bound complex I are important for the

transduction of the signal (Walczak, 2011). Recently it has been shown, that cIAP dependent recruitment of the linear ubiquitin chain assembly complex (LUBAC), consisting of SHANK-associated RH domain interacting protein (SHARPIN) and heme-oxidized IRP2 ubiquitin ligase 1 homolog (HOIL-1) as well as HOIL-1-interacting protein (HOIP), is essential for TNF mediated activation of NF- κ B and JNK. LUBAC catalyses linear ubiquitin onto RIP1 and NF-kappa-B essential modulator (NEMO), an essential component of the IKK complex, which ultimately mediates NF- κ B activation. Linear ubiquitination of these proteins stabilises the receptor bound complex and promotes NF- κ B- and JNK activation. (Gerlach et al., 2011; Haas et al., 2009; Ikeda et al., 2011; Tokunaga et al., 2011; Tokunaga et al., 2009).

Activation of TNFR1 signalling can also lead to the formation of two secondary cytoplasmic complexes after TNFR1 internalisation, complex IIa and IIb (Micheau and Tschopp, 2003). Contrary to the outcome of complex I signalling, which is mainly cell survival, the formation of these cytosolic complexes can lead to cell death. Dissociation of TRAF2 and RIP1 from TRADD allows binding of FADD to TRADD and subsequent recruitment of Caspase 8 through FADD to this cytosolic complex IIa. Alternatively, RIP1 can bind FADD and thereby recruit Caspase 8 to cytosolic complex IIb. Another component of complex II is Receptor (TNFRSF)-interacting serine-threonine kinase 3 (RIP3), although it is not clear whether RIP3 is constantly associated, directly or indirectly, to the FADD containing complex (Cho et al., 2009; O'Donnell et al., 2011) or whether this association is transient (Oberst et al., 2011). The apoptotic cell death effector of complex II is Caspase-8. Formation of homotypic procaspase-8 dimers, by recruitment of two single procaspase-8 molecules to FADD, induces the activation of Caspase 8 by reciprocal cleavage of the procaspase 8 isoform. Once Caspase 8 is activated, signalling to apoptosis is mediated through the activation of a caspase cascade (Medema et al., 1997). The caspase cascade is activated through Caspase 8 by cleavage mediated activation of the executioner caspases 3, 6 and 7 either directly (Type I cells) or via a mitochondrial amplification loop (Type II cells) (Barnhart et al., 2003; Wilson et al., 2009). Executioner caspases mediate cell death by cleaving cytoskeletal and nuclear proteins critical for maintenance of cell structure, as well as enzymes involved in metabolism and repair (Alenzi et al., 2010).

TNFR1 dependent signalling to apoptosis can be regulated on different levels. On one hand, signalling towards apoptosis can be inhibited by different targets of the

transcription factor NF- κ B. For example, different isoforms of cellular FLICE-like inhibitory protein (c-FLIP), which is a Caspase 8 homologue lacking the caspase activity, compete with procaspase 8 for binding to FADD. Heterodimers of c-FLIP and procaspase 8 cannot induce procaspase 8 cleavage and therefore inhibit complex II induced apoptosis (Irmeler et al., 1997). Expression levels of c-FLIP can be increased by survival signals like NF- κ B and degradation of c-FLIP can be induced by stress pathways through JNK signalling (Wilson et al., 2009). Other targets of NF- κ B are the cIAPs, which negatively regulate complex II formation by ubiquitin mediated stabilisation of complex I (Micheau and Tschopp, 2003; Wang et al., 2008). On the other hand, signalling to cell death can also be promoted, for example by the deubiquitination of RIP1 by Cylindromatosis (CYLD). Deubiquitination of RIP1 is an important event for the formation of the pro-death complex II to occur (Wang et al., 2008; Wertz et al., 2004; Wright et al., 2007). Therefore, the cell fate, survival or death, in response to TNFR1 signalling depends on a very tight regulation of signalling to complex I and complex II.

1.2.2.2. FASL-induced apoptosis

In contrast to TNFR1, binding of FASL to FAS leads to the recruitment of FADD instead of TRADD via the DD to the receptor (Schutze et al., 2008). Thus, FADD is part of the receptor-bound complex, which is essential for FAS-dependent signalling to cell death. In the absence of FADD signalling to cell death, triggered by FASL/FAS, is completely blocked *in vitro* (Holler et al., 2000; Zhang et al., 1998). After binding of FASL to FAS, higher order complexes of the receptor are formed (Henkler et al., 2005), which promote the recruitment of FADD, procaspase-8, different c-FLIP isoforms, RIP1 and the cIAPs (Boldin et al., 1996; Budd et al., 2006; Deveraux et al., 1998; Galluzzi et al., 2011; Holler et al., 2000; Irmeler et al., 1997). Internalisation of the receptor bound complex to the endosomal compartment is followed by the full activation of the signalling complex, leading to the induction of apoptosis (Algeciras-Schimmich et al., 2002; Lee et al., 2006). Also a secondary cytosolic complex II has been reported that might further enhance apoptosis (Lavrik et al., 2008). FAS dependent signalling has also been implicated in cell proliferation and tumourigenesis presumably through signalling to JNK and Jun (Chen et al., 2010; Strasser et al., 2009).

1.2.2.3. TRAIL-induced apoptosis

Like FAS mediated signalling, TRAIL induced signalling through TRAILR1 and TRAILR2 in humans, or TRAILR in mice, also leads to the recruitment of FADD to the receptor via the DD. Subsequently, FADD recruits procaspase-8 and c-FLIP to form the receptor bound complex (Kuang et al., 2000; Wiley et al., 1995). Other than in FAS dependent apoptosis, internalisation of the TRAILR complex is not necessary for the induction of apoptosis in type I cells (Guicciardi and Gores, 2009). TRAIL induced signalling can also lead to the activation of NF- κ B, p38 MAPK and JNK via a secondary cytosolic signalling complex containing RIP1, TRADD, TRAF2, FADD, Caspase 8 and NEMO (Varfolomeev et al., 2005).

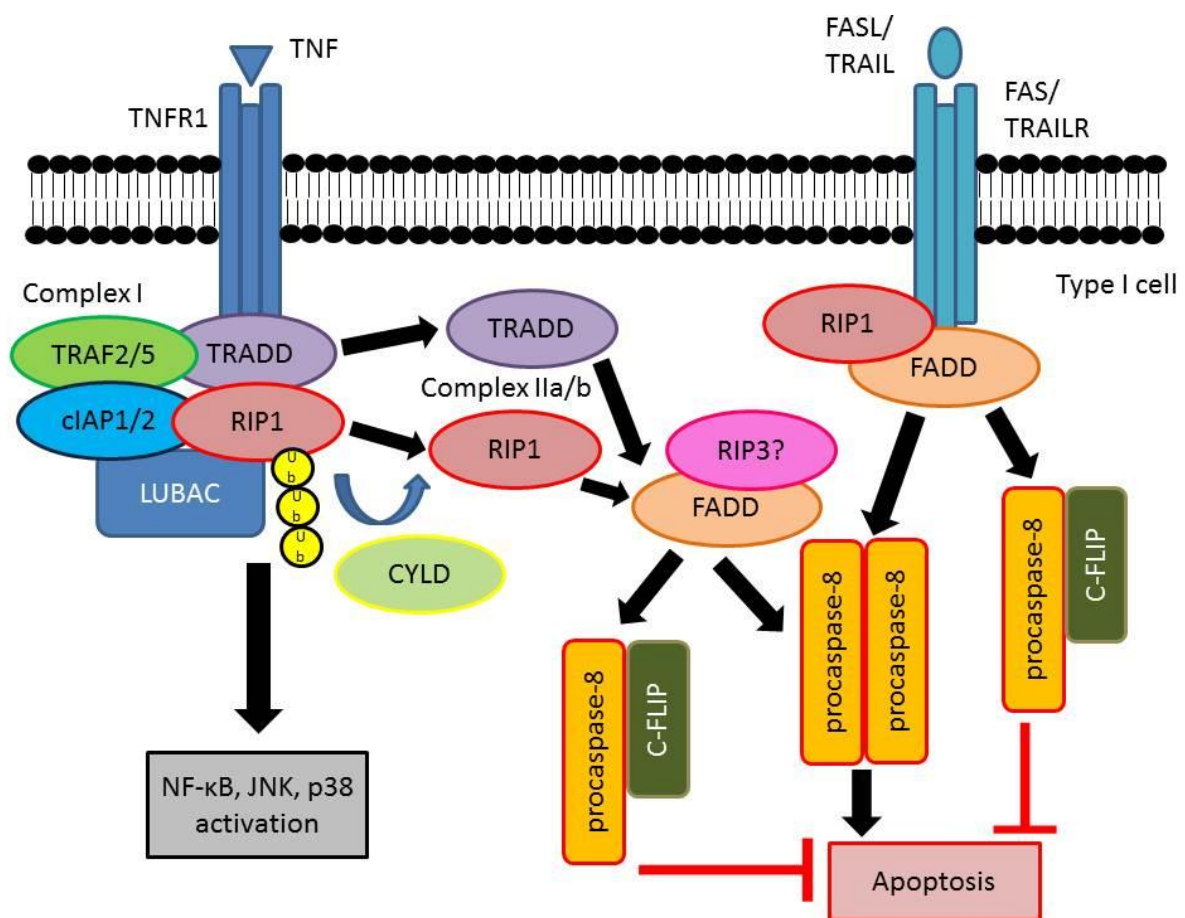


Figure 1: Death receptor induced apoptosis

Upon binding to their cognate receptor the DR-ligands TNF, FASL and TRAIL are able to induce several intracellular signalling pathways. TNF induced signalling leads to the assembly of a receptor-bound complex I, which can either lead to the activation of prosurvival and proinflammatory signalling through NF- κ B, JNK and p38 or to pro-death signalling. Cell death signalling is induced by the assembly of an either TRADD or deubiquitinated RIP1 dependent secondary cytoplasmic complex II. In this complex II FADD serves as a central adaptor-protein, leading to the recruitment of procaspase-8 homodimers or procaspase-8/c-FLIP heterodimers. In case of FASL and TRAIL induced signalling FADD is directly recruited to the receptor, leading to the assembly of the death inducing complex at the receptor. In procaspase-8 homodimers reciprocal cleavage leads to the formation of the enzymatically active Caspase 8 that is able to induce apoptosis. Ub=ubiquitin

1.2.3. Cell autonomous immunity and apoptosis

Extrinsically triggered cell death is not the only way how an immune response can induce death of potentially harmful cells. Also cell autonomous immune mechanisms can lead to apoptosis of the affected cell. Recognition of pathogen-associated molecular pattern (PAMPs) by pattern recognition receptors (PRRs) can induce signalling that can terminate in the death of the cell.

In response to viral infection, cells can induce their own death. The PRR Toll-like receptor 3 (TLR3), located at the endosomal membrane, senses virus derived double-stranded RNA or its synthetic homolog poly(I:C) (Kenny and O'Neill, 2008). TLR3 signalling can induce the expression of cytokines through the activation of NF- κ B, MAPK or interferon regulatory factor 3 (IRF3) signalling (Takeuchi and Akira, 2010). TLR3 can also trigger apoptosis through the adaptor protein TIR domain-containing adaptor inducing interferon-beta (TRIF) which recruits RIP1, Receptor (TNFRSF)-interacting serine-threonine kinase 3 (RIP3), FADD, Caspase 8 and c-FLIP (Kaiser and Offermann, 2005).

In addition to viral infections, infections with bacterial pathogens can also induce PRR dependent cell death. Toll-like receptor 4 (TLR4), a PRR located at the cytoplasmic membrane sensing lipopolysaccharides from the cell walls of gram-negative bacteria as well as some antigens from gram positive bacteria (Park et al., 2004), is also able to induce TRIF dependent apoptosis through the FADD, Caspase 8 signalling axis after internalisation to the endosome (De Trez et al., 2005; Ma et al., 2005; Ruckdeschel et al., 2004). TLR4 signalling through the adaptor protein MyD88 can additionally induce the expression of cytokines by activating NF- κ B and MAPK signalling and exhibit cytoprotective effects (Takeuchi and Akira, 2010).

Thus, in TLR3 and TLR4 induced signalling TRIF functions as a signalling platform combining sensing of pathogens to FADD dependent apoptosis.

1.2.4. Immunity and regulated necrosis

As described above, cytokine induced apoptosis can be an important part of the immune response. Apoptosis leads to plasma membrane blebbing, to cell body shrinkage (pyknosis), to nuclear condensation and fragmentation (karyorrhexis) as well as formation of membrane-bound cell fragments (apoptotic bodies). Apoptotic bodies get rapidly phagocytosed. Since the cytoplasmic content is retained in

vesicles, release of intracellular danger-associated molecular pattern (DAMP) is prevented. Thus, cells dying by apoptosis do normally not induce inflammation. Necrosis, on the other hand, has long been considered an accidental, unregulated form of cell death. Necrotic cell death appears less organized and ordered and differs in many regards from apoptotic cell death. In contrary to apoptotic death, necrosis leads to cell swelling, a rather disorganized hydrolysis of chromatin and rupture of the cell membrane. Due to the loss of membrane integrity during necrosis, intracellular DAMPs like DNA-binding protein high mobility group box 1 (HMGB1) or uric acid are released, leading to proinflammatory responses and subsequently to increased tissue damage (Lamkanfi and Dixit, 2010).

Recent findings challenged the notion that necrosis is a merely accidental and unregulated form of cell death. First reports about TNF being able to induce necrotic cell death date back to the late 1980s and early 1990s (Fady et al., 1995; Laster et al., 1988). Later on, caspase inhibitors like CrmA or z-VAD were shown to promote necrotic cell death in L929 cells (Vercammen et al., 1998), suggesting that necrosis is negatively regulated by caspases. Beside of TNF, also FAS and TRAIL were found to be able to induce regulated necrosis in primary T-cells lacking Caspase 8 or FADD and this form of necrosis was found to depend on RIP1 (Holler et al., 2000). DR signalling induced regulated necrosis was termed necroptosis, after the RIP1 kinase inhibitor Necrostatin-1 was discovered to block this pathway (Degterev et al., 2008; Degterev et al., 2005). Necroptosis induced by FAS or TRAIL, but not TNF, also depends on FADD (Holler et al., 2000; Zhang et al., 1998). Therefore, the inability to activate caspases in FADD deficient cells only sensitized towards TNF mediated necroptosis, while FAS or TRAIL induced necroptosis is blocked in those cells *in vitro*. RIP1 was the only signalling transducer known to participate in the induction of necroptosis until Cyldromatosis (CYLD) was found to be involved in necroptosis *in vitro* (Hitomi et al., 2008). The deubiquitinase CYLD has been proposed to deubiquitinate RIP1 and thereby to promote formation of the secondary cytosolic death promoting complex in TNF induced signalling (Wang et al., 2008; Wright et al., 2007). However, the detailed mechanism how CYLD is regulating necroptosis is not known. One year after the discovery of CYLD as a regulator of necroptosis, three groups identified RIP3 as the essential switch for TNF induced necroptosis. RIP3 deficiency completely blocks necroptosis. RIP3 was found to be part of complex II together with RIP1, FADD, Caspase 8 and c-FLIP (Cho et al., 2009; He et al., 2009;

Zhang et al., 2009). Under normal conditions, RIP3 dependent necrosis seems to be inhibited by a mechanism including c-FLIP_L and Caspase 8 (Oberst et al., 2011). Not much is known about the signalling events downstream of the RIP1, RIP3, FADD, Caspase 8, c-FLIP complex towards necroptosis, but it has been suggested that RIP3 activation regulates key metabolic enzymes leading to increased production of reactive oxygen species (ROS) (Zhang et al., 2009). To summarise, DRLs can induce necroptosis either through complex II in TNFR1 signalling, or by the receptor-bound death inducing complexes in FAS- and TRAIL signalling, when the activation of Caspase 8 is blocked. Blockade of Caspase 8 releases the inhibition of RIP3 dependent signals, which lead to necrotic cell death, most likely by metabolic changes that favour the production of ROS.

In addition to DRL induced necroptosis, also signalling induced by stimulation of TLR3 and TLR4 has been shown to be able to induce regulated necrosis (Feoktistova et al., 2011; He et al., 2011; Zhang et al., 2009). Induction of regulated necrosis by TLR3 or TLR4 depends on TRIF, which can interact with RIP1 and RIP3 via the Receptor-Interacting Protein Homotypic Interaction Motif (RHIM) domain. Like in DRL induced necroptosis, Caspase 8 activity inhibits TLR3 and TLR4 induced regulated necrosis (Ma et al., 2005). Thus, Caspase 8 activation has to be blocked for TLR induced regulated necrosis to occur. Both, DRL induced necroptosis as well as TLR induced regulated necrosis depend on RIP3 as the central switch towards the induction of necrotic cell death.

No direct marker for the detection of RIP3 dependent regulated necrosis exists up to now, making it difficult, if not impossible, to unambiguously detect regulated necrosis *in vivo* other than by genetic manipulation. Thus, not much is known about the physiological roles of necroptosis in humans. However, several different human and mouse cell types and cell lines, like epithelial colon cancer cells, Fibrosarcoma cells, T lymphocytes, macrophages, or mouse embryonic fibroblasts (MEFs) have been described to be able to undergo necroptosis or TLR induced regulated necrosis once caspase activation is blocked (Degterev et al., 2005; He et al., 2011; He et al., 2009; Holler et al., 2000; Zhang et al., 2009), indicating that RIP3 dependent regulated necrosis can occur in a variety of different cell types in mice as well as in humans. In mice, a physiological role for regulated necrosis has been reported in photoreceptor detachment (Trichonas et al., 2010) and several ischemic models, like ischemic brain injury (Degterev et al., 2005). Additionally, infection with Vaccinia Virus induces TNF

mediated necroptosis, confirming a role for necroptotic cell death in the clearance of virally infected cells (Cho et al., 2009). However, RIP3 deficient mice do not show any developmental phenotype (Newton et al., 2004), therefore RIP3 dependent necrotic death does not seem to play a role during mouse development.

Both, extrinsically induced necroptosis through DRLs as well as cell autonomously induced regulated necrosis through TLR3 and TLR4 have an important function in the removal of infected cells. Nowadays it becomes clear, that even more pathways involved in the immune response to viral infections are able to induce RIP3 dependent necrosis. Cells infected with Cytomegalovirus (CMV) have been shown to die by RIP3 dependent necrosis (Upton et al., 2008, 2010). CMV possesses the inhibitor M45/vIRA, which blocks RHIM domain dependent signalling. Proteins like RIP1, TRIF and RIP3 contain RHIM domains and interaction between RHIM domains is essential for the induction of regulated necrosis by CMV (Upton et al., 2010). Therefore, CMV can block RIP3 dependent regulated necrosis by the M45 inhibitor, while infection with CMV containing a mutated RHIM inhibitor M45 leads to RIP3 dependent regulated necrosis of the infected cell. This RIP3 dependent form of necrosis proceeds independent of RIP1, TRIF and TNF and is therefore different from RIP1 dependent DR induced necroptosis and TRIF dependent TLR3 and TLR4 induced regulated necrosis (Upton et al., 2010). However, up to now it is neither known how this RIP3 dependent necrosis is induced nor how it is molecularly regulated.

Up to now, RIP3 dependent necrosis seems to be an alternative pathway to overcome inhibition of Caspase 8 dependent cell death in various conditions. Whether RIP1 or RIP3 dependent necrosis also occurs independent of Caspase 8 inhibition remains to be shown.

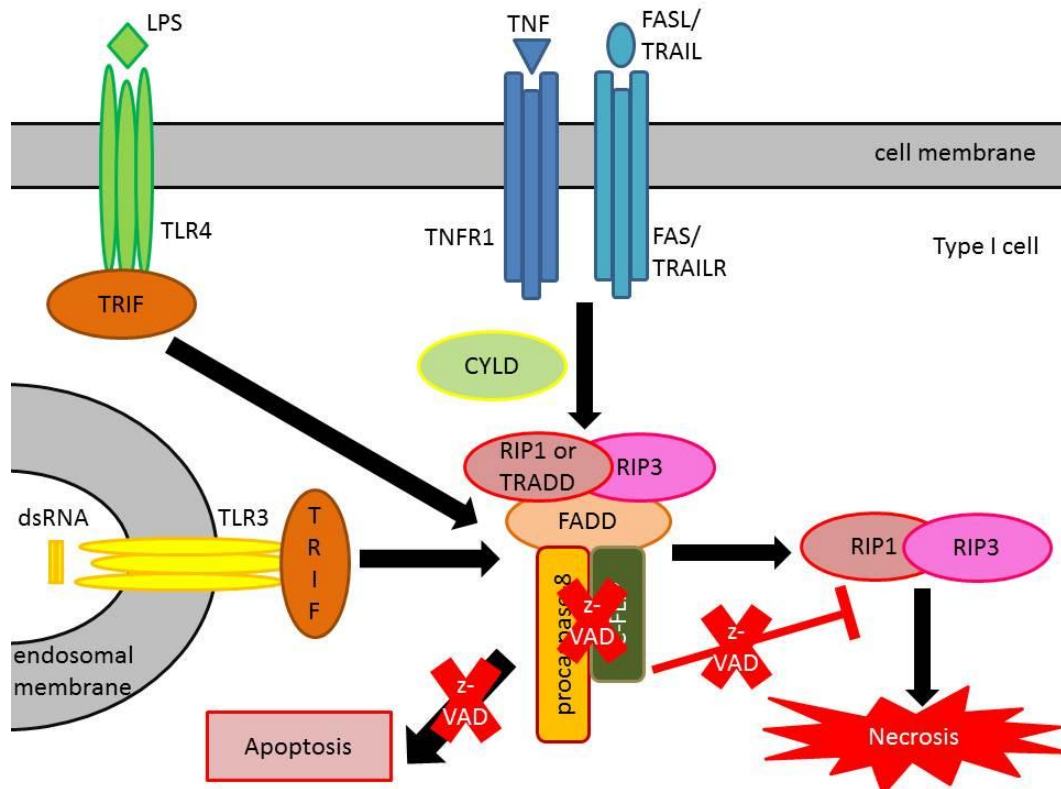


Figure 2: Signaling pathways leading to RIP3 dependent regulated necrosis

TNFR, FAS and TRAILR1/2 as well as TLR3- and most likely also TLR4 induced signalling can lead to RIP1 and RIP3 dependent regulated necrosis. Normally regulated necrosis is blocked by a not fully understood mechanism involving procaspase-8 and c-FLIP. Thus, regulated necrosis takes place, when activation of Caspase 8 is blocked, for example by the pancaspase inhibitor z-VADfmk.

1.3. The gastrointestinal tract

The gastrointestinal tract consists of the small intestine and the large intestine or colon. The small intestine can further be subdivided in the duodenum, the jejunum, and the ileum, and is followed by the caecum. The colon is subdivided into the ascending colon, the descending colon and the rectum. The main function of the gastrointestinal tract is the digestion of food and absorption of nutrients and water, the latter mainly taking place in the colon.

The outer part of the intestine contains two muscle layers, an outer longitudinal and an inner circular muscle, the combined action of both being responsible for the intestinal peristalsis leading to the directional transport of the luminal contents. Inside of the two muscle layers lies the submucosa, which contains blood and lymphatic vessels as well as nerves, which are embedded in an irregular connective tissue. The submucosa is followed by the mucosa. The mucosa consists of three different parts: the muscularis mucosa is a thin smooth muscle layer separating the mucosa from the

submucosa, the lamina propria which contains the immune cells of the gastrointestinal tract in a loose connective tissue, and the intestinal epithelium.

1.3.1. The intestinal epithelium

The intestinal epithelium is a single cell layer lining the intestinal lumen, thereby forming a barrier separating luminal contents of the intestine, which contain the commensal bacteria, from the lamina propria, which is home to the mucosal immune cells. Impairments in this barrier may result in an inappropriate contact of bacterial antigens and mucosal immune cells, which could lead to the activation of immune cells and a subsequent inflammatory response in mice (Catalioto et al., 2011). Also patients suffering from inflammatory bowel disease (IBD), like Ulcerative Colitis (UC) or Crohn's Disease (CD) exhibit impairments in the intestinal epithelial barrier function (Roda et al., 2010). But the intestinal epithelium is not only a passive physical barrier, it also has important active roles in the maintenance of intestinal homeostasis. The intestinal epithelium is thought to actively establish an immunosuppressive environment in the mucosa to prevent the intestinal immune cells from overreacting to commensal bacterial antigens. Additionally, the intestinal epithelium actively shapes the environment at the epithelial luminal boarder by establishing layers of mucus and by the secretion of antimicrobial peptides (Wells et al., 2011).

The architecture of the epithelium and the presence of specialised intestinal epithelial cells (IECs) differ between the colon and the small intestine. While the mucosa of the small intestine protrudes into the lumen with the villi and invaginates into crypts, the colon only contains invaginating crypts but lacks protrusions (see Fig. 4). The crypts and villi enlarge the surface area where the uptake of nutrients takes place. The crypts of both, the colon and the small intestine, harbour the slowly proliferating stem cells at the bottom followed by the more rapidly dividing transit amplifying cells further up in the crypt, which together maintain the cells of the intestinal epithelium. The intestinal epithelium is a highly proliferative tissue being completely renewed every 3 to 5 days (van der Flier and Clevers, 2009). New IECs derive from the stem cells, which divide about once per day giving rise to the transit amplifying cells, which divide a further 4 to 5 times before they lose their ability to divide by undergoing cell cycle arrest. The IECs further differentiate while moving up the crypt until they get shed off at the tip of the crypt or villus. Four different specialised intestinal epithelial

cell types can be found: the absorptive enterocytes, the secretory goblet cells, the enteroendocrine cells and the small intestinal specific Paneth cells (Radtke and Clevers, 2005). Enterocytes are the most abundant cells of the intestinal epithelium. They possess a brush border at the apical side and secrete hydrolases and absorb nutrients. Goblet cells are the most common cells of the secretory cell types. They secrete mucins, which constitute the protective mucus layer that prevents direct contact of commensal bacteria with the epithelium (McGuckin et al., 2009). The rather rare enteroendocrine cells secrete certain hormones, which regulate the secretion of digestive fluids and contraction of the intestinal muscles. Paneth cells are another type of highly secretory cells in the intestinal epithelium. They can be found at the bottom of small intestinal crypts in between the stem cells. They secrete antimicrobial peptides and proteins, like lysozyme or defensins, which contribute to host defense against bacterial pathogens and also seem to have a role in shaping the composition of the intestinal flora. Paneth cells also provide important factors for the stem cell niche of the small intestine (Bevins and Salzman, 2011).

At the end of the life cycle of an IEC at the tip of the small intestinal villus or colonic crypt, the cell gets shed off and expelled into the intestinal lumen. This homeostatic cell death is thought to be induced by the loss of anchorage and is named anoikis. Morphologically, cell detachment coincides with phenotypic alterations resembling apoptotic cell death (Vereecke et al., 2011). To prevent barrier leakage while cells get shed off, neighbouring cells have been reported to dynamically rearrange cytoskeletal elements leading to the formation of a ring like structure of actin and myosin around those cells that are about to be expelled. Contraction of these ring like structures build by the neighbouring cells leads to extrusion of the cell in their middle, while at the same time preventing the formation of holes in the epithelial barrier, at the places where cells get shed off (Madara, 1990; Rosenblatt et al., 2001). Additionally, an impermeable substance was found to plug epithelial discontinuities at the villus tip as a response to cell shedding, further preventing the formation of harmful gaps within the intestinal epithelium due to homeostatic cell shedding (Watson et al., 2005).

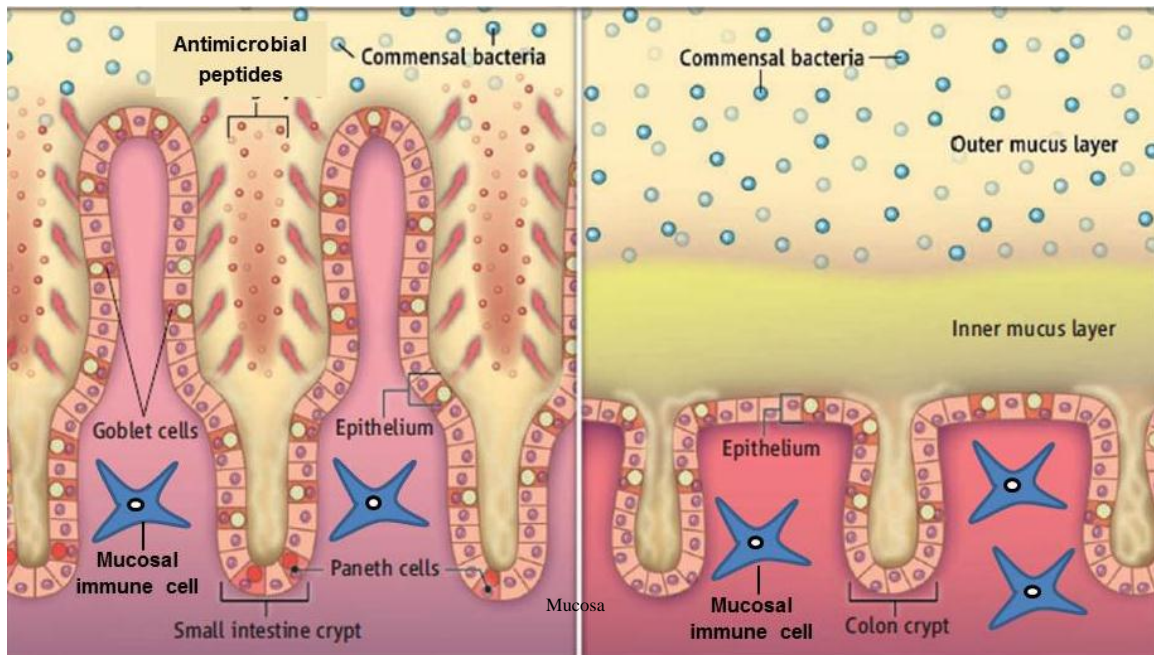


Figure 4: The intestinal epithelium at the mucosal luminal border of the gastrointestinal tract (modified from Johansson and Hansson, 2011).

The intestinal epithelium forms a barrier separating the luminal microbiota from the mucosal immune cells. IECs also establish the protective mucus layer to prevent a too close contact with the microbes. On the other hand IECs also regulate mucosal immune cell behaviour by creating an immunosuppressive environment. The crypts in the colon (right panel) are invaginations increasing the epithelial surface. A thick mucus layer prevents direct contact between the epithelium and the microbiota. The small intestine (left panel) consists of the crypts and the protruding villi. Paneth cells at the bottom of the crypts express important antimicrobial peptides and are important for the establishment of the stem cell niche.

1.3.2. Immunity, epithelial cell death and inflammation in the intestinal tract

Homeostatic cell death in the intestinal epithelium is a tightly regulated process, preventing the epithelial barrier to become leaky. Excessive IEC death could be exceptionally harmful for the organism. Breakdown of the intestinal epithelial barrier would enable microbes to invade the mucosa, where antigen sensing by the mucosal immune cells could cause a severe inflammatory condition. On the other hand, infected or damaged IECs could become harmful, when the infection cannot be brought under control and thus spreads to other cells or otherwise harms the organism. Thus, immune responses regulating survival or death of infected or damaged IECs are a delicate process.

As described above, cytokines like the DRLs can regulate cell survival and cell death as part of the immune response. Not much is known about FASL and TRAIL induced signalling in the intestine, but TNF induced signalling has been shown to play an important role in the regulation intestinal inflammation in IBD patients. TNF levels

were found to be elevated in the mucosa of IBD patients, especially in regions where epithelial apoptosis is increased (MacDonald et al., 1990). Additionally, an IBD susceptibility locus encompassing the TNF gene has been identified, providing additional evidence for a linkage between TNF and IBD. Anti-TNF agents have been successfully used in the treatment of IBD patients (Peyrin-Biroulet, 2010), although the mechanisms by which TNF treatment affects the development of IBD are not very well understood. Mouse models have been used to study the role of TNF in intestinal inflammation. It has been shown, that mice overexpressing TNF develop inflammation in the distal small intestine (ileitis) (Kontoyiannis et al., 1999). Activation of mesenchymal cells by TNF has been suggested to underlie the TNF induced pathology in this mouse model (Armaka et al., 2008). Further on, it has been reported that overexpression of TNF in IECs is sufficient to induce intestinal inflammation, but that action of TNF on IECs is not enough to cause the disease (Roulis et al., 2011). Thus, it seems that TNF does not cause intestinal inflammation by acting on normal, healthy IECs, although other studies imply that high doses of TNF can induce IEC death (Duprez et al., 2011; Marchiando et al., 2011). However, these studies neither analysed the role of TNF induced signalling in infected or otherwise damaged IECs nor did they dissect the potential roles of TNF induced cell survival or cell death signalling in the intestinal epithelium.

IECs express DRs and are therefore generally able to conduct DR induced signalling (Strater and Moller, 2000). TNF induced signalling can promote inflammation but also cell survival by activating signalling to NF- κ B. Interestingly, mice deficient for TAK1 or NEMO, two molecules essential for TNF induced activation of NF- κ B, specifically in the intestinal epithelium showed increased IEC death and spontaneously developed chronic colitis (Kajino-Sakamoto et al., 2008; Nenci et al., 2007). Importantly, TNFR1 deficiency prevented breakdown of the intestinal barrier and development of colitis in those mice deficient for NEMO specifically in the IECs (NEMO^{IEC-KO} mice) (Nenci et al., 2007). These results indicate that TNFR1 induced signalling might regulate IEC survival by NEMO dependent signals.

Much less is known about the role of the DR induced pro-death signalling pathways in the intestinal epithelium *in vivo*. However, *in vitro* studies in intestinal epithelial cell lines have shown, that virus infection can render cells sensitive towards TRAIL induced cell death (Strater et al., 2002), suggesting a role for DR induced cell death in the clearance of infected epithelial cells.

The intestinal epithelium is at the frontline to a huge variety of intestinal pathogens. IECs express various PRRs, among them TLR3 and TLR4, with the latter one being only expressed at low levels in the adult intestinal epithelium (Abreu, 2010). Although TLR4 is expressed at rather low levels in adult IECs, in those cells that are TLR4 positive, the receptor is mainly found at the Golgi apparatus indicating that receptor internalisation is required in IECs (Hornef et al., 2003).

TLR4 induced signalling has been shown to be protective in an experimental colitis model that depends on the intestinal microbiota (Rakoff-Nahoum et al., 2004), although other studies showed the contrary (Stevceva et al., 1999). Thus, bacteria induced signalling through TLR4 seems to influence the inflammatory response, although this TLR4 dependent regulatory mechanism is most likely independent of TLR4 signalling in IECs.

Not much is known about TLR4 induced IEC death during infections. TLR4 deficient mice are sensitive to infection with several enteric bacteria, like *Salmonella typhimorium* and *Escherichia coli* (Vazquez-Torres et al., 2004; Weiss et al., 2004). However, in both studies TLR4 mediated protection from infection has been allocated to impaired cytokine production and other protective effects in non-epithelial cells. In another enteric infection model TLR4 dependent signals were found to be detrimental. A study analysing *Citrobacter rodentium* infection in mice found that TLR4 induced signalling contributes to the development of colitis, potentially by activating NF- κ B signalling (Khan et al., 2006). Thus, while TLR4 signalling is important in the response to enteric infections, the role of TLR4 mediated IEC death remains largely unknown.

TLR4 is discussed to be implicated in necrotizing enterocolitis, a disease condition connected to increased IEC death in premature infants. Activation of TLR4 signalling in small intestinal IECs of new-borns has been suggested to lead to increased IEC death and might thereby potentially cause necrotizing enterocolitis (Leaphart et al., 2007). However, while linking TLR4 signalling to IEC death, this model requires further analysis to detect the exact signalling mechanisms involved.

Not much is known about the role of TLR3 dependent signals in IECs. Some reports suggest a role for TLR3 in the induction of IEC death in response to dsRNA administration and Rotavirus infections (Sato et al., 2006; Zhou et al., 2007), while another study challenges the TLR3 dependency of the immune response to

Rotavirus (Broquet et al., 2011). Other pathogens that might induce TLR3 mediated IEC death still need to be discovered.

In summary, although some reports link TLR3 and TLR4 to IEC death, the exact conditions and signalling pathways involved require further analysis.

1.4. Cre/LoxP conditional gene targeting

Cre/LoxP mediated recombination enables conditional gene targeting that allows cell type specific analysis of gene function in mice. Additionally, conditional gene targeting offers the opportunity to investigate the function of genes that are essential for mouse development as shown by embryonic or premature lethality of the corresponding conventional full body knockout mice (Rajewsky et al., 1996). In order to generate a cell type specific knockout of a certain allele, this allele is flanked by LoxP sites, specific 34 bp sequences, in the same orientation leading to a so called 'floxed' allele. Mice carrying a floxed allele are crossed with mice expressing a bacteriophage P1-derived Cre recombinase transgene (Sauer and Henderson, 1988) under the control of a cell type specific promoter. The Cre recombinase binds to and mediates recombination between the LoxP sites, resulting in the excision of the DNA flanked by the LoxP sites specifically in the Cre producing cell type.

1.5. Project description

The integrity of the intestinal epithelium is central for intestinal immune homeostasis. The intestinal epithelial barrier prevents invasion of the microbiota into the mucosa, where activation of mucosal immune cells could lead to potentially harmful inflammatory disorders. Therefore, homeostatic IEC death is a highly ordered and regulated process, in order to prevent barrier leakage and subsequent development of inflammation. On the other hand, immune responses might be able to trigger excessive IEC death, which could lead to a loss of the intestinal barrier integrity and thereby be extremely dangerous for intestinal homeostasis.

FADD is a central signalling transducer connecting cytokine inducible receptors, as well as antigen sampling through certain PRRs, to signalling to cell death. The role of FADD dependent cell death has mainly been studied in immune cells, while the role of FADD dependent cell death in epithelial tissues is largely unknown.

In this study, the role of FADD dependent signalling in the intestinal epithelium is analysed *in vivo*. Cre/LoxP mediated recombination was applied, to generate mice that were deficient for FADD specifically in the intestinal epithelium. In those mice FADD dependent signals would only be blocked in intestinal epithelial cells, thereby allowing the analysis of the epithelial specific role of FADD dependent signalling in the intestine.

2. Material and Methods

2.1. Material

2.1.1. Chemicals

Chemicals and compounds were bought from AppliChem, Bayer, Dako, GE Healthcare, Li-Cor Biosciences, Merck, MP, Ratiopharm, Roth, VWR, Sigma-Aldrich, Thermo Scientific, Vector Laboratories.

2.1.2. Material for mouse work

High resolution mini-endoscope, *Coloview* with Xenon light source, Karl-Storz (Tuttlingen, Germany)

Ketamin 10mg/ml, Ratiopharm

Rompun 2%, Bayer Healthcare

Syringes, Braun and injection needles, Terumo and Braun

Ampicillin, ICN Biomedicals

Neomycin, Sigma

Ciprofloxacin, Fluka

Meronem, AstraZeneca

Vancomycin, Eberth

2.1.3. Material for histology

Tissue Retriever 2100, PickCell

Tissue Processor, Leica TP1020

Rotary Microtome, Leica RM2255

Modular tissue embedding center, Leica EG1150 and Leica EG1150 C

Microscope, Leica DM5500 B

ABC Kit Vectastain Elite (Vector, PK 6100)

Avidin/Biotin Blocking Kit (Vector, no. SP-2001)

Liquid DAB Substrate Chromogen System (DakoCytomation, Code K3466)

Normal goat serum, Vector Laboratories

Entellan, Merck

Glass slides, Menzel

2.1.4. Material for biochemistry

Homogenizer Precellys 24, PeqLab

2ml tubes for homogenisation, PeqLab

1,4mm Zirconium oxide beads for tissue homogenisation, PeqLab

Gel casting system and SDS-Page system, Biorad

Protease Inhibitor Cocktail complete mini EDTA free, Roche

PhosphoStop, phosphatase inhibitor, Roche

Bradford reagent, Biorad

Protein Marker PeqGold Protein Marker V, PeqLab

PVDF membranes Immobilon-P, Millipore

Films Hyperfilm ECL, Amersham

2.1.5. Molecular biology reagents and equipment

Trizol reagent, Invitrogen

RNA extraction RNeasy mini kit, Qiagen

RNase-free DNase set, Qiagen

Super ScriptIII cDNA synthesis Kit, Invitrogen

RT Cyclor ABI HT 7900 Cyclor, Applied Biosystems

Power SYBR® Green PCR Master Mix, Applied Biosystems

TaqMan® Gene Expression Master Mix, Applied Biosystems

MicroAmp® Optical Adhesive Film, Applied Biosystems

MicroAmp™ Optical 384-Well Reaction Plate, Applied Biosystems

2.1.6. Laboratory equipment

Centrifuges, Eppendorf and Haereus

Thermomixer, Eppendorf

PCR-cyclers, Biorad DNA Engine, Biometra and Eppendorf

DNA ladder, PeqLab

Primers, Metabion and Invitrogen

Bio Photometer, Eppendorf

NanoDrop ND8100, PeqLab

2.1.7. Cell culture

DMEM, Gibco

TrypLE™ Express, Gibco

100x Penicillin (10000 U/ml)/Streptomycin (10000µg/ml), Gibco

100x L-Glutamine (200mM), Gibco

100x Sodiumpyruvate (100mM), Gibco

Fetal Calf Serum, PAN Biotech

DPBS, Gibco

Plastic ware for cell culture from BD Falcon, Millipore, TPP, Corning Tubes

Eppendorf 1,5ml and 2ml reaction tubes

8 x 0,2ml tube stripes Biozym

zVAD-fmk, ENZO

Cycloheximide, Sigma

2.1.8. Software

Photoshop CS3, Leica microscopy Software Leica application suite, Prism Graph, Microsoft Office, Endnote X4

2.1.9. Buffers and solutions

2.1.9.1. Washing buffers

PBS (1x) pH 7.3

NaCl 137mM

KCl 2,7mM

Na₂HPO₄-7H₂O 4,3mM

KH₂PO₄ 1,4mM

TBS (1x) pH 7.5

Tris-Base 24,2g

NaCl 80g

2.1.9.2. Buffers and solutions for immunostainings

Endogenous peroxidase blocking buffer (for IHC)

NaCitrate	0,04M
Na ₂ HPO ₄	0,121M
NaN ₃	0,03M
H ₂ O ₂	3% (v/v)

Citrate Buffer, pH 6.0

Citrate	10mM
Tween	0,05% (v/v)

TEX Protease K Buffer pH 8.0 (for protease mediated antigen retrieval)

Tris-Base	50mM
EDTA	1mM
Triton X-100	0,5% (v/v)

2.1.9.3. Preparation of protein extracts

High salt RIPA lysis buffer (for preparation of total cell extracts)

HEPES (pH 7.6)	20mM
NaCl	350mM
MgCl ₂	1mM
EDTA	0.5mM
EGTA	0.1mM
Glycerol	20% (v/v)

1% Nonident P-40, Protease inhibitor and Phosphatase inhibitors were added prior to use.

2.1.9.4. Buffers and solutions for Western Blot analysis

Tris-glycine electrophoresis buffer

Tris-Base	25mM
Glycine	250mM
SDS	0.1% (w/v)

SDS-polyacrylamide gel

10% resolving gel (for 20ml):

H ₂ O	7.9ml
30% acrylamide	6.7ml
1.5M Tris (pH 8.8)	5.0ml
10% (w/v) SDS	0.2ml
10% (w/v) APS	0.2ml
TEMED	0.012ml

5% stacking gel (for 10ml)

H ₂ O	6.8ml
30% acrylamide	1.7ml
1M Tris (pH 8.8)	1.25ml
10% (w/v) SDS	0.1ml
10% (w/v) APS	0.1ml
TEMED	0.01ml

Transfer Buffer (for semidry transfer)

Tris-Base	25mM
Glycine	192mM
Methanol pH 8.3	20% (v/v)

Blocking Buffer

Tween-20	0.1% (v/v)
nonfat dry milk	5% (w/v)
in PBS	

primary antibody dilution buffer

Tween-20	0.1% (v/v)
nonfat dry milk or BSA	5% (w/v)
in TBS	

5x Laemmli loading buffer

Tris-HCl (pH 6.8)	250mM
SDS	10% (w/v)
Glycerol	50% (v/v)
Bromphenolbue	0.01%
β -Mercaptoetanol	10%

Homemade ECL solution

Stock solutions:

Tris-HCl (pH 8.5)	100mM
Luminol	250mM
Paracoumaric acid (PCA)	90mM
H ₂ O ₂	30% (v/v)

Solution A:

2.5mM Luminol	100 μ l
400 μ M PCA	44 μ l
in 10ml 10mM Tris-HCl (pH 8.5)	

Solution B:

30% H ₂ O ₂	7 μ l
in 10ml 10mM Tris-HCl (pH 8.5)	

Solution A and B were mixed prior to use and applied to the membrane.

2.1.9.5. Buffers and solution for DNA extraction, genotyping PCRs and Southern Blot

Tail lysis buffer

Tris-HCl (pH 8.5)	100mM
EDTA	5mM
NaCl	200mM
SDS	0.2% (w/v)

0.1mg Proteinase K (10mg/ml in 50mM Tris, pH 8.0) per 500 μ l lysis buffer was added prior to use.

TE buffer

Tris-HCl (pH 8)	10mM
EDTA (pH 8)	1mM

10x TAG buffer

Tris-base (pH 8.5)	200mM
KCl	500mM

25x TAE buffer for 10L

Tris-base	1210g
EDTA (pH 8.0)	500ml of 0.5M solution
Acetic acid	285.5ml

DNA loading buffer

15% (w/v) Ficoll 400 was resolved in distilled water at 50°C. Orange G was added until the colour turned red.

Hybridization buffer

NaCl	1M
Tris (pH 7.5)	50 mM
Dextran sulphate	10%
SDS	1%
Salmon sperm DNA	250 g/ml (sonicated)

2.2. Methods

2.2.1. Animal handling and mouse experiments

2.2.1.1. Mouse maintenance

The mice were housed in individually ventilated cages in a specific pathogen free (SPF) mouse facility and in a conventional animal facility in the Institute for Genetics at the University of Cologne. The mice had permanent access to regular chow diet (Teklad Global Rodent 2018, Harlan) and acidified water. The animals were kept at a regular 12 hours light/dark cycle. Mice for breedings were set into one cage at a minimum of 6 weeks of age. Litters were weaned by 3 weeks of age, marked by an eartag and a tail biopsy was taken for the isolation of genomic DNA and following genotyping. Care of all mice was within institutional animal care committee guidelines and all protocols were approved by local government authorities.

Germ-free mice were generated by embryonic transfer into the gnotobiotic facility at the University of Ulm and were conventionalised by co-housing in one cage in case of the females or by exchange of bedding in case of males.

2.2.1.2. Generation of conditional and knock-out mice

To generate mice that were specifically lacking FADD in the intestinal epithelium (FADD^{IEC-KO} mice), FADD^{FL} mice (Mc Guire et al., 2010) were crossed with villin Cre transgenic mice (Madison et al., 2002). To generate FADD^{IEC-KO} mice that were deficient for MyD88, TNF or RIP3, FADD^{IEC-KO} mice were crossed to *Myd88*^{-/-} mice (Adachi et al., 1998), *Tnf*^{-/-} mice (Pasparakis et al., 1996) and *Ripk3*^{-/-} mice (Newton et al., 2004). To generate FADD^{IEC-KO} mice expressing the truncated deubiquitinase deficient CYLD Δ 932 in the intestinal epithelium (FADD^{IEC-KO}/CYLD Δ 932^{IEC} mice), FADD^{IEC-KO} mice were crossed with CYLD Δ 932^{FL} mice as described in Fig. 12.

For all analysis littermates only carrying the loxP flanked alleles served as control mice.

2.2.1.3. Endoscopy

Mice were anaesthetised by intraperitoneal injection of 100 μ l per 10g bodyweight Ketanest/Rampun. A high resolution mouse mini-endoscope, denoted Coloview from

Karl Storz, was employed to analyse the distal colon. The endoscope was gently inserted into the anus and a constant airflow dilated the colon to prevent injuries and allow a proper view on the colonic bowel wall. Disease index was determined as a sum of 5 scoring parameters, each of them indicative for intestinal disease. Every parameter was scored from 0 to 3, with 0 being healthy and 3 indicating severe inflammation (Becker et al., 2005). The following parameters were included in the murine endoscopic index of colitis severity (MEICS): stool consistency, vascularisation pattern, fibrin abundance, thickening of the bowel wall and surface appearance of the mucosa. The MEICS is the sum of the score of these parameters and ranges between 0 and 15. Furthermore, tumours, ulceration and other intestinal lesions could be assessed by endoscopic examination.

After endoscopy mice were allowed to recover or were immediately killed.

2.2.1.4. Antibiotic treatment, generation of germ-free mice and conventionalisation

In order to deplete the intestinal microbiota, mice were treated with 1 g/l ampicillin, 1 g/l neomycin, 0.5 g/l meronem and 0.5 g/l ciprofloxacin in the drinking water beginning at the second day after birth. At weaning, three weeks after birth, ciprofloxacin was exchanged for 0.5 g/l vancomycin. Efficiency of the depletion of the microbiota was tested by plating homogenized faeces in LB medium in different concentrations on agar plates.

Germ-free FADD^{IEC-KO} mice were generated at the gnotobiotic facility of the University of Ulm. For conventionalisation female germ-free mice were either cohoused with conventional FADD^{FL} mice or FADD^{IEC-KO}/CYLD Δ 932^{IEC} mice. For the conventionalisation of male germ-free mice, bedding from conventional FADD^{FL} mice and FADD^{IEC-KO}/Ripk3^{-/-} mice was added into the cage. Mice were dissected after one week of conventionalisation.

2.2.1.5. Sacrifice of mice

Mice were sacrificed by cervical dislocation.

2.2.1.6. Tissue preparation

The abdominal cavity was cut open by a longitudinal incision. The intestine was removed by one cut close to the anus and another one shortly behind the pylorus. The intestine was washed in PBS and the mesentery and fat tissue removed. The colon and the small intestine were separated and the luminal content removed carefully. Either small pieces of about 5mm were taken for histological examination or RNA extraction or a bigger part of the tissue was cut open longitudinally and afterwards rolled up to a “swiss roll”.

2.2.2. Histology

2.2.2.1. Preparation of intestinal tissue for histological analysis

For histological analysis the tissue was transferred into cassettes and fixed overnight at 4°C in 4% paraformaldehyde. In order to dehydrate the samples, they were passed through increasing concentrations of ethanol for 2h each (in 30% (v/v), 50% (v/v), 70% (v/v), 96% (v/v) and 2x in 100% (v/v) ethanol). Afterwards they were incubated in xylol for two times 2h and then transferred to paraffin, for the embedding in paraffin blocks. The fixed intestinal tissue was sectioned by a microtome at 3-5µm thickness and transferred onto glass slides.

2.2.2.2. Haematoxylin and Eosin staining of intestinal tissue sections

To de-wax the tissue sections, they were placed in xylol for 20min, and afterwards rehydrated in decreasing concentrations of ethanol for 2min each (100% (v/v), 95% (v/v), 75% (v/v) ethanol) and then washed in PBS for 5min and in tap water for 1min. For the Haematoxylin and Eosin (H&E) staining the sections were first stained in Mayer’s Haematoxylin for 2min. The sections were washed for 20sec in tepid tap water, 15min in tap water at room temperature and a few seconds in deionized water. For staining with Eosin samples were placed in Eosin staining solution for 1min. Afterwards the sections were washed in tap water up to 7 times. The sections were dehydrated for 2min each in 75% (v/v), 96% (v/v) and 100% (v/v) ethanol and cleared in xylol. Coverslips were mounted with Entellan.

2.2.2.3. Immunostainings

For immunohistochemical (IHC) staining, sections were de-waxed and rehydrated as described for the H&E staining. After the rehydration samples were washed twice in tap water for 5min each. The endogenous peroxidase activity was blocked by incubation in endogenous peroxidase blocking buffer for 15min at room temperature. Afterwards slides were washed three times in tap water for 5 min each. For antigen unmasking by heat induced epitope retrieval sections were either heated in citrate buffer for 20min to 120°C in a pressure steam cooking device or overnight at 80°C. For F4/80 immunostaining antigen unmasking was achieved by Proteinase K digestion with 20µg/ml Proteinase K in TEX buffer for 20min at room temperature. Sections were washed in PBS and unspecific background was blocked by treatment with 10% (v/v) normal goat serum, 0.3% (v/v) Triton X-100 and Avidin in PBS. Incubation with primary antibody diluted in PBS, 0.2% (v/v) cold fish gelatine and Biotin was done overnight at 4°C. Samples were washed three times for 5min in PBS with 0.05% (v/v) Tween-20. Sections were incubated with the secondary antibody diluted in PBS with 10% (v/v) normal goat serum for 1h at room temperature. Samples were again washed three times for 5min in PBS with 0.05% (v/v) Tween-20. Sections were afterwards incubated with an Avidin-Biotin-HRP complex (ABC Kit) for 30min at room temperature. After washing in PBS the staining was developed by incubation with DAB chromogen for up to 20 min. The formation of precipitate was followed by microscopy and the reaction was stopped by washing in PBS in all corresponding samples at the same time after reaching a level of adequate staining. Nuclei were counterstained in Mayer's Haematoxylin for 2min. The sections were either mounted with Kaisers' gelatine or dehydrated in a descending series of ethanol solution as described above and mounted with Entellan.

Table 1: Primary antibodies and conditions for immunostaining

Antigen	Company	Clone	Host	Dilution
F4/80	home made	A3-1	rat	1:100
Gr1	BD Pharmingen	1A8	rat	1:500
CD3	Abcam	Ab 5690	rabbit	1:200
B220	home made	RA3 6B2	rat	1:1000
active Caspase 3	R&D systems	AF835	rabbit	1:2000
Ki-67	Dako	TEC-3	rat	1:1000
Lysozyme	Dako	EC 3.2.1.17	rabbit	1:1000

Table 2: Secondary antibodies and conditions for immunostaining

Antigen	Company	Clone	Host	Dilution
bioinylated rat IgG	Dako	E0468	rabbit	1:1000
biotinylated rabbit IgG	Perkin Elmer	NEF813	goat	1:500

2.2.2.4. Electron microscopy

3-mm-long samples from distal, medial and proximal colon were taken for electron microscopy and immediately fixed in 2.5% glutaraldehyde and 2% paraformaldehyde in phosphate buffer pH 7.4 for 3 h at room temperature. Afterwards, the tissues were post-fixed in 1% OsO₄ and then embedded in Epon resin. The sections were cut at a thickness of 70–90-nm and stained with uranyl acetate and lead citrate. Samples were analysed with a Philips CM-10 transmission electron microscope. Representative pictures were captured using an Orius SC200 CCD camera (Gatan GmbH). Electron microscopy was carried out in collaboration with Vangelis Kondylis.

2.2.3. Biochemistry

2.2.3.1. IEC isolation from colon and small intestine

Colon and small intestine were removed as described above and transferred into cold PBS. Isolation of IECs was performed according to the published protocol (Ukena et al., 2007). Colon and small intestine were cut open longitudinally and the luminal content removed by washing in PBS. Colon or small intestine were

transferred into 50ml Falcon tubes and incubated on a horizontal shaker at 180rpm at 37°C in pre-warmed PBS with 1mM DTT for 10min in order to remove the mucus and debris. After washing the tissue in PBS, it was transferred into a new Falcon 50ml tube and incubated in HANKs salt solution (HBSS) with 1.5mM EDTA for 15min at 37°C and 180rpm. To efficiently detach the IECs and crypts, tubes were vortexed for 1min at full speed. The remaining tissue was removed and IECs were pelleted by centrifugation at 1200rpm for 10min. The supernatant was removed and the IEC pellets were resuspended in 1-2ml PBS and transferred into eppendorf tubes. IECs were centrifuged at 5000rpm for 5min and pellets were frozen in liquid nitrogen or directly used for protein or RNA extraction.

2.2.3.2. Preparation of IEC protein extracts

For total extracts of IECs, cells were lysed in high salt RIPA lysis buffer containing protease- and phosphatase inhibitors. During the lysis cells were kept on ice for 30min and inverted repetitively. Afterwards samples were centrifuged at full speed for 20min at 4°C to pellet the cell debris. The supernatant containing the extracted proteins was used for further analysis.

2.2.3.3. Assessment of protein concentration by Bradford assay

For the determination of protein concentration within a given sample, the sample was diluted in lysis buffer 1:10. 2µl of this dilution were added to 1ml of Bradford solution. A protein standard curve with 0.5µg, 1µg, 2 µg, 5µg and 10µg in of BSA in lysis buffer was obtained by adding 2µl of the different BSA concentrations to 1ml of Bradford dilution each. Protein concentration was measured with a spectrophotometer at an absorbance of 595nm. The standard curve was used to obtain the protein concentration in the sample.

2.2.3.4. Western Blot analysis

Samples were boiled in Laemmli loading buffer for 10min to reduce disulphide bonds and denature proteins. Proteins were separated according to size by electrophoresis in 10% SDS-polyacrylamid gels (SDS-PAGE) under denaturing conditions with Tris-Glycine electrophoresis buffer. Transfer of Proteins to PVDF membranes was achieved by semidry transfer. Therefore the PVDF membrane was activated by

incubation in 100% (v/v) methanol for 2min and then placed in the transfer buffer. 3mm Whatman paper was soaked in semi dry transfer buffer. The setup for the transfer was the following from bottom to top: one piece of whatman paper is followed by the PVDF membrane, followed by the gel and another whatman paper on top. For the transfer 1mA current was applied per cm² membrane for 90min. After blotting the membrane was washed in PBS and blocked under constant agitation with blocking buffer to reduce unspecific binding of antibodies. Incubation with primary antibodies diluted in primary antibody dilution buffer was performed overnight at 4°C. The membrane was washed afterwards three times for 5min in PBS with 0.1% (v/v) Tween-20, followed by 1h of incubation with the secondary HRP-conjugated secondary antibody diluted in blocking buffer at room temperature under agitation. Afterwards the membrane was washed again with three times for 5min in PBS with 0.1% (v/v) Tween-20. Proteins were detected by incubation of the membrane in homemade ECL solution followed by exposition to chemiluminescent films for varying times. The films were developed in AGFA developer solution and fixed in AGFA fixation solution.

Table 3: Primary antibodies used for Western Blot analysis

Antigen	Company	Host	Dilution
FADD	gift from A. Strasser	rat	1:1000
RIP3	Enzo	rabbit	1:1000
CYLD	gift from R. Massoumi	rabbit	1:1000
α-Tubulin	Sigma	mouse	1:5000

Table 4: Secondary antibodies used for Western Blot analysis

Antigen	Company	Clone	Host	Dilution
Rat IgG	Jackson ImmunoResearch		goat	1:3000
Rabbit IgG	Amersham Pharmacia	NA934V	donkey	1:3000
Mouse IgG	Amersham Pharmacia	NA9310V	sheep	1:3000

2.2.4. Molecular Biology

2.2.4.1. Preparation of genomic DNA

Tail biopsies or IECs were digested in 500µl of tail lysis buffer and Proteinase K (10mg/ml) under agitation at 56°C overnight. Undigested material was pelleted by centrifugation at full speed for 10min. The supernatant was transferred to a new tube, 500µl of isopropanol were added and the tube was inverted several times to precipitate the DNA. After 5min of centrifugation at full speed the DNA was washed with 200µl of 70% (v/v) ethanol. To obtain the genomic DNA, samples were centrifuged at full speed for 5min, the supernatant was removed and the DNA pellet dried for 20min and afterwards suspended in 100µl Tris-EDTA buffer.

2.2.4.2. Southern Blot

The genomic DNA was digested overnight with the restriction enzyme SpeI in case of the *Cyld* locus and with EcoRV in case of the *Fadd* locus. DNA fragments were separated on a 0.8% agarose gel, and afterwards overnight transferred from the gel onto a charged nylon membrane by capillary flow. After the transfer the membrane was baked at 80°C for 1h and pre-incubated in hybridization buffer at 65°C for 2h. Specific DNA probes labelled by random priming with ³²Pα-GTP were added to the hybridization buffer and allowed to hybridize with the membrane overnight at 65°C. The membrane was washed afterwards for 20 minutes with 2x SSC/1% SDS at 65°C, followed by more washing steps for 20min each with 1x SSC/0.5% SDS until the background signal was low enough for detection of the specific signals. After sufficient washing the membrane was first exposed to a Phosphorimager screen for 1-2 hours and afterwards a KODAK BioMax MR film was exposed to the membrane for several days at -80°C.

Table 5: primers used for amplification of DNA probes by Southern Blot

locus	forward (5'→3')	reverse (5'→3')
<i>Fadd</i>	CGTGAGGAGCAGGGCAAGCAG	TGGTGAAGCCCTCCAGCCTGT
<i>Cyld</i>	TCATGGCCAGCAGTCTCGAAG	TTTCTGTGGGCCTACATACGG

2.2.4.3. Genotyping PCRs

2µl of genomic tail DNA was used for genotyping by Polymerase-chain-reaction (PCR). The following PCR mix was used: 3µl of 10x TAG buffer, 3µl of 2mM dNTPs, 3µl of 3µM primer mix, 1.8µl 25mM MgCl₂, 1.8µl DNA loading dye, 0.5µl homemade Taq-enzyme and 17µl of H₂O in a final volume of 30µl. Annealing and elongation times during the PCR depend on the individual primer set. 10µl of the PCR reaction was separated on an agarose gel by electrophoresis.

Table 6: Primer sequences for genotyping PCRs and PCR-amplified fragment sizes

typing for	Primer sequence	bands
villin Cre	ACA GGC ACT AAG GGA GCC AAT G AT TGCA GGT CAG AAA GAG GTC ACA G GTT CTT GCG AAC CTC ATC ACT C	WT: 900bp Tg: 350bp
<i>Fadd</i>	TCA CCG TTG CTC TTT GTC TAC GTA ATC TCT GTA GGG AGC CCT CTA GCG CAT AGG ATG ATC AGA	WT: 208bp FL: 280bp
<i>Ripk3</i>	CGC TTT AGA AGC CTT CAG GTT GAC GCC TGC CCA TCA GCA ACT C CCA GAG GCC ACT TGT GTA GCG	WT: 320bp KO: 485bp
CyldΔ932	CCA AGC TCT AGG CCC TAA GGT ATG TCT AAG TCC TTC TGG CAT	WT: 729bp FL : 763bp
<i>Myd88</i>	GAG CAG GCT GAG TGC AAA CTT GGT CTG AGC CTC TAC ACC CTT CTC TTC TCC ACA ATC GCC TTC TAT CGC CTT CTT GAC GAG	WT: 1000bp KO: 1000bp (separate PCRs)
<i>Tnf</i>	AAC CAG GCA GGT TCT GTC CC CTC TTG CTT ATC CCC TCT TCC	WT: 481bp KO: 1200bp

Table 7: programmes for genotyping PCRs

typing for	PCR programme		cycles
villin Cre	94°C	3min	35
	94°C	1min	
	67°C	1min	
	72°C	1min	
	72°C	5min	

Table 7 continued			
<i>Fadd</i>	94°C	3min	34
	94°C	1 sec	
	55°C	30 sec	
	72°C	30 sec	
	72°C	3 min	
<i>Ripk3</i>	94°C	4min	30
	94°C	1 min	
	60°C	30 sec	
	72°C	1 min	
	72°C	10 min	
CYLDA932	94°C	4min	30
	94°C	1 min	
	56°C	30 sec	
	72°C	1 min	
	72°C	4 min	
<i>Myd88</i>	94°C	3min	35
	94°C	30sec	
	67°C	1min	
	72°C	1min	
	72°C	5min	
<i>Tnf</i>	94°C	3min	5
	94°C	1min	
	58°C	30sec	
	72°C	90sec	
	94°C	15sec	25
	58°C	40sec	
	72°C	90sec	

2.2.4.4. Agarose gel electrophoresis

DNA-fragments amplified by PCR were separated by gel electrophoresis according to size. Therefore, depending on the fragment size, either 1% or 2% of Agarose in TAE buffer were boiled and afterwards 0,5mg/ml Ethidiumbromide was added. After polymerisation during the cooling process, gels were run in TAE buffer.

2.2.4.5. Extraction of RNA

For RNA extraction from whole intestinal tissue or IECs, samples were homogenised in 1ml of Trizol (Invitrogen). To ensure the complete lysis of nuclei, samples were incubated for 20 min at room temperature. Cell debris was afterwards pelleted by centrifugation for 10min at full speed. The supernatant was transferred into a new tube and incubated for another 5min. For the extraction of nucleic acids 200µl of chloroform per 1ml of Trizol was added and the samples were thoroughly mixed for 15sec. After incubation for 5min at room temperature, the organic and the aqueous phase was separated by centrifugation for 15min at full speed. The upper aqueous phase was transferred into a new tube and an equal volume of 70% (v/v) ethanol was added. The samples was loaded on a Quiagen RNAeasy column and centrifuged for 1min at 9000g to bind the nucleic acids to the filter of the column. In a washing step washing buffer, provided by the manufacturer, was added to the column and removed by centrifugation for 15sec at 9000g. For DNA digestion the column was incubated with RNase-free DNase in RDD buffer, also provided by the manufacturer. After another two washing steps, the RNA was eluted in nuclease free water by centrifugation for 2min at full speed.

The quality of the RNA was tested on an agarose gel and possible contamination with genomic DNA was checked by a PCR for β -actin. Concentration and purity of the RNA samples was assessed by photometric analysis with a NanoDrop.

2.2.4.6. cDNA synthesis

cDNA synthesis was performed with the Superscript III kit (Invitrogen). In a total reaction volume of 10µl 1µg of RNA was added to 1µl of 10mM dNTPs and 1µl random hexamer primers (50ng/µl). Annealing of the primers to the RNA was achieved by incubation at 65°C for 5min. Afterwards the sample was incubated on ice for several minutes. 10µl of cDNA synthesis mix containing 2µl 10x RT-reaction

buffer, 4µl 25mM MgCl₂, 2µl 0.1M DTT, 1µl RNase OUT (40µl U/µl) and 1 µl of SuperScript III polymerase (200U/µl) was then added to sample and following reaction was carried out on a PCR cycler: 10min at 25°C, 50min at 50°C for cDNA synthesis, 5min at 85°C for termination of the reaction. To digest the RNA the sample was incubated with 1µl of RNase H for 20min at 37°C. Finally the reaction was diluted 10-fold with nuclease free water.

2.2.4.7. Quantitative real time PCR

For quantitative real time PCR (qRT-PCR) each sample was run in duplicates. For probe-based Taqman qRT-PCR 2µl of the cDNA dilution were mixed with 6µl of 2x Mastermix (Applied Biosystems), 0.6µl of primer-probe mix (Applied Biosystems) and 3.4µl of water in 384-well plates. All Taqman probes were purchased from Applied Biosystems. The following PCR programme was used: activation step for 10min at 95°C, for amplification 40 cycles of 10sec at 95°C and 1min at 60°C.

For SYBR-Green qRT-PCR 2µl of the cDNA dilution were mixed with 1.2µl of 20µM primer mix, 6µl of 2x reaction buffer (Applied Biosystems) and 2.8µl of water. The following PCR programme was used: 10min at 95°C, 40 cycles for 10sec at 95°C, 20sec at 60°C and 40sec at 72°C. After the 40 cycles the PCR-amplicons were subjected to a dissociation stage. Primers for SYBR-Green qRT-PCR were purchased from Invitrogen and primer sequences were obtained from pga.mgh.harvard.edu/primerbank/.

The comparative $\Delta\Delta CT$ method was used to determine RNA expression levels. Therefore, in order to generate the ΔCT value, Ct values (corresponding to the cycle number when the amplification plot crosses the fixed threshold) for each gene were subtracted from the Ct values of the endogenous reference gene TATA box binding protein. Relative quantification was achieved by using the $\Delta\Delta CT$ value.

Table 8: Taqman probes used for quantitative RT-PCR analysis

Gene	Taqman probe
<i>Il6</i>	Mm00446190_m1
<i>Il1b</i>	Mm00434228_m1
<i>Ifng</i>	Mm00801778_m1
<i>Tnf</i>	Mm00443258_m1
<i>Fasl</i>	Mm00438864_m1
<i>Tnfsf10</i>	Mm00437174_m1
<i>Ccl5</i>	Mm01302428_m1
<i>Il23, p19</i>	Mm00518984_m1
<i>Il18</i>	Mm00434225_m1
<i>Il12a, p35</i>	Mm00434165_m1
<i>Il10</i>	Mm00439616_m1
<i>Tnfr1</i>	Mm01182929_m1
<i>Fas</i>	Mm00433237_m1
<i>Defa20</i>	Mm00842045_g1
<i>Lyz1</i>	Mm00657323_m1
<i>Defa-rs1</i>	Mm00655850_m1
<i>Ang4</i>	Mm03647554_g1
<i>Ccnd1</i>	Mm00432359_m1
<i>Tbp</i>	Mm00446973_m1

Table 9: primer sequences for SYBR-Green qRT-PCR

gene	forward (5'->3')	reverse (5'->3')
<i>Ccl2</i>	TTA AAA ACC TGG ATC GGA ACC AA	GCATTAGCTTCAGATTTACGGG T
<i>Ripk1</i>	GAAGACAGACCTAGACAGCGG	CCAGTAGCTTCACCACTCGAC
<i>Ripk3</i>	TCTGTCAAGTTATGGCCTACTGG	GGAACACGACTCCGAACCC
<i>Casp8</i>	TGCTTGGACTACATCCCACAC	TGCAGTCTAGGAAGTTGACCA
<i>Tbp</i>	GCTCTGGAATTGTACCGCAG	CTGGCTCATAGCTCTTGGCTC

2.2.5. Cell Biology

2.2.5.1. Culture of mouse embryonic fibroblasts (MEFs)

Primary MEFs were isolated from wild-type and homozygous CYLD Δ 932 mice. MEFs were cultured in growth medium (DMEM supplemented with 10% (v/v) FCS, Penicillin/Streptomycin, Pyruvate and Glutamine). Cells were grown to confluency in 15cm Petri dishes and incubated at 37°C and 5% (v/v) CO₂. Once cells had grown to confluence they were treated trypsinated in order to detach the cells from the dish. Cells were incubated for 5min with trypsin solution at 37°C, afterwards trypsin activity was blocked by addition of DMEM supplemented with 10% (v/v) FCS, Penicillin/Streptomycin, Pyruvate and Glutamine. After centrifugation and removal of the medium, cells were resuspended in fresh growth medium and either replated after dilution on 15cm Petri dishes or used for the cell death assay.

2.2.5.2. Cell death assay with MEFs

For the cell death assay early passage MEFs were trypsinated as described above. Concentration of cells was determined using a Neubauer chamber. After resuspending, 10⁴ cells per well were plated in 100 μ l of growth medium on a 96-well plate and incubated overnight at 37°C and 5% (v/v) CO₂. For the induction of necroptosis cells were pretreated for one hour with 1 μ g/ml cycloheximide (CHX; Sigma) and 20 μ M zVAD-fmk (ENZO) and subsequently stimulated with 1, 10 or 30ng/ml murine TNF for 12h. Cell survival was determined by spectrophotometric measurement of crystal violet incorporation. All samples were tested in triplicates and values are presented as per cent survival of triplicates compared to untreated cells.

2.2.6. Statistics

Results are presented as the mean +/- standard deviation (SD). Statistical significance between experimental groups was determined by an unpaired two-tailed Student's t-test.

3. Results

3.1. Deletion of FADD in IECs results in chronic spontaneous colitis and enteritis

3.1.1. Generation of mice deficient for FADD only in the intestinal epithelium

To investigate the role of FADD dependent signalling pathways in the intestinal epithelium, a genetic mouse model was generated, in which FADD was deleted specifically in intestinal epithelial cells (IECs). Mice carrying *Fadd* alleles with the second exon of *Fadd* flanked by loxP sites (FADD^{FL} mice) (Mc Guire et al., 2010) were crossed with mice expressing the Cre recombinase under the control of the IEC specific villin promoter (Madison et al., 2002). In FADD^{FL} mice that express the Cre recombinase under the control of the villin promoter, the Cre recombinase excises the second exon of *Fadd* only in IECs. This results in mice expressing FADD in all cells except for the FADD deficient intestinal epithelium (FADD^{IEC-KO} mice). FADD was efficiently deleted in IECs on the genomic level as shown by Southern Blot analysis and on the protein level as shown by Western Blot analysis from extracts of isolated colonic IECs (Fig. 4a and 4b).

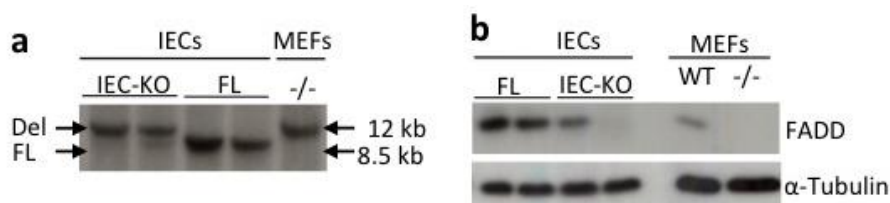


Figure 4 Conditional ablation of FADD in the intestinal epithelium of mice (FADD^{IEC-KO} mice)
a. and b. Efficient deletion of the *Fadd*-allele in isolated IECs from FADD^{IEC-KO} mice (IEC-KO) compared to FADD^{FL} mice (FL) was detected by Southern Blot (b) and Western Blot (c). Wildtype (WT) and FADD^{-/-} (-/-) MEFs served as controls. α-Tubulin served as loading control.

3.1.2. FADD^{IEC-KO} mice develop spontaneous chronic colitis

FADD^{IEC-KO} mice were born at mendelian ratios but grew slower and gained less bodyweight than FADD^{FL} littermates. About half of the FADD^{IEC-KO} mice died within the first three weeks after birth. Endoscopy of 10 week old animals revealed severe colitis in FADD^{IEC-KO} mice as displayed by a thickened and less translucent mucosa, ulceration, increased deposition of fibrin, an altered vascularization and severe diarrhoea leading to a significantly increased murine endoscopic index of colitis

severity (MEICS) compared to FADD^{FL} mice (Fig. 5a). Colons from FADD^{IEC-KO} mice were significantly shorter than those of FADD^{FL} mice (Fig 5b).

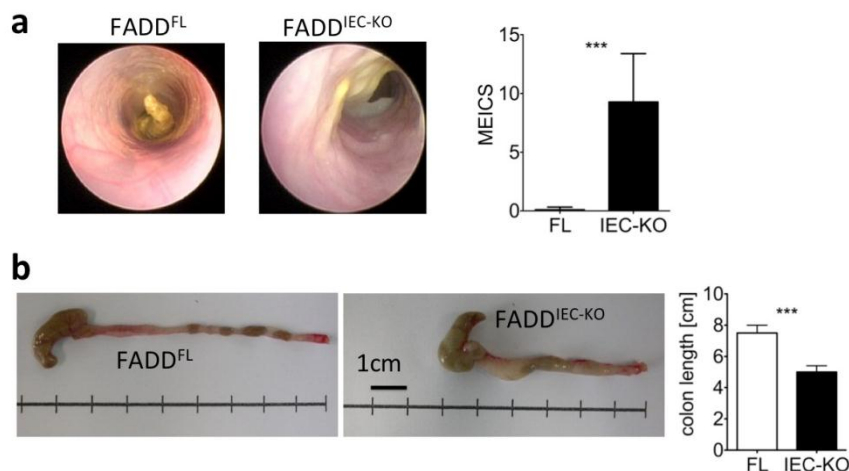


Figure 5 Spontaneous development of colitis in FADD^{IEC-KO} mice

a. Representative endoscopic images of 10 week old FADD^{FL} control and FADD^{IEC-KO} mice and a significantly increased MEICS (murine endoscopic index for colitis severity) showed colonic inflammation. FADD^{IEC-KO} (n=31) and FADD^{FL} (n=37) **b.** The colon of FADD^{IEC-KO} mice was significantly shorter than the colon of FADD^{FL} mice. FADD^{IEC-KO} (n=4) and FADD^{FL} littermates (n=5). Scale bar, 1 cm

For histological analysis sections from colons of 2-, 3- and 10 week old mice were stained with Haematoxylin, which indicates the nuclei, and Eosin (H&E), which highlights the cytoplasm. Increased epithelial cell death was detected already in 2 week old FADD^{IEC-KO} mice, but not in FADD^{FL} controls. Immune cell infiltrations into the mucosa became visible in 2 week old FADD^{IEC-KO} mice and elongated crypts were detectable in 3 week old mice throughout the whole colon, with increasing intensity to the proximal part. Both, immune cell infiltration and crypt elongation further increased in 10 week old FADD^{IEC-KO} mice (Fig 6a), which is reflected in a significantly increased Histological Colitis Score (HCS) for sections from 10 week old FADD^{IEC-KO} mice compared to FADD^{FL} mice (Fig 6b).

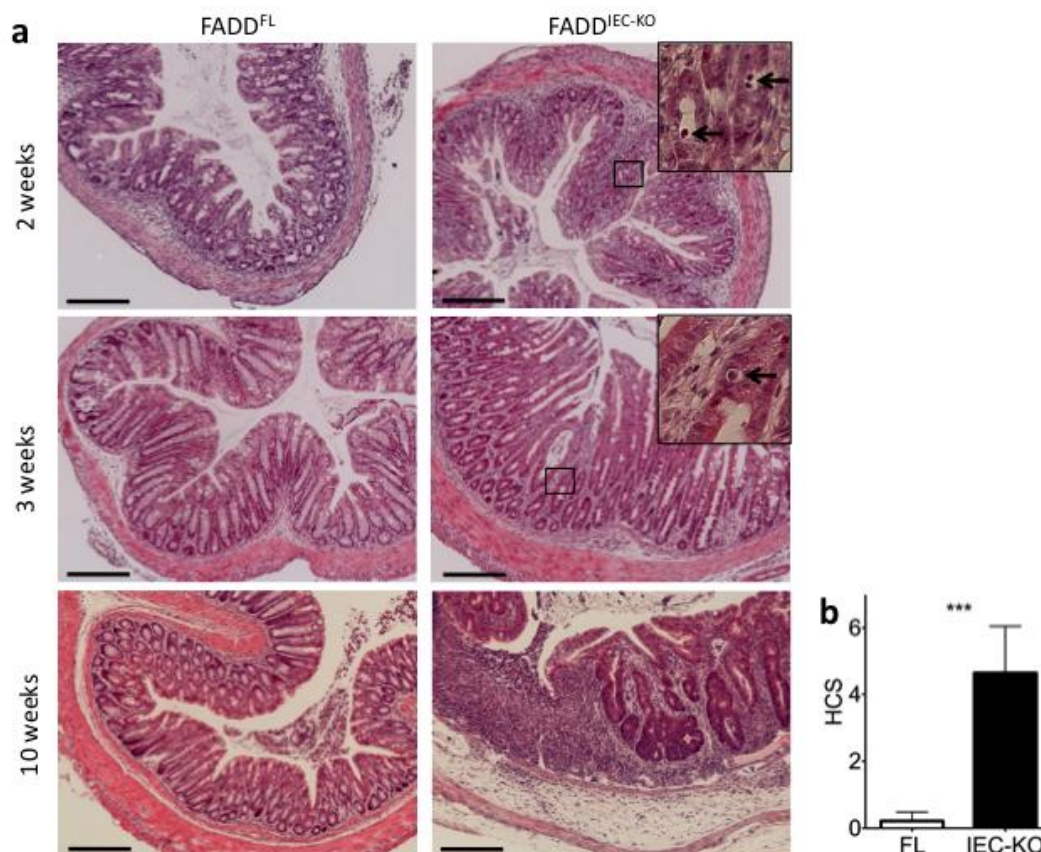


Figure 6 Development of inflammation and tissue damage in FADD^{IEC-KO} mice

a. H&E stained colonic sections from 2-, 3- and 10 week old FADD^{IEC-KO} mice showed increased infiltration of immune cells into the mucosa, hyperproliferation and increased cell death compared to FADD^{FL} mice. Arrows in insets indicate dying epithelial cells in 2- and 3-week-old mice. Scale bars: 100 μ m. **b.** Significantly increased HCS (Histologic Colitis Score) confirmed the colonic inflammation in 10 week old FADD^{IEC-KO} mice. FADD^{FL} (n=7) and FADD^{IEC-KO} (n=7)

Quantitative real time PCR (qRT-PCR) on colonic extracts was employed to further analyse the inflammatory response in the colon of FADD^{IEC-KO} animals, revealing increased expression of several inflammatory cytokines and chemokines in FADD^{IEC-KO} mice compared to FADD^{FL} mice (Fig 7a). Ccl2 and Ccl5, chemokines that attract different sets of immune cells like monocytes or dendritic cells in case of Ccl2 and T cells as well as eosinophils and basophils in case of Ccl5, were expressed at significantly higher levels in the FADD^{IEC-KO} mice than in the control mice. Several pro-inflammatory cytokines from the interleukin family like IL-1 β , IL-6 or IL-12a were expressed at a much higher level in the FADD^{IEC-KO} mice compared to the controls. Beside of the pro-inflammatory interleukins also the anti-inflammatory IL-10 was significantly upregulated, indicating that additionally to the pro-inflammatory response mechanisms were activated to keep the inflammation under control. Additionally, expression of the DR ligands TNF, FASL and TRAIL was upregulated in the FADD^{IEC-KO} animals as well as Interferon- γ .

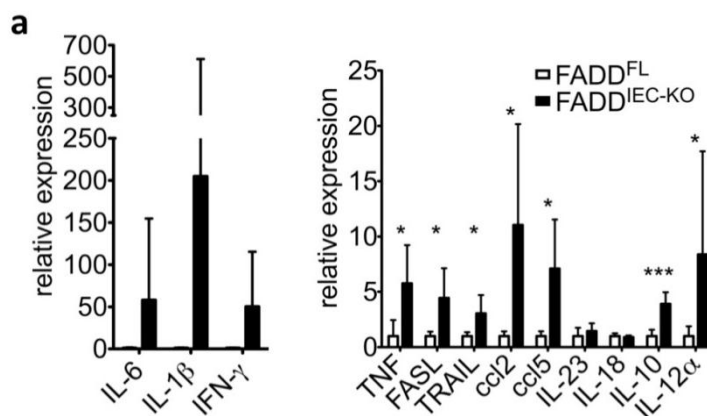


Figure 7 Increased expression of proinflammatory cytokines and chemokines of 10 week old FADD^{IEC-KO} mice

a. qRT-PCR analysis revealed increased cytokine and chemokine expression in colons from 10-week-old FADD^{IEC-KO} and FADD^{FL} mice (n=5–8 for each genotype). All graphs show mean values ± standard deviation (s.d.).

The nature of the immune response in the colon was further dissected by immunohistochemical (IHC) stainings for the infiltrating immune cells on sections from 2-, 3- and 10-week old mice. An increased amount of F4/80 positive macrophages was detectable in the mucosa of two week old FADD^{IEC-KO} mice compared to FADD^{FL} control mice. The number of F4/80 positive macrophages increased even more in older FADD^{IEC-KO} mice (Fig. 8a). A similar pattern could be found for Gr1 positive granulocytes which were already abundant in 2-week old FADD^{IEC-KO} mice and further increased in 3- and 10-week old FADD^{IEC-KO} mice, while they were hardly detectable in the control mice (Fig. 8a). Neither increased infiltration of B220 positive B-cells nor of CD3 positive T-cells could be detected in 2-week old FADD^{IEC-KO} animals compared to FADD^{FL} control animals. Both cell types were moderately increased in 3-week old FADD^{IEC-KO} mice compared to FADD^{FL} control mice and further increased in the mucosa of 10-week old FADD^{IEC-KO} mice compared to FADD^{FL} control mice (Fig. 8a). Therefore the primary immune response in young FADD^{IEC-KO} animals seems to rely on innate immune cells of the myeloid lineage, while cells of the adaptive immune response contributed to the inflammation in the colons of FADD^{IEC-KO} animals only in later stages.

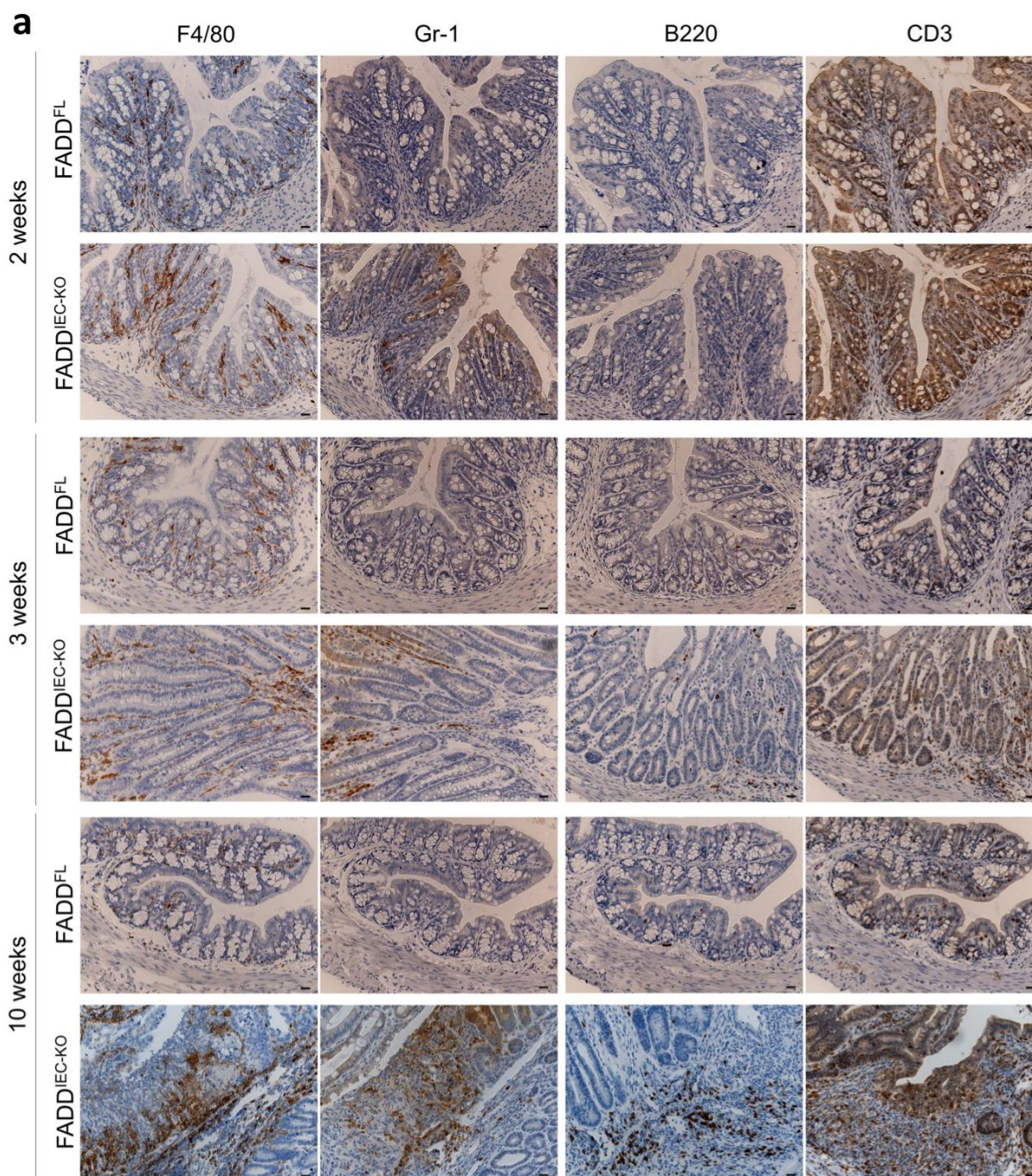


Figure 8 Increased infiltration of immune cells into the mucosa of 10 week old FADD^{IEC-KO} mice
a. Colonic cross-sections from FADD^{IEC-KO} and FADD^{FL} mice were immunostained for F4/80, Gr-1, B220, CD3 (brown) and counterstained with haematoxylin (blue). Macrophage (F4/80+) and granulocyte (Gr-1+) infiltration into the colonic mucosa was detectable already in 2- and 3-week-old FADD^{IEC-KO} mice, while large inflammatory infiltrates were detected at 10 weeks of age. Increased B- (B220+) and T-cell (CD3+) infiltration was detectable in the mucosa of 10-week-old FADD^{IEC-KO} mice, while small numbers of lymphocytes were observed in 2- and 3-week old animals. Scale bar: 10µm.

To investigate whether the elongation of the colonic crypts in FADD^{IEC-KO} animals (Fig 6a) was due to a hyper-proliferative response of the intestinal epithelium, IHC staining for Ki-67 positive proliferating intestinal epithelial cells was performed (Fig. 9a). The number of proliferating IECs was slightly higher in colonic sections from 2-week old FADD^{IEC-KO} mice compared to FADD^{FL} control mice and further increased in

the colon of 3- and 10-week old mice. In line with the increased amount of proliferative epithelial cells detected by IHC staining, qRT-PCR on isolated colonic IECs showed a significant increase of Cyclin D1 mRNA expression in FADD^{IEC-KO} mice compared to FADD^{FL} control mice (Fig. 9b). Taken together the data suggest that elongation of colonic crypts in FADD^{IEC-KO} animals is due to a hyper-proliferative response of the intestinal epithelium, most likely as a response to the chronic inflammation and tissue damage in FADD^{IEC-KO} animals.

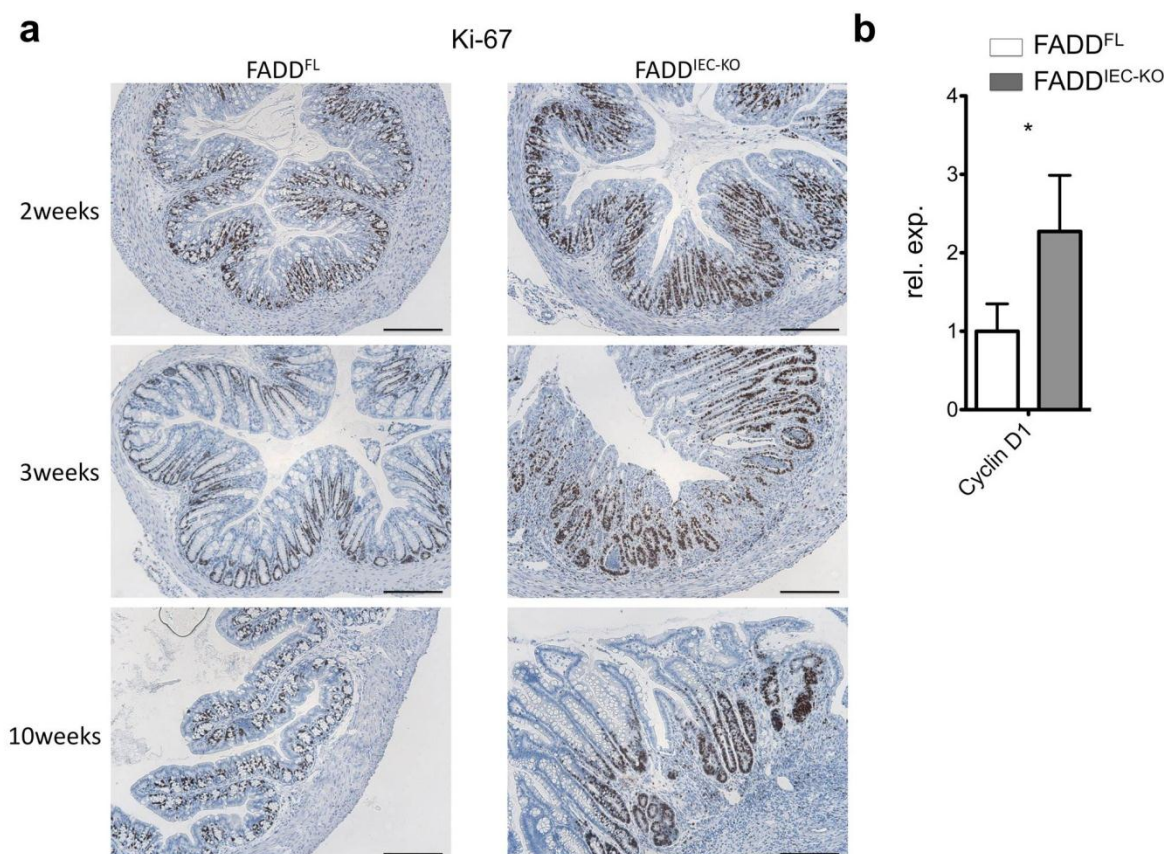


Figure 9 Increased proliferation of epithelial cells in the colon

a. Representative pictures from colonic cross-sections from 2-, 3- and 10-week-old FADD^{IEC-KO} and FADD^{FL} mice immunostained with antibodies recognising Ki-67 (brown) and counterstained with haematoxylin (blue). Elevated epithelial proliferation was detectable in FADD^{IEC-KO} mice already at 2 weeks of age, which was further increased at 3 and 10 weeks. Scale bar: 100µm. **b.** Quantitative RT-PCR analysis on mRNA isolated from primary colonic IECs showed increased Cyclin D1 expression in FADD^{IEC-KO} compared to FADD^{FL} animals (n=4).

3.1.3. FADD^{IEC-KO} mice develop spontaneous chronic enteritis and have reduced numbers of Paneth cells

Since FADD deficiency in the colonic epithelium causes spontaneous chronic colitis, we wanted to analyse whether FADD deficiency also affects the small intestine. Histological sections from the distal small intestine stained with H&E showed increased infiltration of immune cells into the mucosa of FADD^{IEC-KO} mice compared

to FADD^{FL} control mice (Fig. 10a). Increased epithelial death was detectable all over the crypt and villus axis. Additionally, a severely reduced amount of eosin rich cells at the bottom of the small intestinal crypts suggested a reduced amount of Paneth cells in FADD^{IEC-KO} mice. Like in the colon also small intestinal crypts were found to be elongated in FADD^{IEC-KO} animals. These findings were also reflected by a significantly increased Histological Score (HS) for FADD^{IEC-KO} mice compared to FADD^{FL} control mice (Fig. 10b).

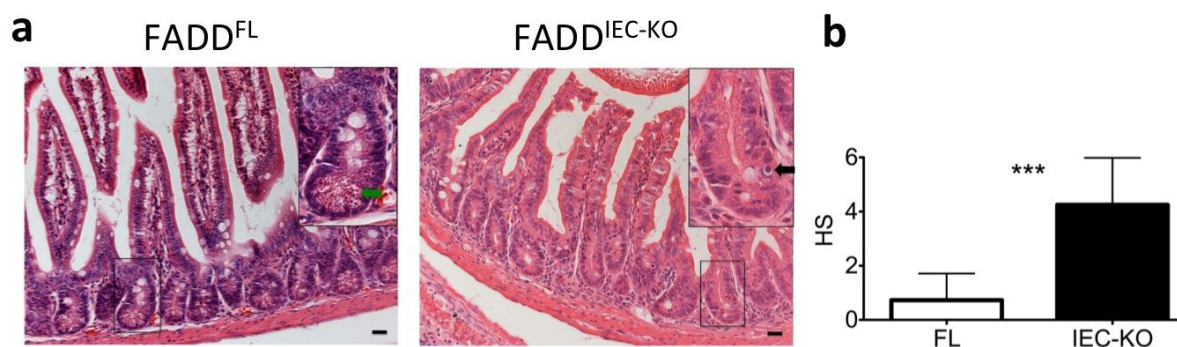


Figure 10 Development of enteritis in FADD^{IEC-KO} mice

a. Representative histological images from the small intestine of 10 week old FADD^{IEC-KO} mice showed increased cell death and a lack of Paneth cells compared to FADD^{FL} mice. Green arrow indicates a Paneth cell, black arrow indicates a dying epithelial cell **b.** Significantly increased histological score (HS) indicated small intestinal inflammation in FADD^{IEC-KO} mice. FADD^{FL} (FL, n=11), FADD^{IEC-KO} (IEC-KO, n=8)

Paneth cells are important producers of antimicrobial peptides and proteins and therefore have an important role in the regulation of the microbiota in the small intestine. Thus we analysed the amount of Paneth cells by IHC staining for the Paneth cell marker Lysozyme. The number of Lysozyme positive Paneth cells at the bottom of the small intestinal crypts was severely reduced in FADD^{IEC-KO} animals (Fig. 11a). To test whether reduced numbers of Paneth cells influenced the amount of antimicrobial peptides and proteins in the small intestine of FADD^{IEC-KO} mice, qRT-PCR analysis of small intestinal RNA extracts was applied. RNA expression of the tested antimicrobial peptides and proteins Defa20, Lyz1, Defa-rs1 and Ang4 was significantly decreased in FADD^{IEC-KO} mice compared to FADD^{FL} control mice (Fig. 11b).

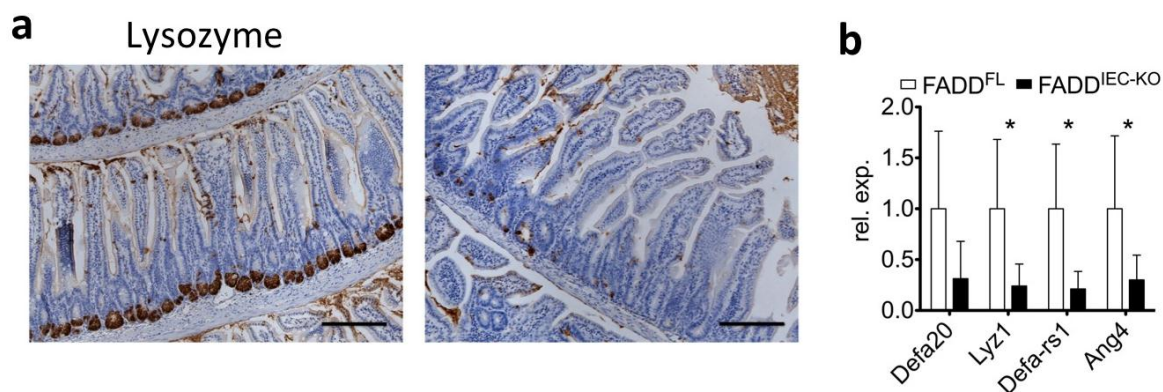


Figure 11 Reduced numbers of Paneth cells in FADD^{IEC-KO} mice

a. Small intestinal sections were immunostained for lysozyme (brown) and counterstained with haematoxylin (blue). Less Paneth cells were detectable in FADD^{IEC-KO} mice. **b.** Expression of the Paneth-cell-specific genes *Defa20*, *Lyz1*, *Defa-rs1* and *Ang4* was significantly decreased in FADD^{IEC-KO} mice compared to FADD^{FL} mice as measured by qRT-PCR in small intestinal mRNA samples. FADD^{FL} (n=6), FADD^{IEC-KO} (n=6)

As reported above, H&E stained small intestinal sections showed increased infiltration of immune cells into the small intestinal mucosa of FADD^{IEC-KO} mice, as well as elongated crypts. IHC staining for Gr1 confirmed increased infiltration of Gr1 positive granulocytes into the small intestinal mucosa of FADD^{IEC-KO} mice compared to FADD^{FL} control mice (Fig. 12a). To test, whether increased proliferation of IECs causes the elongation of small intestinal crypts in FADD^{IEC-KO} animals, IHC staining for Ki-67 was applied. An increased amount of Ki-67 positive proliferating epithelial cells was detected within the crypts of FADD^{IEC-KO} mice compared to FADD^{FL} control mice (Fig. 12b), suggesting that the elongated crypts in FADD^{IEC-KO} mice are indeed due to an increase of epithelial proliferation.

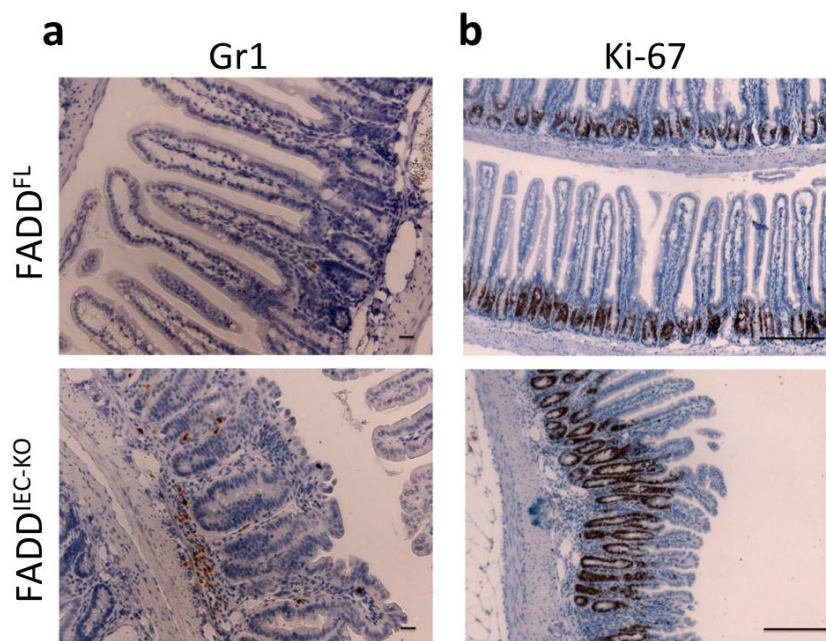


Figure 12 Infiltration of granulocytes into the mucosa and epithelial hyperproliferation in the small intestine of FADD^{IEC-KO} mice

a. and b. Small intestinal sections were immunostained against Gr1 (brown) (a) and Ki-67 (brown) (b) and counterstained with haematoxylin. Increased infiltration of granulocytes into the small intestinal mucosa and increased proliferation in the small intestinal epithelium was found in FADD^{IEC-KO} mice. Scale bars: a=10 μ m and b=100 μ m

3.2. FADD deficient IECs are sensitised towards cell death with necrotic features

3.2.1. FADD^{IEC-KO} mice show increased colonic epithelial cell death

Although FADD is an essential component of extrinsically induced apoptosis, increased intestinal epithelial cell death was found already on H&E stained sections from 2 week old FADD^{IEC-KO} animals, which further increased in older animals leading to areas with a completely eroded epithelium (Fig. 6a). To dissect the nature of the increased epithelial cell death in FADD^{IEC-KO} mice, colonic sections from 3 week old mice were IHC stained against active Caspase 3, a marker of apoptotic cell death. Despite the presence of some active Caspase 3 positive dying or dead cells, many active Caspase 3 negative dying or dead epithelial cells could be detected in FADD^{IEC-KO} animals (Fig. 13a). No active Caspase 3 negative epithelial cell death was found in FADD^{FL} control animals. The increased epithelial cell death of FADD deficient IECs differed from the homeostatic IEC death at the tip of the crypts, because epithelial cells were affected at any position within the crypt and the amount of dying cells was by far higher than the amount of cell death involved in normal

epithelial cell turnover. The incidence of a large amount of active Caspase 3 negative dying cells suggested that FADD deficient IECs die by caspase independent necrotic mechanisms. And indeed, electron microscopy on colon sections from 10 week old $FADD^{IEC-KO}$ mice revealed many dying epithelial cells with signs of necrosis, like low electron density within the cytoplasm, disruption of the plasma membrane, swollen organelles and lack of chromatin condensation (Fig. 13b). Necrosis therefore seemed to be the major form of cell death in FADD-deficient IECs in the colon.

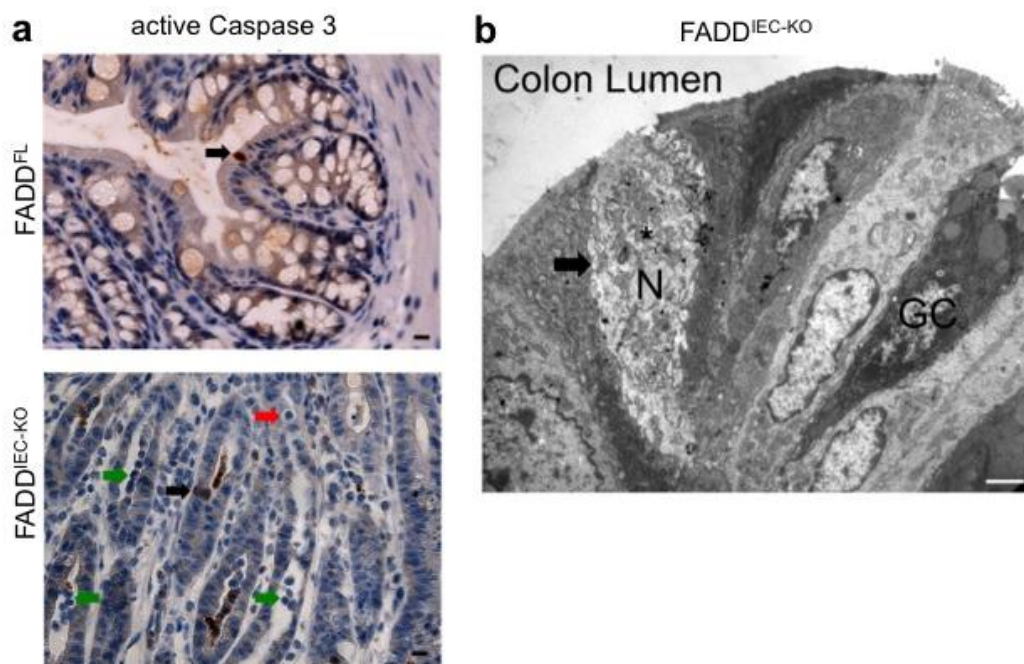


Figure 13 Increased caspase independent cell death with necrotic features in $FADD^{IEC-KO}$ mice
a. Colon sections from $FADD^{IEC-KO}$ and $FADD^{FL}$ mice were immunostained for active caspase 3 (brown) and counterstained with haematoxylin (blue). Black arrow indicates apoptotic, red arrow shows early resident necrotic and green arrows show late detached necrotic epithelial cells. Necrotic cells could only be detected in $FADD^{IEC-KO}$ mice but not in $FADD^{FL}$ control mice. Scale bar: $10\mu m$
b. Small intestinal sections from 10 week old $FADD^{IEC-KO}$ and $FADD^{FL}$ mice were immunostained for active caspase 3 (brown) and counterstained with haematoxylin (blue). Red arrow shows early resident necrotic epithelial cells. Scale bar: $100\mu m$
b. Representative electron microscopy picture of a necrotic epithelial cell (arrow) in the colon of a $FADD^{IEC-KO}$ mouse. GC: goblet cell; N: nucleus. Scale bar: $2\mu m$.

3.2.2. $FADD^{IEC-KO}$ mice show increased epithelial cell death in the small intestine

As described before, FADD deficiency leads to increased cell death of IECs in the colon. In line with these observations on colonic sections, increased cell death was also found on small intestinal sections from $FADD^{IEC-KO}$ mice (Fig. 10a). IHC staining for active Caspase 3 on small intestinal sections of $FADD^{IEC-KO}$ mice also revealed many active Caspase 3 negative dying epithelial cells, which were absent in sections from $FADD^{FL}$ control mice (Fig 14a). Like in the colon, increased cell death was

observed throughout the whole crypt and villus length. Thus, increased and mainly Caspase 3 negative cell death of colonic as well as small intestinal epithelial cells was found to occur from very early on in the pathology of FADD^{IEC-KO} mice.

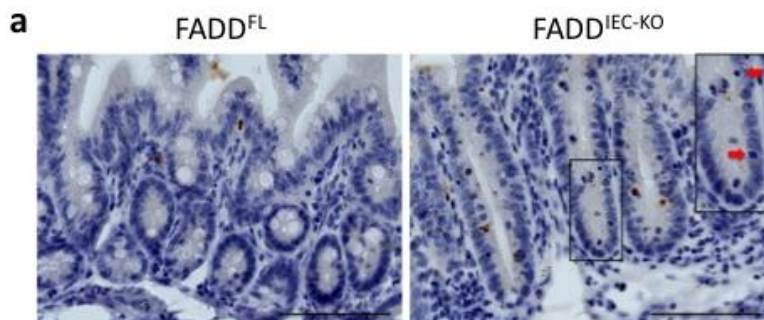


Figure 14 Increased active Caspase 3 negative IEC death in the small intestine of FADD^{IEC-KO} mice

a. Small intestinal sections from FADD^{IEC-KO} mice were stained for active caspase-3 (brown) and counterstained with haematoxylin. Caspase 3 negative dying epithelial cells were detected in FADD^{IEC-KO} mice but not in FADD^{FL} controls. Red arrows in inset mark active Caspase 3 negative dying IECs. Scale bars, 100 μ m

3.3. Development of colitis in FADD^{IEC-KO} mice depends on RIP3-dependent regulated necrosis

3.3.1. IEC death in the colon and development of colitis in FADD^{IEC-KO} mice is RIP3 dependent

Recently an alternative regulated cell death pathway has been described in cells, where activation of the extrinsic apoptotic pathway was blocked by the inhibition of Caspases or by FADD deficiency. This alternative pathway depends on RIP1 and RIP3 and results in necrotic cell death (Cho et al., 2009; He et al., 2009; Zhang et al., 2009). Interestingly RIP3 was upregulated on mRNA- and protein-level in extracts from isolated IECs of FADD^{IEC-KO} mice compared to FADD^{FL} control mice, as shown by qRT-PCR and Western Blot (Fig. 15a and 15b).

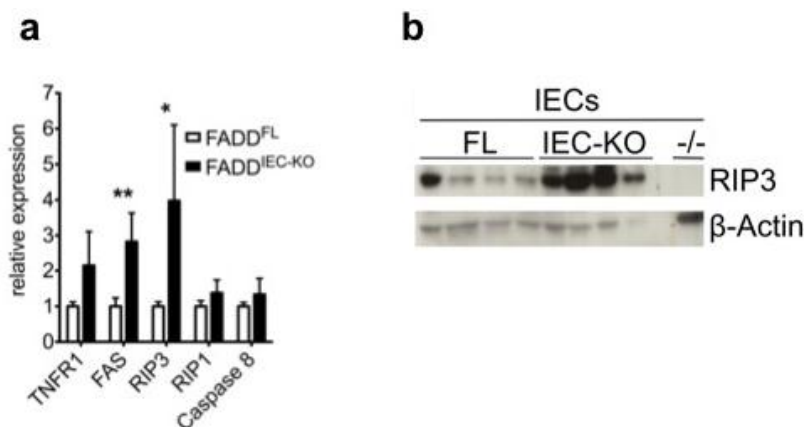


Figure 15 Increased expression of RIP3 in FADD deficient IECs

a. qRT-PCR showed increased expression of *Tnfr1*, *Fas* and *Ripk3* in colonic IECs from FADD^{IEC-KO} mice (n=3) compared to FADD^{FL} (n=4) mice. **b.** Western Blot for RIP3 in colonic IECs from FADD^{IEC-KO} (IEC-KO), FADD^{FL} (FL) and *Ripk3*^{-/-} (-/-) mice. β -actin serves as loading control. Lanes represent IECs from individual mice.

In order to assess the impact of RIP3 dependent cell death in FADD deficient IECs, FADD^{IEC-KO} mice were crossed with *Ripk3*^{-/-} mice (Newton et al., 2004). FADD^{IEC-KO}/*Ripk3*^{-/-} mice, which lack FADD only in IECs and RIP3 in all cells, were born in mendelian ratios and had a healthy appearance. Colon sections from FADD^{IEC-KO}/*Ripk3*^{-/-} mice stained with H&E did not show increased cell death, inflammation or hyperproliferation of the intestinal epithelium (Fig. 16a). The sections from FADD^{IEC-KO}/*Ripk3*^{-/-} mice were indistinguishable from those of FADD^{FL}/*Ripk3*^{-/-} control mice as also confirmed by the HCS (Fig. 16b).

Thus RIP3 is essential for the development of colitis in FADD^{IEC-KO} mice. The prevention of increased necrotic IEC death in RIP3 deficient FADD^{IEC-KO} mice strongly suggests that FADD deficiency sensitises IECs towards RIP3 dependent necrotic cell death in the colon. This RIP3 dependent IEC death seems to be the initial trigger causing colitis in FADD^{IEC-KO} animals.

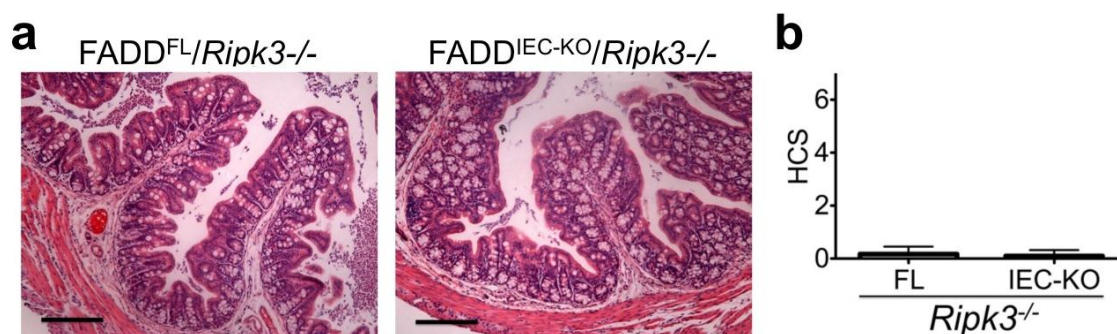


Figure 16 Development of Colitis in FADD^{IEC-KO} mice depends on RIP3

a. Representative histological images showing no differences between FADD^{IEC-KO}/*Ripk3*^{-/-} mice and FADD^{FL}/*Ripk3*^{-/-} mice. **b.** Quantification of HCS in colon sections confirmed that FADD^{IEC-KO}/*Ripk3*^{-/-} mice are comparably healthy like the FADD^{FL}/*Ripk3*^{-/-} control mice. FADD^{IEC-KO}/*Ripk3*^{-/-} (n=5), FADD^{FL}/*Ripk3*^{-/-} (n=3) Scale bar: 100 μ m

3.3.2. Cell death and inflammation in the colon of FADD^{IEC-KO} mice depends on CYLD

CYLD is a deubiquitinase that has an important regulatory role in TNF induced cell death. Its main proposed function during the induction of TNF induced cell death is the deubiquitination of RIP1, which is important for the cytosolic death inducing complex to form (Wang et al., 2008; Wright et al., 2007). CYLD has also been implicated in TNF induced necrotic cell death *in vitro*, when apoptosis is inhibited (Hitomi et al., 2008). Treatment with TNF induced necrotic cell death in primary mouse embryonic Fibroblasts (MEFs) after blocking apoptosis via the caspase inhibitor z-VAD-fmk and simultaneously blocking protein synthesis with the inhibitor Cycloheximide. Primary MEFs expressing a mutated deubiquitinase deficient CYLD Δ 932 Protein were largely protected from this TNF induced necrotic death (Fig. 17a). In order to analyse whether CYLD, and more specifically its deubiquitinating function, is also necessary for the necrosis that occurs in FADD deficient IECs, FADD^{IEC-KO} mice were crossed with mice expressing the CYLD Δ 932 mutant deficient in its deubiquitinating activity only in IECs (CYLD Δ 932^{IEC} mice). In this mouse model a stop cassette was placed behind the wildtype exon 17, both of which were flanked with loxP sites. Additionally a mutated last exon (exon 17) of the *Cyld* gene, containing a nonsense mutation at position 932, was introduced behind the wildtype *Cyld* exon 17 (Fig. 17b). This mutation leads to a premature termination Codon at position 932 of the *Cyld* gene resulting in a truncation of the last 20 amino acids of the protein, which contain subdomain III of the His box that is essential for the catalytic activity of the deubiquitinating domain. In CYLD Δ 932^{FL} mice the stop cassette prevents transcriptional read-through and expression of the mutated exon 17. In CYLD Δ 932^{IEC} mice, the Cre recombinase under the control of the villin promoter excises the loxP-flanked fragment containing the wild type exon 17 and the stop cassette only in IECs, resulting in the replacement of wild type exon 17 with the mutated exon 17 in these cells. After crossing CYLD Δ 932^{FL} mice to the FADD^{IEC-KO} mice, the resulting FADD^{IEC-KO}/CYLD Δ 932^{IEC} mice expressed the catalytically inactive truncated CYLD Δ 932 protein in IECs while at the same time lacking FADD in IECs, as shown by Southern Blot and Western Blot on isolated IECs (Fig. 17c and 17d).

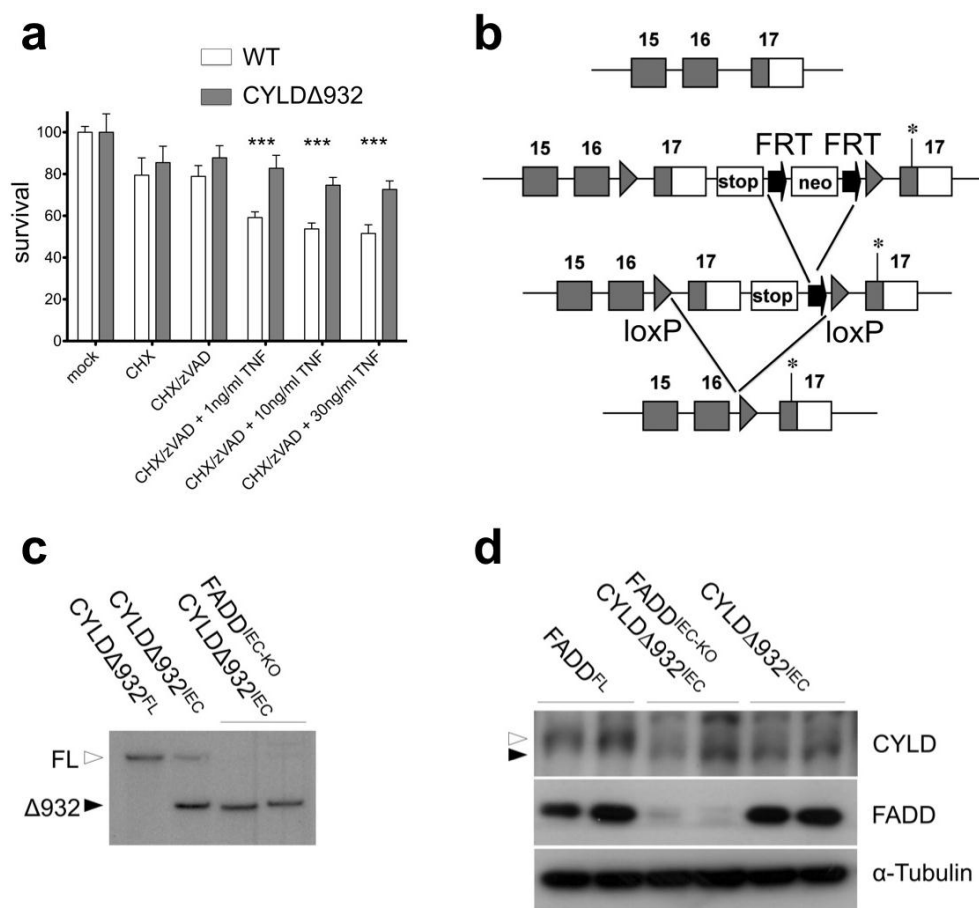


Figure 17 CYLD Δ 932 protects from TNF induced necrotic cell death and generation of FADD^{IEC-KO}/CYLD Δ 932^{IEC} mice

a. The catalytically inactive CYLD Δ 932 protects from TNF induced necroptosis in MEFs after pretreatment with cycloheximide and z-VAD (mean values of triplicates \pm SD shown). **b.** A stop cassette was inserted behind Exon 17 of CYLD and both Exon 17 and the stop cassette were flanked with LoxP sites. A mutated Exon 17 was inserted behind the LoxP flanked region. Upon Cre mediated recombination the wildtype Exon 17 was excised and catalytically inactive CYLD containing the mutated Exon 17 got expressed (for details see text). **c.** Efficient recombination of the mutated CYLD locus was detected by Southern Blot on DNA isolated from IECs of FADD^{IEC-KO}/CYLD Δ 932^{IEC} mice. DNA from IECs of CYLD Δ 932^{IEC} and CYLD Δ 932^{FL} mice served as controls. White arrowhead indicates the floxed allele, black arrowhead indicates the mutated allele **d.** Efficient deletion of FADD and efficient expression of mutated CYLD on protein level was shown by Western Blot. α -Tubulin served as loading control. White arrowhead indicates the wildtype CYLD protein, black arrowhead indicates the mutated, slightly smaller CYLD Δ 932 protein

FADD^{IEC-KO}/CYLD Δ 932^{IEC} mice were born at mendelian ratios and endoscopic analysis (Fig 18a) as well as H&E stained colonic sections (Fig. 18b) revealed that 10 week old FADD^{IEC-KO}/CYLD Δ 932^{IEC} mice did not show increased cell death nor did they develop colitis and were therefore indistinguishable from FADD^{FL}/CYLD Δ 932^{FL} control mice. Although the exact molecular mechanism by which CYLD regulates necrosis *in vivo* is not known, these observations suggest that the deubiquitinating activity of CYLD is important for RIP3-dependent necrotic cell death to occur in FADD deficient colonic IECs. Beyond that, prevention of necrotic IEC death by

inhibition of CYLD specifically in IECs proves, that an IEC intrinsic mechanism causes the development of colitis in $FADD^{IEC-KO}$ mice.

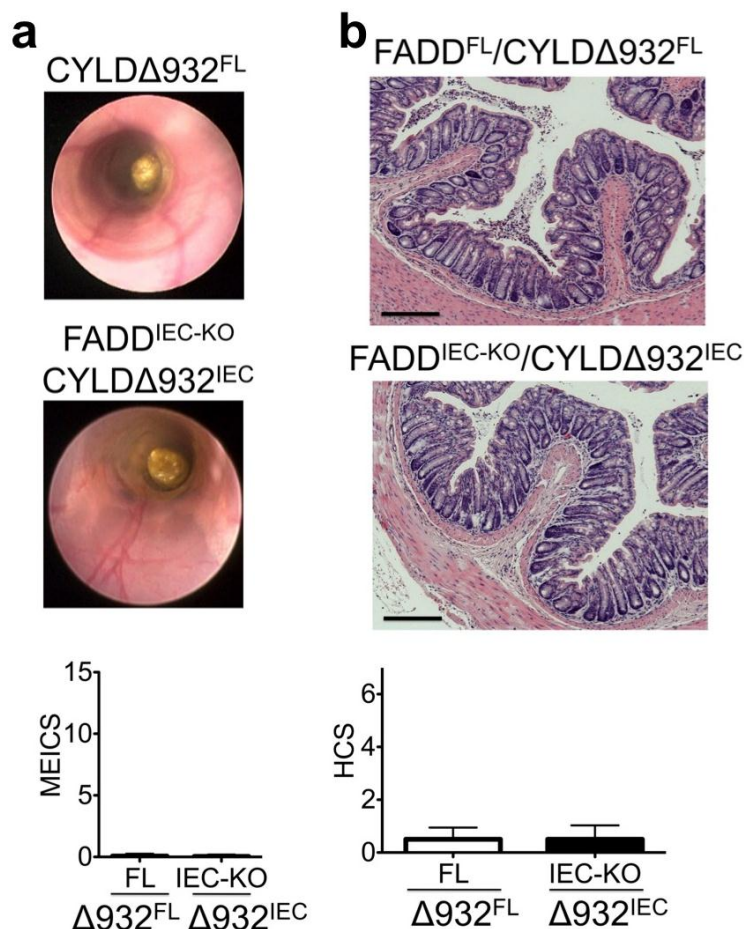


Figure 18 Cell death and colitis development in $FADD^{IEC-KO}$ mice depends on the deubiquitinating activity of CYLD

a. Representative endoscopic images and quantification of MEICS in colons from $FADD^{IEC-KO}/CYLD\Delta932^{IEC}$ and $FADD^{FL}/CYLD\Delta932^{FL}$ mice did not show significant differences. $FADD^{IEC-KO}/CYLD\Delta932^{IEC}$ (n=11), $FADD^{FL}/CYLD\Delta932^{FL}$ (n=7) **b.** No inflammation or increased cell death can be detected on representative histological images and by quantification of HCS in colon sections from 10 week old $FADD^{IEC-KO}/CYLD\Delta932^{IEC}$ and $FADD^{FL}/CYLD\Delta932^{FL}$ mice. $FADD^{IEC-KO}/CYLD\Delta932^{IEC}$ (n=10), $FADD^{FL}/CYLD\Delta932^{FL}$ (n=6)

3.3.3. Cell death and inflammation in the colon of $FADD^{IEC-KO}$ mice depends partially on TNF

TNF has been shown to induce necrotic cell death in FADD deficient T-cells (Holler et al., 2000). To investigate whether necrosis of FADD deficient IECs in the colon is induced by TNF, $FADD^{IEC-KO}$ mice were crossed to TNF deficient mice (Pasparakis et al., 1996) resulting in mice deficient for FADD in IECs while lacking TNF in the whole organism ($FADD^{IEC-KO}/Tnf^{-/-}$ mice). $FADD^{IEC-KO}/Tnf^{-/-}$ mice developed significantly less severe colitis compared to $FADD^{IEC-KO}$ mice as shown by endoscopic analysis and the corresponding MEICS score (Fig. 19a). However, $FADD^{IEC-KO}/Tnf^{-/-}$ mice still

developed significantly more colitis than FADD^{FL}/*Tnf*^{-/-} control mice (Fig. 19a). H&E stained colonic sections of FADD^{IEC-KO}/*Tnf*^{-/-} animals showed less overall infiltration of immune cells into the mucosa compared to FADD^{IEC-KO} mice, but some patchy areas with increased cell death and local infiltration of immune cells were detectable (Fig. 19b). Therefore, it seems that TNF either has a role in the induction of colonic IEC necrosis or in the development of inflammation in FADD^{IEC-KO} mice or maybe in both. On the other hand TNF can neither be the only inducer of death in FADD deficient colonic IECs nor the only cytokine responsible for the induction of the inflammatory response in the colon of FADD^{IEC-KO} mice.

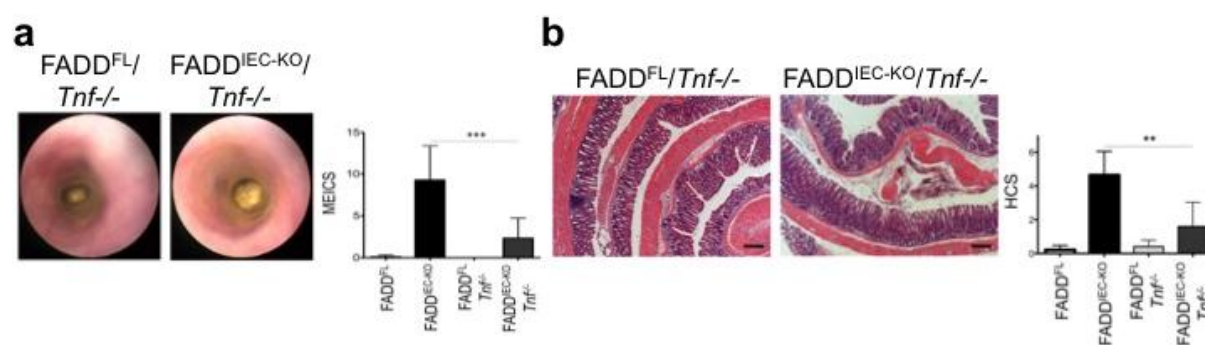


Figure 19 TNF deficiency ameliorates colitis development in FADD^{IEC-KO} mice

a. The catalytically inactive CYLDA932 protects from TNF induced necroptosis in MEFs after pretreatment with cycloheximide and z-VAD (mean values of triplicates ± SD shown). **b.** Representative endoscopic images and quantification of MEICS showing only mild inflammation in colons from FADD^{IEC-KO}/*Tnf*^{-/-} mice compared to FADD^{FL}/*Tnf*^{-/-} mice. FADD^{IEC-KO}/*Tnf*^{-/-} (n=6), FADD^{FL}/*Tnf*^{-/-} (n=6) **c.** Representative histological images and quantification of HCS in colon sections from FADD^{IEC-KO}/*Tnf*^{-/-} mice show only patchy areas with mild infiltration of immune cells compared to healthy FADD^{FL}/*Tnf*^{-/-} control mice. FADD^{IEC-KO}/*Tnf*^{-/-} (n=5), FADD^{FL}/*Tnf*^{-/-} (n=6)

3.4. Role of the microbiota in the development of colitis in FADD^{IEC-KO} mice

3.4.1. The development of chronic colitis but not the increased cell death in FADD^{IEC-KO} mice depends on MyD88

Recognition of bacteria by Toll-like Receptors (TLR) on immune cells can lead to the induction of intestinal inflammation. MyD88 is an essential adaptor molecule for most TLRs and signalling through MyD88 has been shown to be important for the development of inflammatory responses in several mouse models of colitis (Nenci et al., 2007; Rakoff-Nahoum et al., 2006). To analyse the role of MyD88 dependent signalling in the development of colitis in FADD^{IEC-KO} mice, MyD88 deficient mice (*Myd88*^{-/-} mice) were crossed to FADD^{IEC-KO} mice (FADD^{IEC-KO}/*Myd88*^{-/-} mice). The colon of FADD^{IEC-KO}/*Myd88*^{-/-} mice had an overall healthy appearance comparable to FADD^{FL}/*Myd88*^{-/-} control mice, as shown by endoscopy (Fig. 20a). H&E stained

sections from $FADD^{IEC-KO}/Myd88^{-/-}$ mice did not show increased infiltration of immune cells into the colonic mucosa compared to $FADD^{FL}/Myd88^{-/-}$ control mice (Fig. 20b). However, IHC staining for active Caspase 3 revealed a slight increase of Caspase 3 negative and positive epithelial cell death in the colon of $FADD^{IEC-KO}/Myd88^{-/-}$ mice compared to $FADD^{FL}/Myd88^{-/-}$ control mice (Fig. 20c), although the level of cell death was by far lower than in $FADD^{IEC-KO}$ animals. Therefore, MyD88 dependent signalling seems to be important for the initiation of the immune response in the colon, but not for the initial cell death of colonic IECs. Furthermore, colonic inflammation in $FADD^{IEC-KO}$ mice seems to substantially increase the amount of dying epithelial cells.

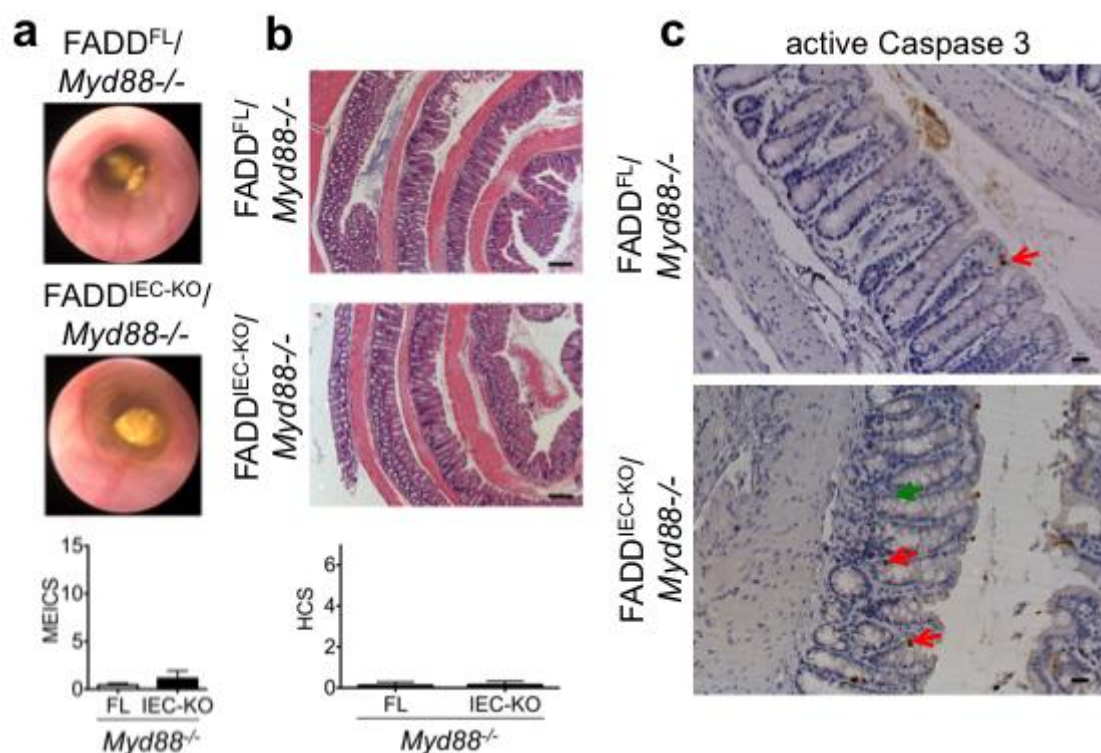


Figure 20 MyD88 is necessary for colitis development but not for increased cell death in $FADD^{IEC-KO}$ mice

a. Representative endoscopic images and quantification of MEICS in colons from $FADD^{IEC-KO}/Myd88^{-/-}$ and $FADD^{FL}/Myd88^{-/-}$ mice showed no differences between the two genotypes. $FADD^{IEC-KO}/Myd88^{-/-}$ (n=9), $FADD^{FL}/Myd88^{-/-}$ (n=6) **b.** No inflammation was detectable on representative histological images from $FADD^{IEC-KO}/Myd88^{-/-}$ mice and quantification of HCS on colon sections from $FADD^{IEC-KO}/Myd88^{-/-}$ and $FADD^{FL}/Myd88^{-/-}$ mice did not show any differences between the two genotypes. $FADD^{FL}/Myd88^{-/-}$ (n=6), $FADD^{IEC-KO}/Myd88^{-/-}$ (n=9) **c.** Colon sections from $FADD^{IEC-KO}/Myd88^{-/-}$ and $FADD^{FL}/Myd88^{-/-}$ mice were immunostained for active caspase 3 (brown) and counterstained with haematoxylin (blue). Slightly increased epithelial cell death was detectable in $FADD^{IEC-KO}/Myd88^{-/-}$ mice. Red arrow shows apoptotic and green arrow indicates early resident necrotic epithelial cells. Necrotic epithelial cells were found in $FADD^{IEC-KO}/Myd88^{-/-}$ mice, but not in $FADD^{FL}/Myd88^{-/-}$ control mice. Scale bar: 10 μ m

3.4.2. The development of chronic colitis in FADD^{IEC-KO} mice depends on microbiota induced signals

To further dissect, whether the effect of MyD88 dependent signalling on the development of inflammation in the colon of FADD^{IEC-KO} mice depends on bacterial induced signalling, FADD^{IEC-KO} mice were treated with a cocktail of broad-spectrum antibiotics to diminish the bacterial burden in the intestinal tract. Antibiotics were administered in the drinking water, starting from the second day after birth. Endoscopic analysis and H&E staining of colon sections from FADD^{IEC-KO} mice treated with antibiotics revealed a significantly diminished pathology compared to untreated FADD^{IEC-KO} mice, as shown by endoscopy and H&E stained histological sections (Fig. 21a and 21b). Inflammation in the colon of FADD^{IEC-KO} mice treated with antibiotics was strongly attenuated, which suggests that indeed bacterial induced MyD88 dependent signalling, most likely in mucosal immune cells, is important for the development of colitis.

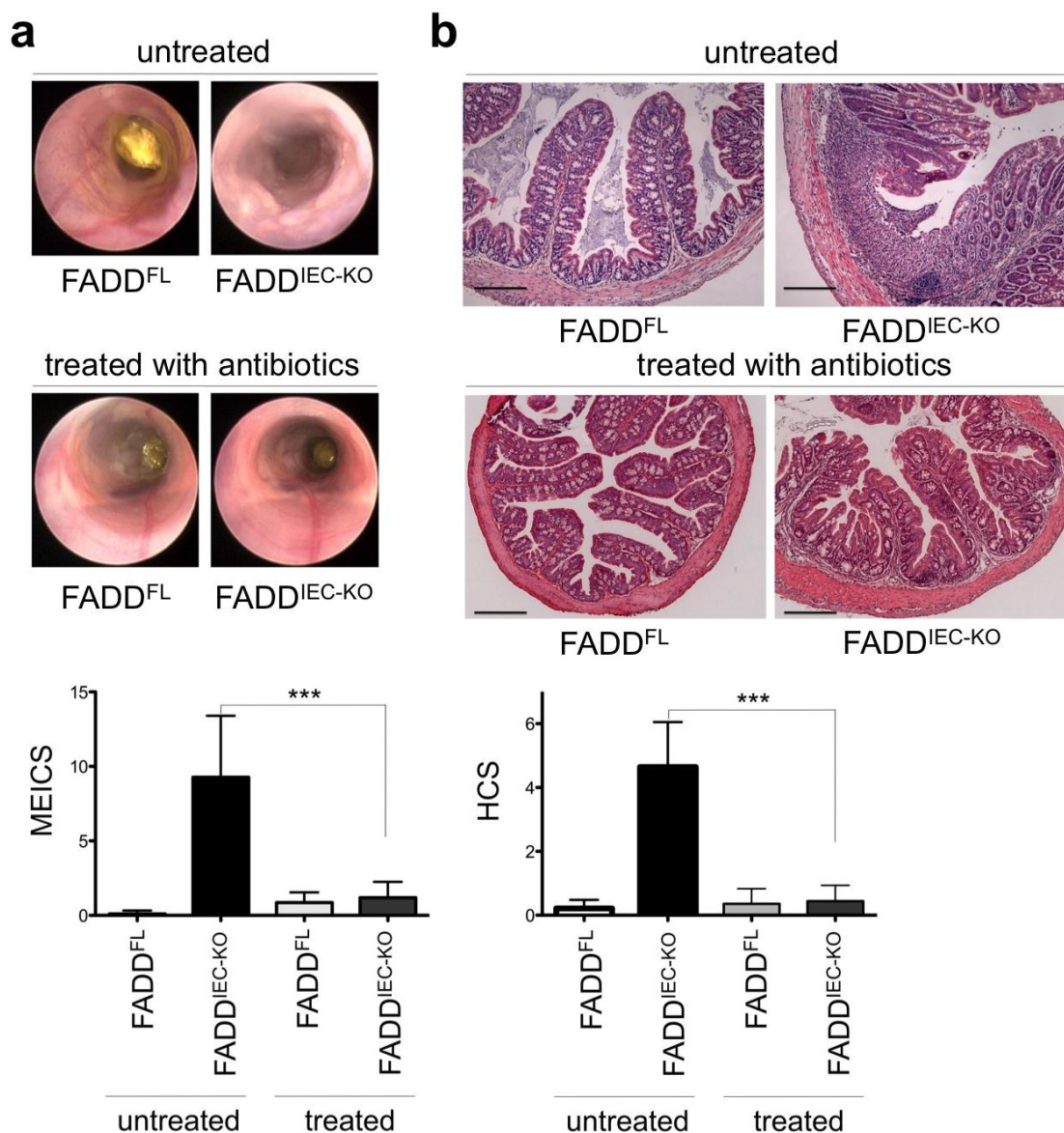


Figure 21 Antibiotic treatment reduces the development of colitis in FADD^{IEC-KO} mice

a. Representative endoscopic images and quantification of MEICS showed that antibiotic treated FADD^{IEC-KO} mice have a largely normal colonic mucosa compared to the severe colitis seen in untreated animals. FADD^{FL} untreated, n=37; FADD^{IEC-KO} untreated, n=31; FADD^{FL} treated, n=7; FADD^{IEC-KO} treated, n=8.

b. Representative histological images of colonic sections showed that antibiotic treated FADD^{IEC-KO} mice have a largely normal colonic mucosa comparable to FADD^{FL} control mice, in contrast to the severe inflammatory lesions seen in the colon of untreated FADD^{IEC-KO} animals. Scale bar, 100 μ m. Quantification by HCS indicated significantly increased inflammation and tissue damage in untreated FADD^{IEC-KO} mice compared to treated FADD^{IEC-KO} mice. FADD^{FL} untreated, n=7; FADD^{IEC-KO} untreated, n=7; FADD^{FL} treated, n=7; FADD^{IEC-KO} treated, n=8. Scale bar, 100 μ m.

In order to unambiguously assess the role of bacterial induced signalling in the colon of FADD^{IEC-KO} mice, germfree FADD^{IEC-KO} mice were generated in the gnotobiotic facility at the University of Ulm. Endoscopic analysis revealed no differences between germ-free FADD^{FL} control mice and germ-free FADD^{IEC-KO} mice (Fig. 22a). H&E stained sections from germfree FADD^{IEC-KO} mice did not show increased infiltration of immune cells into the colonic mucosa compared to germfree FADD^{FL} control mice

(Fig. 22b). On the other hand, when germfree $FADD^{IEC-KO}$ mice were conventionalized either by cohousing the females with conventionally housed $FADD^{FL}$ or $FADD^{IEC-KO}/CYLDA932^{IEC}$ mice or by exposing the male mice to the bedding from conventionally housed mice, the former germfree $FADD^{IEC-KO}$ mice developed severe colitis within less than a week, as shown by endoscopic analysis and H&E staining (Fig. 22c and 22d). 4 out of 12 mice died within one week of conventionalization, probably due to massive intestinal inflammation. qRT-PCR revealed significantly increased expression of the proinflammatory cytokines TNF and IL-1 β in the colon of conventionalized $FADD^{IEC-KO}$ animals compared to germfree $FADD^{IEC-KO}$ animals (Fig. 22e). Taken together, development of the inflammatory response in the colon of $FADD^{IEC-KO}$ mice depends on bacterial induced and MyD88 dependent signalling. Since colitis can be induced by cohousing germ-free $FADD^{IEC-KO}$ mice with healthy control mice harbouring a normal composition of the microbiota, the development of colitis in $FADD^{IEC-KO}$ mice cannot be caused by a possibly altered composition of the microbiota in $FADD^{IEC-KO}$ mice.

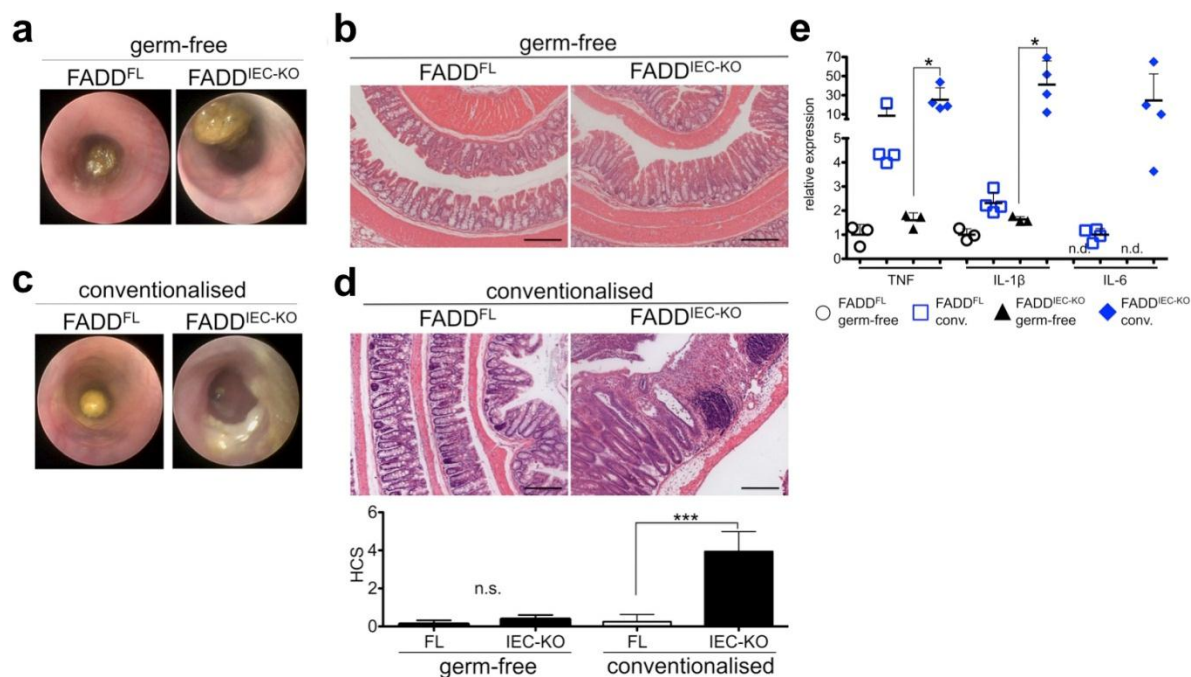


Figure 22 Colitis development in $FADD^{IEC-KO}$ mice depends on the presence of the microbiota
a. Representative endoscopic colon images of germ-free $FADD^{IEC-KO}$ mice do not show signs of inflammation. **b.** Representative histological images showed no signs of inflammation in germfree $FADD^{IEC-KO}$ mice. Scale bars, 100 μ m **c.** Representative endoscopic colon images of conventionalised $FADD^{IEC-KO}$ mice show signs of severe colitis, like diarrhoea, ulceration and reduced translucency of the bowel wall. **d.** Representative histological images showed severe infiltration of immune cells into the mucosa and epithelial erosion in conventionalised $FADD^{IEC-KO}$ mice. Quantification by H&S revealed significantly increased inflammation and tissue damage in conventionalized $FADD^{IEC-KO}$ mice compared to conventionalized $FADD^{FL}$ control mice. $FADD^{FL}$ (n=5), germ-free $FADD^{IEC-KO}$ (n=7), conventionalized $FADD^{FL}$ (n=8) and conventionalized $FADD^{IEC-KO}$ (n=8) Scale bars, 100 μ m **e.** qRT-PCR analysis demonstrated increased expression of TNF, IL-1 β and IL-6 in colons of conventionalized (conv.) $FADD^{IEC-KO}$ mice compared to germfree $FADD^{IEC-KO}$ mice. n.d.= not detectable.

3.5. Development of enteritis in FADD^{IEC-KO} mice depends on RIP3-dependent regulated necrosis

3.5.1. IEC death in the small intestine and development of enteritis in FADD^{IEC-KO} mice is RIP3 dependent

As shown above, IEC necrosis in the colon and development of spontaneous chronic colitis was prevented in RIP3 deficient FADD^{IEC-KO} mice. Thus we wanted to analyse whether RIP3 is also essential for the small intestinal epithelial cell death and the development of enteritis. Neither increased cell death, nor infiltration of immune cells, Paneth cell loss or elongation of the crypts could be found on H&E stained sections from FADD^{IEC-KO}/*Ripk3*^{-/-} mice (Fig. 23a). The healthy appearance of the small intestinal sections from FADD^{IEC-KO}/*Ripk3*^{-/-} mice was also reflected in the low HS, which was comparable to the HS of the FADD^{FL}/*Ripk3*^{-/-} control mice (Fig. 23a). IHC staining against Lysozyme on small intestinal sections revealed a normal amount and distribution of Paneth cells in FADD^{IEC-KO}/*Ripk3*^{-/-} mice comparable to FADD^{FL}/*Ripk3*^{-/-} control mice (Fig. 23b). Accordingly, also the mRNA-level of the antimicrobial peptides Defa20, Lyz1, Defa-rs1 and Ang4 was not significantly altered in FADD^{IEC-KO}/*Ripk3*^{-/-} mice compared to FADD^{FL}/*Ripk3*^{-/-} control mice, as shown by qRT-PCR (Fig. 23c). IHC staining against active Caspase 3 revealed no increased cell death in the small intestine of FADD^{IEC-KO}/*Ripk3*^{-/-} animals (Fig. 23d).

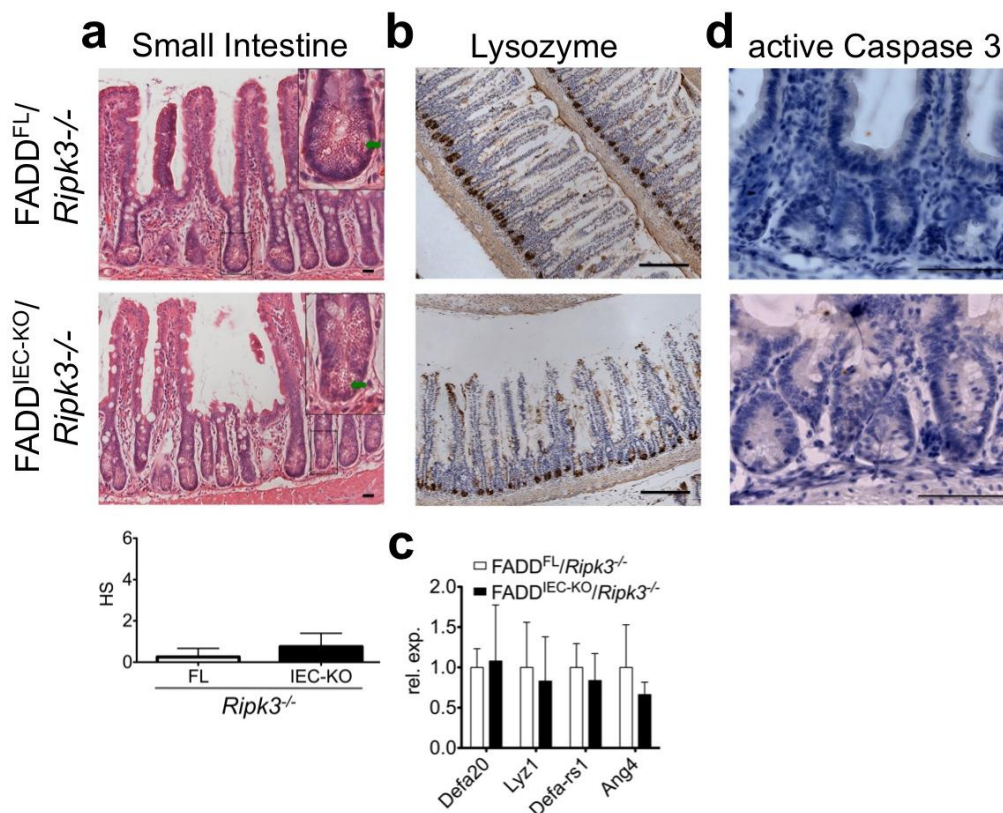


Figure 23 Development of enteritis, increased cell death and Paneth cell loss in FADD^{IEC-KO} mice is RIP3 dependent

a. Representative histological images of FADD^{IEC-KO}/*Ripk3*^{-/-} mice showed a completely healthy small intestine. The histological score (HS) of FADD^{IEC-KO}/*Ripk3*^{-/-} and FADD^{FL}/*Ripk3*^{-/-} mice was comparable. FADD^{FL}/*Ripk3*^{-/-} (n=6), FADD^{IEC-KO}/*Ripk3*^{-/-} (n=4); Scale bars: 10 μ m **b.** Small intestinal sections were immunostained for lysozyme (brown) and counterstained with haematoxylin (blue). FADD^{IEC-KO}/*Ripk3*^{-/-} mice had normal numbers of Paneth cells. Scale bars: 100 μ m **c.** Expression levels of the Paneth-cell-specific genes *Defa20*, *Lyz1*, *Defa-rs1* and *Ang4* measured by qRT-PCR were not significantly altered in the small intestine of FADD^{IEC-KO}/*Ripk3*^{-/-} mice. FADD^{FL}/*Ripk3*^{-/-} (n=3), FADD^{IEC-KO}/*Ripk3*^{-/-} (n=5) **d.** No increased cell death was detectable in small intestinal sections of FADD^{IEC-KO}/*Ripk3*^{-/-} mice immunostained for active Caspase 3 (brown), counterstained with haematoxylin (blue). Scale bars: 100 μ m

IHC staining against Gr1 showed no increased infiltration of granulocytes into the small intestinal mucosa of FADD^{IEC-KO}/*Ripk3*^{-/-} animals compared to FADD^{FL}/*Ripk3*^{-/-} control mice (Fig 24a). The small intestinal epithelium of FADD^{IEC-KO}/*Ripk3*^{-/-} mice also didn't show any signs of hyper proliferation, as demonstrated by IHC staining against Ki-67 (Fig. 24b).

Therefore, like in the colon, RIP3 dependent regulated necrosis of FADD deficient small intestinal IECs seems to cause the spontaneous development of chronic enteritis and Paneth cell loss.

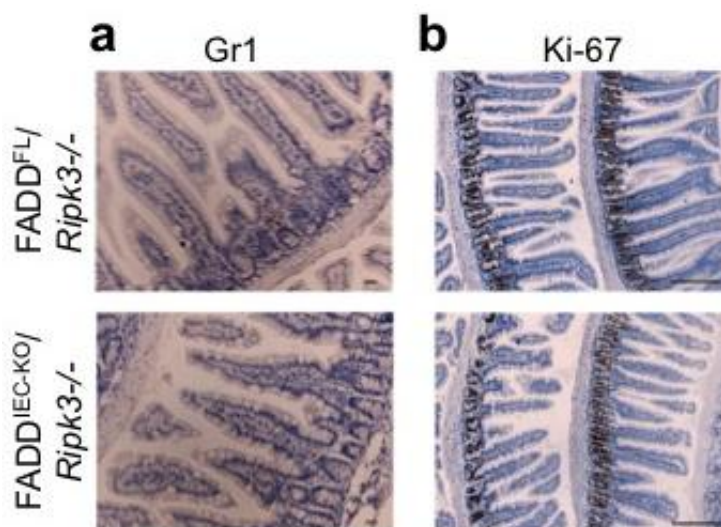


Figure 24 No increased infiltration of granulocytes or hyperproliferation in FADD^{IEC-KO} mice
a. and b. Small intestinal sections were immunostained against Gr1 (brown) (a) and Ki-67 (brown) (b) and counterstained with haematoxylin. Neither increased infiltration of granulocytes into the small intestinal mucosa or increased proliferation in the small intestinal epithelium was found in FADD^{IEC-KO}/Ripk3^{-/-} mice. Scale bars: e=10 μ m and f=100 μ m

3.5.2. Cell death and inflammation in the small intestine of FADD^{IEC-KO} mice is independent of CYLD

To investigate whether the inhibition of the deubiquitinating activity in the CYLD Δ 932 mutant is also able to abrogate the small intestinal cell death, the Paneth cell loss and the inflammatory response in FADD^{IEC-KO} mice, small intestinal sections from FADD^{IEC-KO}/CYLD Δ 932^{IEC} mice were analysed. Surprisingly H&E stained sections from 10 week old FADD^{IEC-KO}/CYLD Δ 932^{IEC} mice still showed increased cell death, Paneth cell loss, an increased infiltration of immune cells into the mucosa and elongated crypts compared to FADD^{FL}/CYLD Δ 932^{FL} control mice (Fig. 25a). The loss of Paneth Cells in FADD^{IEC-KO}/CYLD Δ 932^{IEC} animals was confirmed by IHC staining for Lysozyme on small intestinal sections (Fig. 25b). Dying small intestinal epithelial cells in FADD^{IEC-KO}/CYLD Δ 932^{IEC} mice were largely, but not exclusively, active Caspase 3 negative, as shown by IHC staining (Fig. 25c).

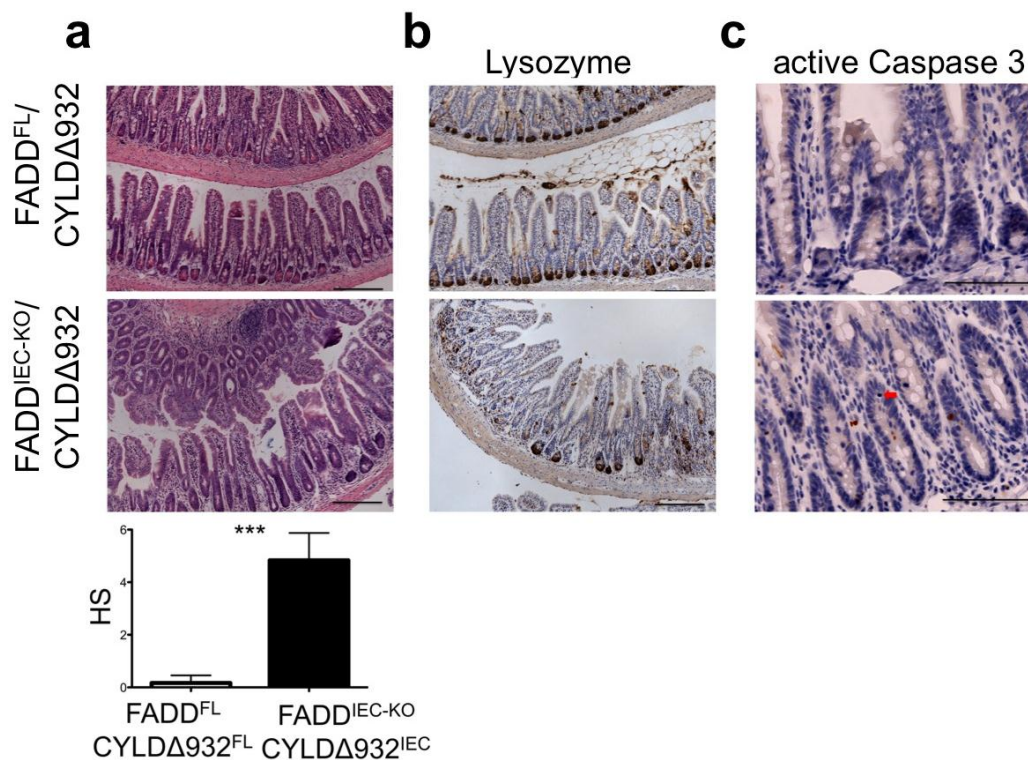


Figure 25 Increased cell death. Paneth cell loss and development of enteritis in FADD^{IEC-KO} mice is independent of the deubiquitinating activity of CYLD

a. Representative histological images of small intestinal sections from 10 week old FADD^{IEC-KO}/CYLDA932^{IEC} mice showed decreased numbers of Paneth cells, dying enterocytes and increased infiltration of immune cells into the mucosa. The histological score (HS) of FADD^{IEC-KO}/CYLDA932^{IEC} mice was significantly increased compared to FADD^{FL}/CYLDA932^{FL} mice. FADD^{FL}/CYLDA932^{FL} (n=3), FADD^{IEC-KO}/CYLDA932^{IEC} (n=3); Scale bars: 100µm **b.** Small intestinal sections were immunostained for lysozyme (brown) and counterstained with haematoxylin (blue). FADD^{IEC-KO}/CYLDA932^{IEC} mice had decreased numbers of Paneth cells. Scale bars: 100µm **c.** Increased cell death was detected in small intestinal sections of FADD^{IEC-KO}/CYLDA932^{IEC} mice immunostained for active Caspase 3 (brown) and counterstained with haematoxylin (blue) compared to FADD^{FL}/CYLDA932^{FL} mice. Red arrow indicates active caspase-3 negative dying enterocyte. Scale bars: 100µm

Increased infiltration of Gr1 positive granulocytes into the small intestinal mucosa of FADD^{IEC-KO}/CYLDA932^{IEC} mice compared to FADD^{FL}/CYLDA932^{FL} control mice, shown by IHC staining for Gr1, further highlighted the inflammatory response in those mice (Fig. 26a). Increased numbers of proliferating Ki-67 positive IECs confirmed the hyper proliferative response of the epithelium as detected by IHC staining for Ki-67 (Fig. 26b).

The deubiquitinating activity of CYLD therefore doesn't seem to be involved in the regulation of necrosis in FADD deficient small intestinal IECs and the subsequent development of enteritis.

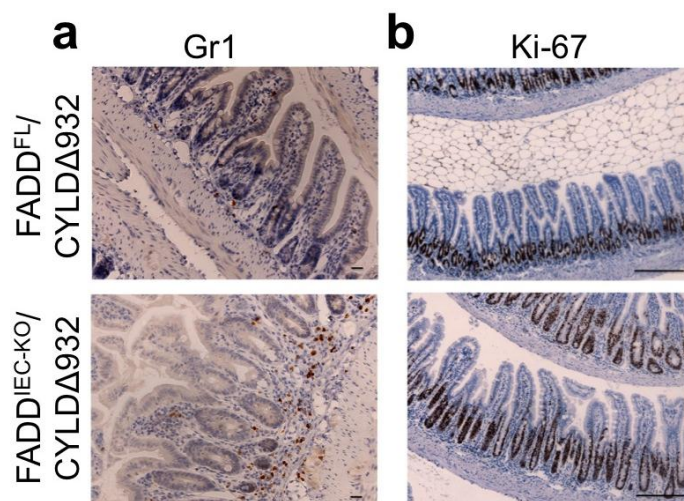


Figure 26 Infiltration of granulocytes into the mucosa and epithelial hyperproliferation in $FADD^{IEC-KO}$ mice is independent of the deubiquitinating activity of CYLD

a. and b. Small intestinal sections were immunostained against Gr1 (brown) (e) and Ki-67 (brown) (e) and counterstained with haematoxylin. Increased infiltration of granulocytes into the small intestinal mucosa and increased proliferation in the small intestinal epithelium was found in $FADD^{IEC-KO}/CYLDA932^{IEC}$ mice. Scale bars: d=10 μ m and e=100 μ m

3.5.3. Cell death and inflammation in the small intestine of $FADD^{IEC-KO}$ mice is not induced by TNF

TNF induced signalling is at least partially involved in the induction of colitis in $FADD^{IEC-KO}$ mice. To check whether TNF induced signalling also plays a role in the necrosis of FADD deficient small intestinal IECs and the development of enteritis, small intestinal sections from TNF deficient $FADD^{IEC-KO}$ mice were analysed. H&E stained small intestinal sections from 10 week old TNF deficient $FADD^{IEC-KO}$ mice showed increased cell death and Paneth cell loss as well as massive infiltration of immune cells into the mucosa and elongated crypts compared to $FADD^{FL}/Tnf^{-/-}$ control mice (Fig. 27a). IHC staining for Lysozyme confirmed the pronounced Paneth cell loss (Fig. 27b) and also in the $FADD^{IEC-KO}/Tnf^{-/-}$ mice the epithelial cell death was mainly active Caspase 3 negative, as shown by IHC staining (Fig. 27c).

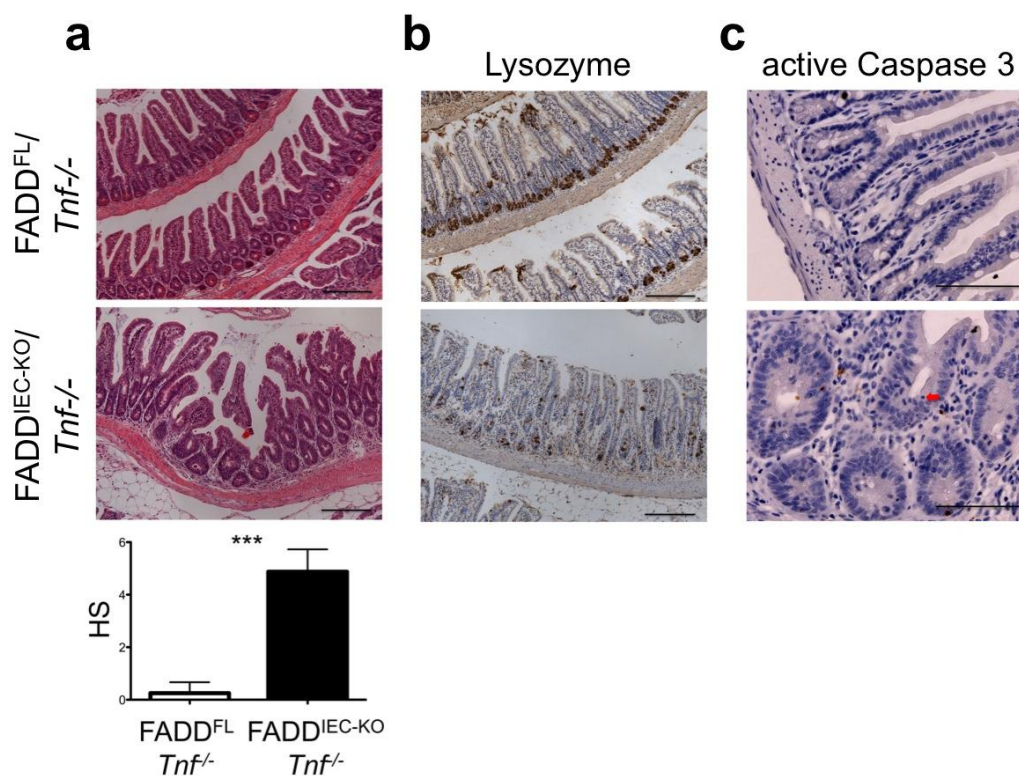


Figure 27 Increased cell death. Paneth cell loss and development of enteritis in FADD^{IEC-KO} mice is independent of TNF

a. Representative histological images of small intestinal sections from 10 week old FADD^{IEC-KO}/Tnf^{-/-} mice showed decreased numbers of Paneth cells, dying enterocytes and an increased infiltration of immune cells into the mucosa. The histological score (HS) of FADD^{IEC-KO}/Tnf^{-/-} mice was significantly increased compared to FADD^{FL}/Tnf^{-/-} mice. FADD^{FL}/Tnf^{-/-} (n=6), FADD^{IEC-KO}/Tnf^{-/-} (n=4); Scale bars: 100µm **b.** Small intestinal sections were immunostained for lysozyme (brown) and counterstained with haematoxylin (blue). FADD^{IEC-KO}/Tnf^{-/-} mice had decreased numbers of Paneth cells. Scale bars: 100µm **c.** Increased cell death was detected in small intestinal sections of FADD^{IEC-KO}/Tnf^{-/-} mice immunostained for active Caspase 3 (brown) and counterstained with haematoxylin (blue) compared to FADD^{FL}/Tnf^{-/-} mice. Red arrow indicates active caspase-3 negative dying enterocytes. Scale bars: 100µm

A massive infiltration of granulocytes into the mucosa of FADD^{IEC-KO}/Tnf^{-/-} mice was detected on IHC stained sections for Gr1 (Fig. 28a), indicating that the inflammatory response in FADD^{IEC-KO} mice might even be elevated in the absence of TNF. IHC staining for Ki-67 revealed a strongly increased amount of proliferating epithelial cells in FADD^{IEC-KO}/Tnf^{-/-} mice compared to FADD^{FL}/Tnf^{-/-} control mice (Fig. 28b).

Thus TNF, while contributing to colitis development in FADD^{IEC-KO} mice, does not have a role in the development of enteritis in FADD^{IEC-KO} mice. Taken together, the results obtained for the contribution of CYLD and TNF to the pathology of FADD^{IEC-KO} mice indicate, that the mechanisms inducing and regulating RIP3 dependent necrosis of FADD deficient IECs differ between colonic and small intestinal IECs.

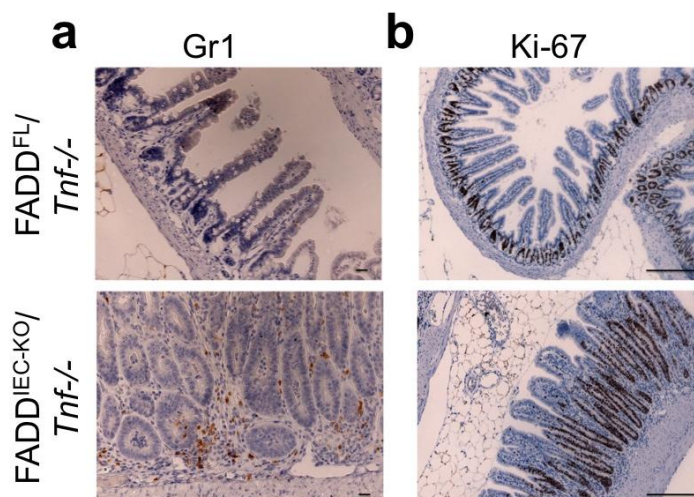


Figure 28 Infiltration of granulocytes into the mucosa and epithelial hyperproliferation in FADD^{IEC-KO} mice is independent of TNF

a. and b. Small intestinal sections were immunostained against Gr1 (brown) (d) and Ki-67 (brown) (e) and counterstained with haematoxylin. Increased infiltration of granulocytes into the small intestinal mucosa and increased proliferation in the small intestinal epithelium was found in FADD^{IEC-KO}/Tnf^{-/-} mice. Scale bars: d=10µm and e=100µm

3.6. Role of the microbiota in the development of enteritis in FADD^{IEC-KO} mice

3.6.1. Enteritis and IEC death in FADD^{IEC-KO} mice does not depend on MyD88

As shown before, bacterial induced and MyD88 dependent signalling is necessary for the development of colitis in FADD^{IEC-KO} mice. To investigate whether MyD88 dependent signalling is also involved in the development of enteritis in FADD^{IEC-KO} mice, small intestinal sections of FADD^{IEC-KO}/Myd88^{-/-} mice were stained with H&E. Analysis of those sections revealed, that neither the increased epithelial cell death, nor Paneth cell loss or inflammation was diminished in the small intestine of FADD^{IEC-KO}/Myd88^{-/-} mice compared to FADD^{FL}/Myd88^{-/-} control mice (Fig. 29a). IHC staining for Lysozyme confirmed decreased numbers of Paneth cells (Fig. 29b). In addition, the increased epithelial cell death in FADD^{IEC-KO}/Myd88^{-/-} mice compared to FADD^{FL}/Myd88^{-/-} control mice was mainly active Caspase 3 negative as shown by IHC staining for active Caspase 3 (Fig. 29c).

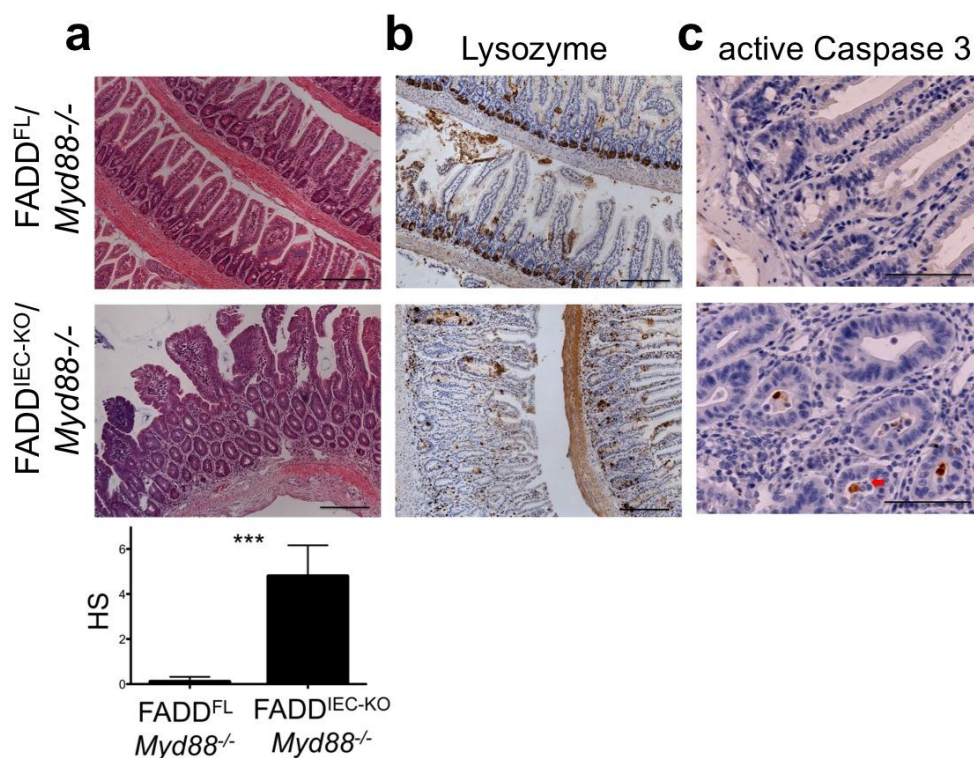


Figure 29 Increased cell death, Paneth cell loss and development of enteritis in FADD^{IEC-KO} mice is independent of MyD88

a. Representative histological images of small intestinal sections from 10 week old FADD^{IEC-KO}/Myd88^{-/-} mice showed decreased numbers of Paneth cells, dying enterocytes and increased infiltration of immune cells into the mucosa. The histological score (HS) of FADD^{IEC-KO}/Myd88^{-/-} mice was significantly increased compared to FADD^{FL}/Myd88^{-/-} mice. FADD^{FL}/Myd88^{-/-} (n=5), FADD^{IEC-KO}/Myd88^{-/-} (n=7); Scale bars: 100µm **b.** Small intestinal sections were immunostained for lysozyme (brown) and counterstained with haematoxylin (blue). FADD^{IEC-KO}/Myd88^{-/-} mice had decreased numbers of Paneth cells. Scale bars: 100µm **c.** Increased cell death was detected in small intestinal sections of FADD^{IEC-KO}/Myd88^{-/-} mice immunostained for active Caspase 3 (brown) and counterstained with haematoxylin (blue) compared to FADD^{FL}/Myd88^{-/-} mice. Red arrow indicates active caspase-3 negative dying enterocytes. Scale bars: 100µm

IHC staining for Gr1 demonstrated strongly increased numbers of Granulocytes (Fig. 30a) in FADD^{IEC-KO}/Myd88^{-/-} mice compared to FADD^{FL}/Myd88^{-/-} control mice, further verifying the inflammatory response in the small intestine of FADD^{IEC-KO}/Myd88^{-/-} mice. An increased amount of proliferating cells leading to a hyper proliferative response of the small intestinal epithelium in FADD^{IEC-KO}/Myd88^{-/-} animals compared to FADD^{FL}/Myd88^{-/-} control animals was revealed by IHC staining for Ki-67 (Fig. 30b). MyD88 dependent signalling thus is neither essential for the initial cell death in FADD deficient small intestinal IECs, nor for the development of small intestinal inflammation in FADD^{IEC-KO} mice.

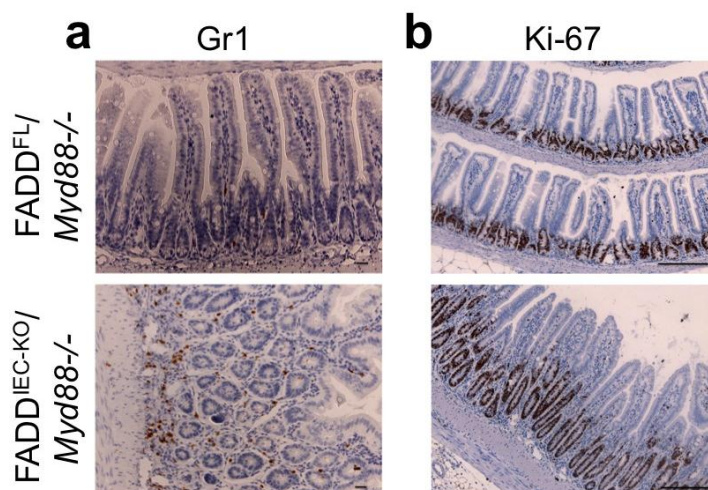


Figure 30 Infiltration of granulocytes into the mucosa and epithelial hyperproliferation in FADD^{IEC-KO} mice is independent of MyD88

a. and b. Small intestinal sections were immunostained against Gr1 (brown) (d) and Ki-67 (brown) (e) and counterstained with haematoxylin. Increased infiltration of granulocytes into the small intestinal mucosa and increased proliferation in the small intestinal epithelium was found in FADD^{IEC-KO}/Myd88^{-/-} mice. Scale bars: d=10 μ m and e=100 μ m

3.6.2. Enteritis and IEC death does not depend on the presence of the microbiota

In line with the finding that MyD88 dependent signalling did not affect enteritis development in the FADD^{IEC-KO} mice, also H&E stained small intestinal sections from germfree FADD^{IEC-KO} mice showed increased epithelial cell death compared to germfree FADD^{FL} control mice, Paneth cell loss and some inflammatory infiltrates in the small intestine of germfree FADD^{IEC-KO} mice (Fig. 31a). Paneth cell loss was visualized by IHC staining for Lysozyme (Fig. 31b). Loss of Paneth cells coincided with decreased expression of antimicrobial peptides in the small intestine of germfree FADD^{IEC-KO} animals compared to germfree FADD^{FL} control animals as revealed by qRT-PCR analysis on small intestinal mRNA (Fig. 31c). The increased epithelial cell death in germfree FADD^{IEC-KO} mice was confirmed to be mainly active Caspase 3 negative by IHC staining for active Caspase 3 (Fig. 31d).

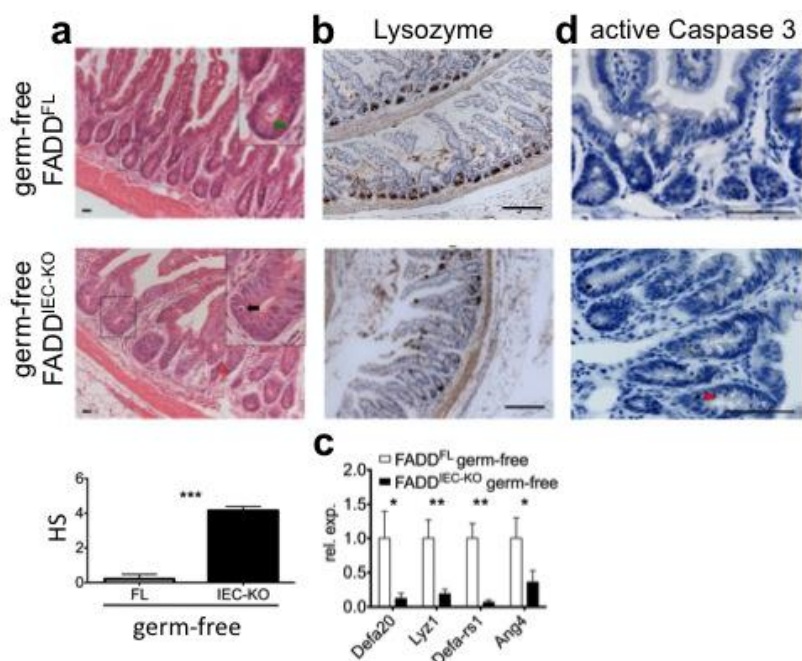


Figure 31 Increased cell death. Paneth cell loss and development of enteritis in FADD^{IEC-KO} mice is independent of microbiota

a. Representative histological images of small intestinal sections from 10 week old germ-free FADD^{IEC-KO} mice showed decreased numbers of Paneth cells, dying enterocytes and increased infiltration of immune cells into the mucosa. The histological score (HS) of germ-free FADD^{IEC-KO} mice was significantly increased, compared to germ-free FADD^{FL} mice. germ-free FADD^{FL} (n=5), germ-free FADD^{IEC-KO} (n=7); The green arrow indicates a Paneth cell, the black arrow shows a dying epithelial cell. Scale bars: 100µm **b.** Small intestinal sections were immunostained for lysozyme (brown) and counterstained with haematoxylin (blue). Germ-free FADD^{IEC-KO} mice had decreased numbers of Paneth cells. Scale bars: 100µm **c.** Expression of the Paneth-cell-specific genes *Defa20*, *Lyz1*, *Defa-rs1* and *Ang4* was significantly decreased in germ-free FADD^{IEC-KO} mice compared to germ-free FADD^{FL} mice as measured by qRT-PCR in small intestinal mRNA samples. germ-free FADD^{FL} (n=3), germ-free FADD^{IEC-KO} (n=3) **d.** Increased cell death was detected in small intestinal sections of germ-free FADD^{IEC-KO} mice immunostained for active Caspase 3 (brown) and counterstained with haematoxylin (blue) compared to germ-free FADD^{FL} mice. Red arrow indicates active caspase-3 negative dying enterocytes. Scale bars: 100µm

The inflammatory response was confirmed by detection of some granulocyte infiltrates in the small intestinal mucosa of germfree FADD^{IEC-KO} mice by IHC staining for Gr1 (Fig. 32a). IHC staining for Ki-67 revealed some hyper proliferative areas in the small intestinal epithelium of germfree FADD^{IEC-KO} mice with increased numbers of proliferative epithelial cells (Fig. 32b). Taken together, unlike in the colon of FADD^{IEC-KO} mice where bacterial induced signalling is necessary for the development of an inflammatory response, bacterial induced and MyD88 mediated signalling is not important for the initiation of inflammation in the small intestine of FADD^{IEC-KO} mice. This implies that not only the initial cell death is differentially regulated in the colon compared to the small intestine of FADD^{IEC-KO} animals, but apparently also different mechanisms are involved in the development of inflammation in both parts of the intestine of FADD^{IEC-KO} mice.

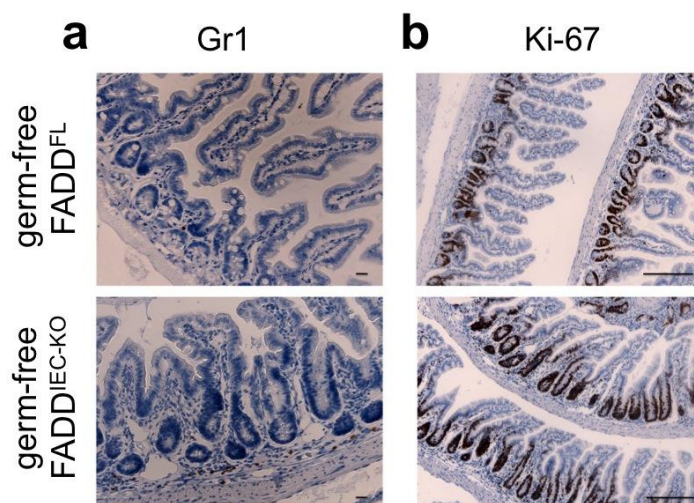


Figure 32 Infiltration of granulocytes into the mucosa and epithelial hyperproliferation in $FADD^{IEC-KO}$ mice is independent of the microbiota

a. and b. Small intestinal sections were immunostained against Gr1 (brown) (e) and Ki-67 (brown) (f) and counterstained with haematoxylin. Increased infiltration of granulocytes into the small intestinal mucosa and increased proliferation in the small intestinal epithelium was found in germ-free $FADD^{IEC-KO}$ mice. Scale bars: d=10 μ m and e=100 μ m

3.6.3. Differential regulation of cell death and inflammation in the colon and small intestine of $FADD^{IEC-KO}$ mice

The results described above strongly suggest a different regulation for the initial cell death and the subsequent inflammation occurring in $FADD^{IEC-KO}$ animals. RIP3 is essential in both, the colon and the small intestine, for necrosis to occur in FADD deficient IECs. However, the initial triggers inducing the cell death probably differ between colon and small intestine of $FADD^{IEC-KO}$ mice. While TNF seems to be at least partially involved in inducing necrosis in the colon of $FADD^{IEC-KO}$ mice, TNF deficiency did not have a beneficial effect in the small intestine of those mice. The regulation of this necrotic pathway also appears to be different between colon and small intestine since the deubiquitinating activity of CYLD only affects the cell death of FADD deficient IECs in the colon but not in the small intestine.

The inflammatory response, but not the epithelial cell death, in the colon depends on the microbiota and MyD88 dependent signalling. Thus, it seems that necrosis of FADD deficient IECs results in an inflammatory response, which is probably triggered by microbiota induced signalling in the mucosal immune cells. Contrary to the colon, neither Myd88 deficiency nor depletion of the microbiota prevented inflammation in the small intestine of $FADD^{IEC-KO}$ animals (Fig. 33a and 33b). The triggers inducing inflammation in the small intestine of $FADD^{IEC-KO}$ animals have not been identified yet.

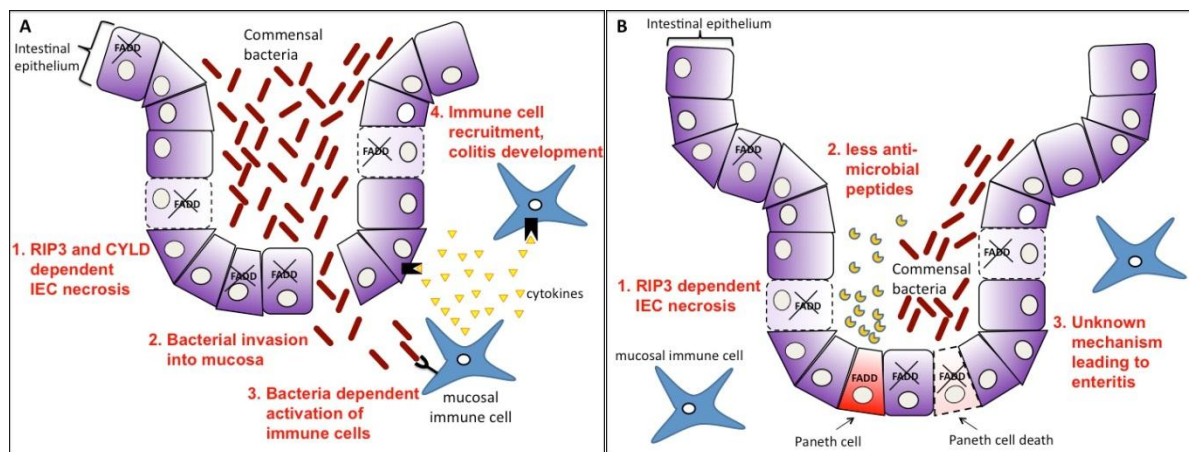


Figure 33 Model for colitis and enteritis development in FADD^{IEC-KO} mice

a. TNF-signalling and other mechanisms induce excessive RIP3 dependent necrosis of FADD deficient colonic IECs, thereby compromising epithelial barrier integrity. Commensal bacteria are able to breach the epithelial barrier and invade into the mucosa. MyD88 dependent sensing of bacteria by mucosal immune cells provokes a proinflammatory response. Secretion of cytokines like TNF accelerates IEC necrosis and stimulates development of chronic colitis.

b. Unknown triggers induce RIP3 dependent IEC necrosis of FADD deficient small intestinal IECs. The reduced amount of Paneth cells leads to decreased levels of antimicrobial peptides in the small intestine. How chronic enteritis develops in FADD^{IEC-KO} mice is currently not understood. For details see text.

4. Discussion

4.1. FADD protects IECs from RIP3 dependent necrosis

The incidence and relevance of regulated necrosis *in vivo* started to unfold only very recently. While it was known since many years that caspase inhibition can lead to DR dependent necroptosis *in vitro* in different cell types (Holler et al., 2000; Vercammen et al., 1998), the first evidence of regulated necrosis to occur *in vivo* was only reported much later in ischemic brain injury (Degterev et al., 2005), an acute pancreatitis model (He et al., 2009), during Vaccinia Virus infection (Cho et al., 2009) and in photoreceptor detachment (Trichonas et al., 2010). Lately, the implications of regulated necrosis during embryonic development have been unravelled. Full body deficiency for Caspase 8 or FADD is embryonically lethal around embryonic day E11.5 (Varfolomeev et al., 1998; Yeh et al., 1998), implying a role for these two molecules during embryonic development. Now it has been shown that the lethality of Caspase 8 deficiency depends on RIP3 (Kaiser et al., 2011; Oberst et al., 2011) and the defects in the embryonic development of FADD deficient mice depend on RIP1 (Zhang et al., 2011). Thus embryonic development depends on the inhibition of RIP3/RIP1 regulated necrosis by Caspase 8 and FADD. These findings confirm that also *in vivo* inhibition of FADD and Caspase 8 dependent apoptosis can lead to increased RIP3 dependent regulated necrosis.

The results presented in this work show for the first time a role for RIP3 dependent regulated necrosis in epithelial cells *in vivo* and highlight the impact of FADD mediated inhibition of regulated necrosis for intestinal homeostasis. Meanwhile, another report has shown that Caspase 8 deficiency in the intestinal epithelium also sensitises IECs towards regulated necrosis (Gunther et al., 2011), further supporting the results obtained with the FADD^{IEC-KO} mice. Furthermore, it was shown that FADD also inhibits RIP3 dependent regulated necrosis in the epidermis of the skin (Bonnet et al., 2011) and in T cells (Lu et al., 2011), while another report suggested that Caspase 8 deficiency can lead to regulated necrosis of Hepatocytes (Liedtke et al., 2011).

In summary, FADD and Caspase 8 have a central role in the regulation of cell survival and cell death *in vivo* by on one hand inducing apoptosis and on the other hand by the inhibition of RIP3 dependent regulated necrosis in several tissues. It

seems that, at least in the intestinal epithelium, regulation of cell death and survival by inhibition of RIP3 mediated regulated necrosis is the dominant role of FADD.

4.2. Regulation of RIP3 dependent IEC necrosis by FADD and CYLD

FADD deficient IECs are sensitised towards RIP3 dependent IEC necrosis (Fig. 16 and 23), showing that in IECs signalling to FADD inhibits RIP3 dependent necrosis. How FADD inhibits RIP3 dependent necrosis is not completely understood, but most likely it acts through the recruitment of Caspase 8 and c-FLIP_L, which together have been shown to regulate RIP3 dependent necrosis (Oberst et al., 2011; Pop et al., 2011). Although binding of c-FLIP_L to procaspase 8 inhibits cleavage-mediated maturation of procaspase 8 to active Caspase 8, the procaspase 8 - c-FLIP_L interaction has been shown to inhibit regulated necrosis by proaspase 8 mediated RIP1 and RIP3 cleavage (Cho et al., 2009; Feng et al., 2007; Feoktistova et al., 2011; Oberst et al., 2011; Rebe et al., 2007). Thus, Caspase 8 dependent apoptosis and regulated necrosis can be inhibited simultaneously by c-FLIP dependent mechanisms.

Whether FADD has any direct function in the inhibition of RIP3 dependent necrosis, independent of procaspase 8 mediated cleavage of RIP1 and RIP3, is not known. FADD has been shown to be constantly associated, directly or indirectly, to RIP3 in MEFs and Jurkat T-cells (Cho et al., 2009; O'Donnell et al., 2011). Therefore, FADD might be able to regulate RIP3 dependent necrosis by directly acting on RIP3 and its positioning within the complex.

Since FADD has been reported to be necessary for FAS and TRAIL induced necroptosis (Holler et al., 2000; Zhang et al., 1998), it is likely that FADD even has a pronecrotic function in some signalling pathways, most likely by recruiting RIP1. And indeed, overexpression and artificial dimerization of FADD has been shown to induce RIP1 dependent necrosis even when caspase activation is not inhibited (Kawahara et al., 1998; Vanden Berghe et al., 2004). Thus, FADD might directly influence, and under certain conditions even promote, regulated necrosis. However, IECs obviously do not depend on FADD for the induction of RIP3 dependent regulated necrosis.

The deubiquitination deficient CYLD Δ 932 mutant prevented sensitisation of FADD deficient IECs to necrosis in the colon (Fig. 18). The deubiquitinating activity of CYLD

is therefore necessary for RIP3 dependent necrosis to occur in FADD deficient colonic IECs. Deubiquitination of RIP1 by CYLD is an important precondition in order to signal towards cell death (Wang et al., 2008; Wright et al., 2007). CYLD deficiency prevents RIP1 recruitment to FADD in response to stimulation with TNF (O'Donnell et al., 2011), preventing the formation of the death inducing complex IIb consisting of RIP1, FADD, RIP3, Caspase 8 and c-FLIP. Furthermore, without the deubiquitinating activity of CYLD ubiquitinated RIP1 remains bound to NEMO, thereby supporting prosurvival signalling (O'Donnell et al., 2011). Thus, the deubiquitination deficient CYLD Δ 932 mutant might prevent RIP3 dependent necrosis of FADD deficient IECs by preventing deubiquitination of RIP1 and subsequent formation of the death inducing protein complex.

Recently, TNF was also shown to induce Caspase 8 mediated cleavage of CYLD. Inhibition of this cleavage, in cells expressing CYLD mutants lacking the cleavage site, switches cell death towards necroptosis even in the presence of Caspase 8 and c-FLIP_L (O'Donnell et al., 2011). Thus, CYLD might not only promote formation of the death inducing complex IIb by deubiquitination of RIP1, but also have an active role in specifically supporting necroptosis. The exact mechanism, how CYLD might specifically support necroptosis is not known.

The deubiquitination deficient CYLD Δ 932 mutant prevented cell death in the colon but not in the small intestine (Fig. 18 and Fig. 25), raising the question why necrosis of colonic IECs is depending on the deubiquitinating activity of CYLD, while necrosis in the small intestinal IECs is not. So far, CYLD has only been implicated in the regulation of apoptotic and necroptotic cell death induced by TNF (O'Donnell et al., 2011; Wang et al., 2008). Whether CYLD is also regulating RIP3 dependent necrosis induced by other stimuli is currently not known. TNF mediated necroptosis apparently only plays a role in the induction of IEC necrosis in the colon (Fig. 19), but not in the small intestine (Fig. 27). Thus, small intestinal IEC necrosis might involve signalling pathways that are not regulated by CYLD.

4.3. Possible inducers of RIP3 dependent regulated necrosis in IECs and their physiological impact

FADD deficient IECs are sensitised towards cell death, because FADD dependent mechanisms can no longer inhibit RIP3 dependent necrosis. The sensitisation of

FADD deficient IECs to regulated necrosis seems to be independent of infections and the corresponding immune responses, since in the small intestine FADD deficient IECs even die under germfree conditions. Thus, triggers that can potentially induce RIP3 dependent IEC necrosis have to be constantly abundant, independent of acute immune responses to infections. Identification of these triggers is important in order to be able to understand the role of FADD dependent regulation of cell death in IECs.

However, while in the FADD^{IEC-KO} mouse model RIP3 dependent necrosis is generally not inhibited by FADD dependent mechanisms, RIP3 dependent necrosis is normally inhibited under physiological conditions in healthy IECs. Thus, while triggers of IEC necrosis in FADD^{IEC-KO} mice have the potential to constantly induce death, under physiological conditions they will only be able to induce cell death in certain situations, which still need to be identified.

In the following chapters potential triggers of RIP3 dependent necrosis in the FADD^{IEC-KO} mouse model as well as their possible physiological impact will be discussed.

4.3.1. Extrinsically induced necroptosis in IECs

Signalling to FADD can be extrinsically induced by cytokines. TNF, FASL and TRAIL have been shown to be able to induce apoptosis as well as necroptosis (Holler et al., 2000). TNF deficiency ameliorates development of colitis but not small intestinal enteritis in FADD^{IEC-KO} mice (Fig. 19 and Fig. 27), suggesting different triggers to be responsible for inducing regulated necrosis in FADD deficient colonic and small intestinal IECs. TNF is thus a likely inducer of necroptosis in FADD deficient colonic IECs, although it remains to be shown, whether TNF directly affects the induction of IEC necroptosis or whether it rather has a proinflammatory role in the colon of FADD^{IEC-KO} mice.

TNF induces signalling to cell death through TNFR1. Beside of TNF also Lymphotoxin- α (LT α) has been shown to be able to activate TNFR1 signalling. LT α is therefore another potential inducer of RIP3 dependent IEC necrosis in FADD^{IEC-KO} mice. In mice, deficient for FADD in the skin epidermis (FADD^{E-KO} mice), keratinocytes are sensitised to RIP3 dependent necrosis, leading to severe skin inflammation and premature death at about one week after birth. Like in FADD^{IEC-KO}

mice, TNF deficiency ameliorated the disease, but did not completely prevent it. Interestingly, while TNF deficient FADD^{E-KO} mice developed skin lesions at two to three weeks after birth, TNFR1 deficient FADD^{E-KO} mice developed skin lesions even later. This discrepancy between TNF and TNFR1 signalling in FADD^{E-KO} mice suggests that LT α is involved in the induction of regulated necrosis in the skin epithelium (Bonnet et al., 2011). Further investigation will have to reveal the impact of LT α dependent signalling on regulated necrosis in epithelial cells, in IECs as well as in Keratinocytes.

Also FASL and TRAIL are potential inducers of IEC necroptosis in FADD^{IEC-KO} mice. However, at least *in vitro* FASL and TRAIL induced necroptosis has been shown to depend on FADD (Holler et al., 2000; Zhang et al., 1998). Therefore, while both FAS and TRAIL might be possible inducers of IEC necrosis in conditions where caspase activation is blocked by other means than by FADD deletion, it is rather unlikely that they induce necroptosis in FADD deficient IECs.

Under physiological conditions, TNF induced necroptosis of IECs might be employed as a control mechanism for the removal of cells that are blocked in their ability to undergo caspase dependent apoptosis. Vaccinia Virus, for example, possesses a viral caspase inhibitor (Spi2) which blocks DR induced apoptosis but sensitises several cell types towards necroptosis (Li and Beg, 2000). Infection with Vaccinia Virus leads to increased TNF expression and RIP3 dependent regulated necrosis (Cho et al., 2009). It has not been reported, whether infection with Vaccinia Virus also induces regulated necrosis of IECs. However, in this infection model TNF induced signalling kills virally infected cells despite the inhibition of caspase dependent apoptosis. The TNF induced removal of virally infected cells by RIP3 dependent necrosis might also occur in the intestinal epithelium.

Caspase inhibition seemed to be a necessary precondition for regulated necrosis to occur until recently, when RIP3 dependent cell death was found to be involved in two sepsis models, even when caspase signalling was not blocked. In a TNF-injection induced sepsis model, as well as in the model of cecal puncture and ligation, RIP3 deficiency was shown to protect from cell death and the lethal aftermath (Duprez et al., 2011). It was suggested that IEC necrosis only plays a minor role in the TNF-injection induced sepsis model. In the cecal puncture and ligation model puncture of the cecum leads to a bacterial infection followed by sepsis. The role of IEC necrosis

in the cecal puncture and ligation model was not analysed and the triggers that might cause RIP3 dependent necrosis in this model remain unknown. Nevertheless, this study indicates, that RIP3 dependent necrosis might also be induced independent of caspase inhibition, implying that RIP3 dependent necrosis might also have an important role in physiological conditions where caspase activation is not blocked. However, if such situations occur in the intestinal epithelium and under which physiological conditions such induction of RIP3 dependent necrosis might play a role, has to be evaluated.

4.3.2. Cell autonomous immunity as a possible trigger for RIP3 dependent IEC necrosis

Viral and bacterial PAMPs can activate the PRRs TLR3 and TLR4, which have been shown to be able to signal to protein complexes that can induce cell death depending on FADD (Kaiser and Offermann, 2005; Ma et al., 2005). The same triggers have also been shown to be able to induce RIP3 dependent regulated necrosis, when caspase activation is inhibited (He et al., 2011). Thus, FADD deficient IECs might be sensitised to bacteria or virus induced regulated necrosis through TLR3 or TLR4. At least in the colon, bacterial induced signalling depending on MyD88 protects from the development of inflammation (Fig. 20-22). However, TLR3/TLR4 induced signalling towards cell death depends on the adaptor protein TRIF, but not on the adaptor protein MyD88 (Kaiser and Offermann, 2005) and the initial induction of cell death in the colon of FADD^{IEC-KO} mice seems to be independent of MyD88 (Fig. 20c). Therefore, the results obtained so far, do not suggest that signalling induced by the normal microbiota is involved in the induction of RIP3 dependent IEC necrosis in FADD^{IEC-KO} animals. However, whether TRIF mediated signalling in IECs, induced by sampling of PAMPs through TLR3 or TLR4, has any impact on IEC necrosis in FADD^{IEC-KO} mice, remains to be shown.

Although IEC necrosis in FADD^{IEC-KO} animals is apparently not directly affected by the normal microbiota, infections with certain viral or even bacterial pathogens might still be able to induce RIP3 dependent IEC necrosis in the host animal. As discussed above, pathogens containing caspase inhibitors could be potential inducers of RIP3 dependent IEC necrosis. Cytomegalovirus, for example, contains a caspase inhibitor and an inhibitor of regulated necrosis. Inactivation of this necrosis inhibitor directly induces RIP3 dependent necrosis (Upton et al., 2010). Infections with

Cytomegalovirus have been reported to cause colitis and ileitis in immunocompetent patients in some rather rare cases (Tejedor Cerdena et al., 2011) and to exacerbate inflammation in immunodeficient patients (Goodgame, 1993). However, these patients have not been tested for the potential involvement of RIP3 dependent regulated necrosis of IECs.

Up to date, no bacterial infection has been described to cause RIP3 dependent regulated necrosis. Thus, it remains to be shown, whether bacterial IEC infections can be cleared by inducing RIP3 dependent regulated necrosis and which pathogens might be involved.

4.3.3. Paneth cell death and endoplasmic reticulum (ER) stress

While it seems that RIP3 dependent necrosis of FADD deficient IECs at least partially depends on TNF, so far no trigger was identified to be involved in small intestinal IEC necrosis. Small intestinal IECs necrosis was detected all over the crypt and villus area, suggesting that probably all the different intestinal epithelial cell types are sensitised to RIP3 dependent necrosis. However, the striking loss of Paneth cells in the small intestine of FADD^{IEC-KO} mice potentially has a considerable impact on the development of enteritis, due to the important role of Paneth cells in the antimicrobial defence as well as in the establishment of the stem cell niche.

Interestingly, similar to the FADD^{IEC-KO} mice, a decrease in the number of Paneth cells by increased active Caspase 3 negative cell death was found in mice lacking X-box-binding protein 1 (XBP1) in the intestinal epithelium (Kaser et al., 2008). XBP1 is part of the Inositol-requiring enzyme-1 (IRE1) dependent signalling pathway, which is one of the three pathways involved in the endoplasmic reticulum (ER) stress response, also called unfolded protein response (UPR). XBP1 is a transcription factor that promotes cell survival and helps the cell to cope with ER-stress. How XBP1 deficiency might induce cell death is not very well understood, but increased signalling through JNK has been linked to IRE1 induced cell death (Tabas and Ron, 2011). Indeed, JNK signalling was increased in the XBP1 deficient small intestinal epithelium, leading to increased expression of proinflammatory cytokines and maybe also contributing to increased cell death (Kaser et al., 2008). It is noteworthy that TNF induced JNK signalling can inhibit c-FLIP through the ubiquitin ligase itchy, E3 ubiquitin protein ligase (ITCH). ITCH ligates K48-linked ubiquitin to c-FLIP leading to

proteasomal degradation of c-FLIP (Chang et al., 2006), providing a possible link between JNK signalling and FADD dependent apoptosis. However, whether there is any linkage between ER-stress and RIP3 dependent necrosis in FADD deficient Paneth cells remains to be shown.

XBP1 has been linked to the development of IBD (Kaser et al., 2008). If ER-stress induced loss of Paneth cells indeed depends on RIP3 mediated necrosis, RIP3 dependent regulated necrosis could be linked to the development of IBD. Interestingly, a recent study implicated regulated necrosis in dying Paneth cells of IBD patients (Gunther et al., 2011). RIP3 is highly expressed in Paneth cells of the human intestine, which could render them sensitive towards regulated necrosis. Dying Paneth cells showing necrotic features were detected in IBD patients by an electron microscopic analysis. Additionally, treatment with the RIP1 kinase inhibitor Necrostatin-1 protected from Paneth cell death induced by TNF treatment in biopsies from IBD patients (Gunther et al., 2011), suggesting that Paneth cells are highly sensitive towards RIP1 kinase dependent regulated necrosis and that regulated necrosis of Paneth cells might be implicated in the pathogenesis of IBD. The physiological trigger of Paneth cell necrosis in those IBD patients still has to be identified, but ER-stress is one possible candidate.

4.3.4. Other possible inducers of RIP3 dependent regulated necrosis

FADD has been reported to interact with the DNA mismatch repair machinery through MBD4 (Screaton et al., 2003). Although the role of FADD in DNA damage repair is not completely understood yet, these findings suggest that cell death induced by genotoxic stress might involve FADD. Whether the interaction of FADD with the DNA mismatch repair induces cell death and if this cell death could also lead to regulated necrosis is not known.

Interestingly, a FADD containing protein complex, called the Ripoptosome, has been found to be involved in signalling to cell death induced by genotoxic stress in cancer cells (Tenev et al., 2011). The ripoptosome is a protein complex consisting of RIP1, FADD, Caspase 8 and c-FLIP. Etoposide, an inhibitor of topoisomerases, can induce cell death in cancer cells through the ripoptosome. This cell death appears to be apoptotic unless caspase activation is blocked, which leads to RIP3 dependent

regulated necrosis. Although it is rather unlikely that genotoxic stress is a primary inducer of regulated necrosis in FADD deficient IECs, it might be possible that genotoxic stress triggers RIP3 dependent necrosis of IECs in certain physiological conditions.

In summary, TNF seems to be one, but not the only, inducer of RIP3 dependent necrosis in the FADD deficient colonic intestinal epithelium but not in the small intestine. Thus, different stimuli apparently trigger IEC necrosis in the colon and small intestine. While additional triggers of necrosis in FADD deficient IECs still need to be identified, it becomes more and more apparent, that FADD dependent apoptosis as well as RIP3 dependent regulated necrosis seem to play a role in a great variety of stress conditions. Therefore, FADD dependent apoptosis and RIP3 dependent IEC necrosis might not only be involved in immune responses to infection, but maybe also in responses to genotoxic stress or in responses to ER-stress. Discovery of the triggers of regulated necrosis in FADD deficient IECs might help to understand the role of RIP3 dependent necrosis of IECs under physiological conditions.

However, the results obtained in this work clearly show that the homeostatic programmed cell death involved in the turnover of the intestinal epithelial cells, termed anoikis, does neither involve FADD nor RIP3 dependent necrosis, because RIP3 deficient FADD^{IEC-KO} mice develop normally without showing any obvious alterations in the intestinal epithelium.

4.4. RIP3 dependent IEC necrosis and inflammation

FADD deficiency sensitises IECs towards RIP3 dependent regulated necrosis, resulting in increased IEC death and subsequent development of colitis and enteritis. However, not only the initial triggers for IEC necrosis in colon and small intestine seem to differ, but also the mechanisms leading to inflammation in the colon and the small intestine are apparently different.

4.4.1. Development of colitis in FADD^{IEC-KO} mice

FADD deficient colonic IECs are sensitised towards RIP3 and CYLD dependent necrosis. Increased IEC necrosis leads to colitis development in FADD^{IEC-KO} mice, which depends on MyD88 dependent signalling and the commensal bacteria (Fig.

20-22). Since MyD88 deficient FADD^{IEC-KO} mice, despite not developing colitis, still show slightly increased IEC death, it is unlikely that epithelial MyD88 directly influences RIP3 dependent necrosis in FADD deficient IECs. Overexpression studies have shown that only TRIF dependent signalling can lead to cell death, while overexpression of MyD88 did not result in increased cell death (Kaiser and Offermann, 2005) further supporting a role for MyD88 dependent signalling in FADD^{IEC-KO} mice that is independent of signalling to cell death. Hence, mucosal MyD88 dependent signalling probably contributes to the induction of inflammation. MyD88 is a central adaptor of several TLRs. These pattern recognition receptors recognise a variety of PAMPs. In case of the FADD^{IEC-KO} mouse model, excessive IEC necrosis presumably leads to barrier leakage and most likely to subsequent invasion of the microbiota into the mucosa. Antigen recognition by TLRs on mucosal immune cells probably induces proinflammatory signalling, which would also explain the dependency on the microbiota for the development of colitis in FADD^{IEC-KO} mice. Increased expression of proinflammatory cytokines like TNF presumably leads to even more IEC necrosis, resulting in a vicious cycle (for a model of the development of colitis in FADD^{IEC-KO} mice see Fig. 33a). Since MyD88 deficient FADD^{IEC-KO} mice, which do not develop colitis, show much lower levels of epithelial cell death compared to FADD^{IEC-KO} mice expressing MyD88, inflammation seems to be necessary to reach the devastating levels of epithelial cell death that lead to epithelial erosion seen in FADD^{IEC-KO} animals.

In a mouse model where NEMO is specifically deleted in IECs (NEMO^{IEC-KO} mice), increased cell death also leads to colitis development (Nenci et al., 2007), similarly to FADD^{IEC-KO} mice. It has been shown, that in NEMO^{IEC-KO} mice the increased IEC death leads to invasion of bacteria into the mucosa (Nenci et al., 2007) and to MyD88 dependent development of colitis. Thus, in both models excessive IEC death is the causative event in the development of colitis. Colitis development in FADD^{IEC-KO} mice at least partially depends on TNF induced signalling, while colitis development in NEMO^{IEC-KO} mice completely depends on TNFR1 induced signalling. Therefore, TNF/TNFR1 mediated regulation of cell survival and cell death in IECs seems to be important for intestinal homeostasis in the colon, although the cell types targeted by TNF still have to be clarified.

Casp8^{ΔIEC} mice do not spontaneously develop colitis (Gunther et al., 2011). It seems though that colonic IEC in Casp8^{ΔIEC} mice are sensitised towards cell death, because

Casp8^{ΔIEC} mice are highly sensitive to the development of colitis after administration of the IEC irritant dextran sodium sulphate (DSS). Differences in the amount of IEC death as well as in the constitution of the microbiota might explain the different phenotype in the colon of Casp8^{ΔIEC} mice compared to FADD^{IEC-KO} mice.

4.4.2. Development of enteritis in FADD^{IEC-KO} mice

FADD deficiency in the small intestine also leads to increased RIP3 dependent IEC necrosis, decreased numbers of Paneth cells and decreased expression of antimicrobial peptides (Fig. 10, 11 and 23). In contrary to the colon, the development of enteritis is independent of MyD88 or commensal bacteria (Fig. 29-32). Whether also the small intestinal epithelial barrier is breached in FADD^{IEC-KO} mice, remains to be shown. But regardless of whether the small intestinal barrier in FADD^{IEC-KO} mice is still intact or not, bacterial induced signalling is not the main cause of the development of spontaneous chronic enteritis in FADD^{IEC-KO} mice (for a model including what is known about enteritis development in FADD^{IEC-KO} mice see Fig. 33b).

The stimuli that might trigger small intestinal inflammation in FADD^{IEC-KO} mice are currently not known. One possible trigger is necrotic cell death itself, which can elicit an inflammatory response by the release of danger associated molecular patterns (DAMPs). Since one of the main characteristics of necrotic cell death is the loss of plasma membrane integrity, intracellular material can escape from necrotic cells and act as DAMP (Chen and Nunez, 2010). DAMPs released by necrotic cells comprise uric acid (Kono et al., 2010), high-mobility group protein B1 (HMGB1) (Scaffidi et al., 2002), heat shock proteins (Quintana and Cohen, 2005), RNA (Cavassani et al., 2008), DNA and adenosine triphosphate (ATP) (Bours et al., 2006). DAMPs are recognised by several PRRs and induce a sterile inflammatory response (Chen and Nunez, 2010). Interestingly, IL-1β, one of the main mediators of sterile inflammation (Chen and Nunez, 2010), is highly upregulated in the colon of FADD^{IEC-KO} mice (Fig. 7a). In addition, intracellular stores of proinflammatory cytokines can be released from necrotic cells, leading to an inflammatory response (Moussion et al., 2008).

Keratinocytes, epithelial cells of the skin, die by RIP3 dependent necrosis in a mouse model deficient for FADD in the epidermis. Released HMGB1 has been found in the epidermis of those FADD^{E-KO} mice, while HMGB1 was not detectable in FADD^{E-KO}

mice deficient for RIP3 (Bonnet et al., 2011). Sterile inflammation might therefore play a role in the development of skin inflammation. Whether sterile inflammation is an inducer of small intestinal enteritis in FADD^{IEC-KO} mice has to be dissected in future research.

5. Concluding Remarks

The data presented within this thesis show that FADD mediated inhibition of RIP3 dependent regulated necrosis in the intestinal epithelium is essential for intestinal homeostasis. Thus, FADD probably does not only mediate signalling to apoptotic cell death in response to various stress-factors, but it is also essential for IEC survival under homeostatic conditions.

The finding that IECs can undergo regulated necrosis might have far reaching implications. Regulated necrosis might have a role in the development of IBD, as suggested by the necrotic features of dying Paneth cells in IBD patients. Successful treatment of IBD patients with anti-TNF was mainly discussed to benefit from the anti-inflammatory role of these drugs, while the data obtained in this thesis indicate that also the role of TNF in IEC death should be considered to contribute to IBD. Additionally, regulated necrosis in the intestinal epithelium might be involved in several other disease conditions, including intestinal infections and genotoxic stress. Thus, drugs specifically targeting the necrotic pathway might prove useful in the treatment of certain disease conditions.

Bibliography

Abreu, M.T. (2010). Toll-like receptor signalling in the intestinal epithelium: how bacterial recognition shapes intestinal function. *Nat Rev Immunol* 10, 131-144.

Adachi, O., Kawai, T., Takeda, K., Matsumoto, M., Tsutsui, H., Sakagami, M., Nakanishi, K., and Akira, S. (1998). Targeted disruption of the MyD88 gene results in loss of IL-1- and IL-18-mediated function. *Immunity* 9, 143-150.

Alenzi, F.Q., Lotfy, M., and Wyse, R. (2010). Swords of cell death: caspase activation and regulation. *Asian Pac J Cancer Prev* 11, 271-280.

Algeciras-Schimmich, A., Shen, L., Barnhart, B.C., Murmann, A.E., Burkhardt, J.K., and Peter, M.E. (2002). Molecular ordering of the initial signaling events of CD95. *Mol Cell Biol* 22, 207-220.

Ameisen, J.C. (2004). Looking for death at the core of life in the light of evolution. *Cell Death Differ* 11, 4-10.

Armaka, M., Apostolaki, M., Jacques, P., Kontoyiannis, D.L., Elewaut, D., and Kollias, G. (2008). Mesenchymal cell targeting by TNF as a common pathogenic principle in chronic inflammatory joint and intestinal diseases. *J Exp Med* 205, 331-337.

Bannerman, D.D., Tupper, J.C., Kelly, J.D., Winn, R.K., and Harlan, J.M. (2002). The Fas-associated death domain protein suppresses activation of NF-kappa B by LPS and IL-1 beta. *J Clin Invest* 109, 419-425.

Barnhart, B.C., Alappat, E.C., and Peter, M.E. (2003). The CD95 type I/type II model. *Semin Immunol* 15, 185-193.

Becker, C., Fantini, M.C., Wirtz, S., Nikolaev, A., Kiesslich, R., Lehr, H.A., Galle, P.R., and Neurath, M.F. (2005). In vivo imaging of colitis and colon cancer development in mice using high resolution chromoendoscopy. *Gut* 54, 950-954.

Bell, B.D., Leverrier, S., Weist, B.M., Newton, R.H., Arechiga, A.F., Luhrs, K.A., Morrisette, N.S., and Walsh, C.M. (2008). FADD and caspase-8 control the outcome of autophagic signaling in proliferating T cells. *Proc Natl Acad Sci U S A* 105, 16677-16682.

Bevins, C.L., and Salzman, N.H. (2011). Paneth cells, antimicrobial peptides and maintenance of intestinal homeostasis. *Nat Rev Microbiol* 9, 356-368.

Boldin, M.P., Goncharov, T.M., Goltsev, Y.V., and Wallach, D. (1996). Involvement of MACH, a novel MORT1/FADD-interacting protease, in Fas/APO-1- and TNF receptor-induced cell death. *Cell* 85, 803-815.

Boldin, M.P., Varfolomeev, E.E., Pancer, Z., Mett, I.L., Camonis, J.H., and Wallach, D. (1995). A novel protein that interacts with the death domain of Fas/APO1 contains a sequence motif related to the death domain. *J Biol Chem* 270, 7795-7798.

- Bolze, A., Byun, M., McDonald, D., Morgan, N.V., Abhyankar, A., Premkumar, L., Puel, A., Bacon, C.M., Rieux-Laucat, F., Pang, K., *et al.* (2010). Whole-exome-sequencing-based discovery of human FADD deficiency. *Am J Hum Genet* 87, 873-881.
- Bonnet, M.C., Preukschat, D., Welz, P.S., van Loo, G., Ermolaeva, M.A., Bloch, W., Haase, I., and Pasparakis, M. (2011). The Adaptor Protein FADD Protects Epidermal Keratinocytes from Necroptosis In Vivo and Prevents Skin Inflammation. *Immunity* 35, 572-582.
- Bours, M.J., Swennen, E.L., Di Virgilio, F., Cronstein, B.N., and Dagnelie, P.C. (2006). Adenosine 5'-triphosphate and adenosine as endogenous signaling molecules in immunity and inflammation. *Pharmacol Ther* 112, 358-404.
- Broquet, A.H., Hirata, Y., McAllister, C.S., and Kagnoff, M.F. (2011). RIG-I/MDA5/MAVS are required to signal a protective IFN response in rotavirus-infected intestinal epithelium. *J Immunol* 186, 1618-1626.
- Budd, R.C., Yeh, W.C., and Tschopp, J. (2006). cFLIP regulation of lymphocyte activation and development. *Nat Rev Immunol* 6, 196-204.
- Catalioto, R.M., Maggi, C.A., and Giuliani, S. (2011). Intestinal epithelial barrier dysfunction in disease and possible therapeutical interventions. *Curr Med Chem* 18, 398-426.
- Cavassani, K.A., Ishii, M., Wen, H., Schaller, M.A., Lincoln, P.M., Lukacs, N.W., Hogaboam, C.M., and Kunkel, S.L. (2008). TLR3 is an endogenous sensor of tissue necrosis during acute inflammatory events. *J Exp Med* 205, 2609-2621.
- Chang, L., Kamata, H., Solinas, G., Luo, J.L., Maeda, S., Venuprasad, K., Liu, Y.C., and Karin, M. (2006). The E3 ubiquitin ligase itch couples JNK activation to TNFalpha-induced cell death by inducing c-FLIP(L) turnover. *Cell* 124, 601-613.
- Chaudhary, P.M., Eby, M., Jasmin, A., Bookwalter, A., Murray, J., and Hood, L. (1997). Death receptor 5, a new member of the TNFR family, and DR4 induce FADD-dependent apoptosis and activate the NF-kappaB pathway. *Immunity* 7, 821-830.
- Chen, G.Y., and Nunez, G. (2010). Sterile inflammation: sensing and reacting to damage. *Nat Rev Immunol* 10, 826-837.
- Chen, L., Park, S.M., Tumanov, A.V., Hau, A., Sawada, K., Feig, C., Turner, J.R., Fu, Y.X., Romero, I.L., Lengyel, E., *et al.* (2010). CD95 promotes tumour growth. *Nature* 465, 492-496.
- Chinnaiyan, A.M., O'Rourke, K., Tewari, M., and Dixit, V.M. (1995). FADD, a novel death domain-containing protein, interacts with the death domain of Fas and initiates apoptosis. *Cell* 81, 505-512.
- Cho, Y.S., Challa, S., Moquin, D., Genga, R., Ray, T.D., Guildford, M., and Chan, F.K. (2009). Phosphorylation-driven assembly of the RIP1-RIP3 complex regulates programmed necrosis and virus-induced inflammation. *Cell* 137, 1112-1123.

De Trez, C., Pajak, B., Brait, M., Glaichenhaus, N., Urbain, J., Moser, M., Lauvau, G., and Muraille, E. (2005). TLR4 and Toll-IL-1 receptor domain-containing adapter-inducing IFN-beta, but not MyD88, regulate Escherichia coli-induced dendritic cell maturation and apoptosis in vivo. *J Immunol* 175, 839-846.

Degterev, A., Hitomi, J., Gemscheid, M., Ch'en, I.L., Korkina, O., Teng, X., Abbott, D., Cuny, G.D., Yuan, C., Wagner, G., *et al.* (2008). Identification of RIP1 kinase as a specific cellular target of necrostatins. *Nat Chem Biol* 4, 313-321.

Degterev, A., Huang, Z., Boyce, M., Li, Y., Jagtap, P., Mizushima, N., Cuny, G.D., Mitchison, T.J., Moskowitz, M.A., and Yuan, J. (2005). Chemical inhibitor of nonapoptotic cell death with therapeutic potential for ischemic brain injury. *Nat Chem Biol* 1, 112-119.

Deveraux, Q.L., Roy, N., Stennicke, H.R., Van Arsdale, T., Zhou, Q., Srinivasula, S.M., Alnemri, E.S., Salvesen, G.S., and Reed, J.C. (1998). IAPs block apoptotic events induced by caspase-8 and cytochrome c by direct inhibition of distinct caspases. *Embo J* 17, 2215-2223.

Duprez, L., Takahashi, N., Van Hauwermeiren, F., Vandendriessche, B., Goossens, V., Vanden Berghe, T., Declercq, W., Libert, C., Cauwels, A., and Vandenabeele, P. (2011). RIP Kinase-Dependent Necrosis Drives Lethal Systemic Inflammatory Response Syndrome. *Immunity* 35, 908-918.

Ermolaeva, M.A., Michallet, M.C., Papadopoulou, N., Utermohlen, O., Kranidioti, K., Kollias, G., Tschopp, J., and Pasparakis, M. (2008). Function of TRADD in tumor necrosis factor receptor 1 signaling and in TRIF-dependent inflammatory responses. *Nat Immunol* 9, 1037-1046.

Fady, C., Gardner, A., Jacoby, F., Briskin, K., Tu, Y., Schmid, I., and Lichtenstein, A. (1995). Atypical apoptotic cell death induced in L929 targets by exposure to tumor necrosis factor. *J Interferon Cytokine Res* 15, 71-80.

Feng, S., Yang, Y., Mei, Y., Ma, L., Zhu, D.E., Hoti, N., Castanares, M., and Wu, M. (2007). Cleavage of RIP3 inactivates its caspase-independent apoptosis pathway by removal of kinase domain. *Cell Signal* 19, 2056-2067.

Feoktistova, M., Geserick, P., Kellert, B., Dimitrova, D.P., Langlais, C., Hupe, M., Cain, K., MacFarlane, M., Hacker, G., and Leverkus, M. (2011). cIAPs block Ripoptosome formation, a RIP1/caspase-8 containing intracellular cell death complex differentially regulated by cFLIP isoforms. *Mol Cell* 43, 449-463.

Galluzzi, L., Vitale, I., Abrams, J.M., Alnemri, E.S., Baehrecke, E.H., Blagosklonny, M.V., Dawson, T.M., Dawson, V.L., El-Deiry, W.S., Fulda, S., *et al.* (2011). Molecular definitions of cell death subroutines: recommendations of the Nomenclature Committee on Cell Death 2012. *Cell Death Differ*.

Gerlach, B., Cordier, S.M., Schmukle, A.C., Emmerich, C.H., Rieser, E., Haas, T.L., Webb, A.I., Rickard, J.A., Anderton, H., Wong, W.W., *et al.* (2011). Linear ubiquitination prevents inflammation and regulates immune signalling. *Nature* 471, 591-596.

- Gibcus, J.H., Menkema, L., Mastik, M.F., Hermsen, M.A., de Bock, G.H., van Velthuysen, M.L., Takes, R.P., Kok, K., Alvarez Marcos, C.A., van der Laan, B.F., *et al.* (2007). Amplicon mapping and expression profiling identify the Fas-associated death domain gene as a new driver in the 11q13.3 amplicon in laryngeal/pharyngeal cancer. *Clin Cancer Res* 13, 6257-6266.
- Gomez-Angelats, M., and Cidlowski, J.A. (2003). Molecular evidence for the nuclear localization of FADD. *Cell Death Differ* 10, 791-797.
- Goodgame, R.W. (1993). Gastrointestinal cytomegalovirus disease. *Ann Intern Med* 119, 924-935.
- Guicciardi, M.E., and Gores, G.J. (2009). Life and death by death receptors. *Faseb J* 23, 1625-1637.
- Gunther, C., Martini, E., Wittkopf, N., Amann, K., Weigmann, B., Neumann, H., Waldner, M.J., Hedrick, S.M., Tenzer, S., Neurath, M.F., *et al.* (2011). Caspase-8 regulates TNF-alpha-induced epithelial necroptosis and terminal ileitis. *Nature* 477, 335-339.
- Haas, T.L., Emmerich, C.H., Gerlach, B., Schmukle, A.C., Cordier, S.M., Rieser, E., Feltham, R., Vince, J., Warnken, U., Wenger, T., *et al.* (2009). Recruitment of the linear ubiquitin chain assembly complex stabilizes the TNF-R1 signaling complex and is required for TNF-mediated gene induction. *Mol Cell* 36, 831-844.
- He, S., Liang, Y., Shao, F., and Wang, X. (2011). Toll-like receptors activate programmed necrosis in macrophages through a receptor-interacting kinase-3-mediated pathway. *Proc Natl Acad Sci U S A* 108, 20054-20059.
- He, S., Wang, L., Miao, L., Wang, T., Du, F., Zhao, L., and Wang, X. (2009). Receptor interacting protein kinase-3 determines cellular necrotic response to TNF-alpha. *Cell* 137, 1100-1111.
- Henkler, F., Behrle, E., Dennehy, K.M., Wicovsky, A., Peters, N., Warnke, C., Pfizenmaier, K., and Wajant, H. (2005). The extracellular domains of FasL and Fas are sufficient for the formation of supramolecular FasL-Fas clusters of high stability. *J Cell Biol* 168, 1087-1098.
- Hitomi, J., Christofferson, D.E., Ng, A., Yao, J., Degterev, A., Xavier, R.J., and Yuan, J. (2008). Identification of a molecular signaling network that regulates a cellular necrotic cell death pathway. *Cell* 135, 1311-1323.
- Holler, N., Zaru, R., Micheau, O., Thome, M., Attinger, A., Valitutti, S., Bodmer, J.L., Schneider, P., Seed, B., and Tschopp, J. (2000). Fas triggers an alternative, caspase-8-independent cell death pathway using the kinase RIP as effector molecule. *Nat Immunol* 1, 489-495.
- Hornef, M.W., Normark, B.H., Vandewalle, A., and Normark, S. (2003). Intracellular recognition of lipopolysaccharide by toll-like receptor 4 in intestinal epithelial cells. *J Exp Med* 198, 1225-1235.

- Hsu, H., Shu, H.B., Pan, M.G., and Goeddel, D.V. (1996). TRADD-TRAF2 and TRADD-FADD interactions define two distinct TNF receptor 1 signal transduction pathways. *Cell* 84, 299-308.
- Ikeda, F., Deribe, Y.L., Skanland, S.S., Stieglitz, B., Grabbe, C., Franz-Wachtel, M., van Wijk, S.J., Goswami, P., Nagy, V., Terzic, J., *et al.* (2011). SHARPIN forms a linear ubiquitin ligase complex regulating NF-kappaB activity and apoptosis. *Nature* 471, 637-641.
- Irmeler, M., Thome, M., Hahne, M., Schneider, P., Hofmann, K., Steiner, V., Bodmer, J.L., Schroter, M., Burns, K., Mattmann, C., *et al.* (1997). Inhibition of death receptor signals by cellular FLIP. *Nature* 388, 190-195.
- Johansson, M.E., and Hansson, G.C. (2011). Microbiology. Keeping bacteria at a distance. *Science* 334, 182-183.
- Kaiser, W.J., and Offermann, M.K. (2005). Apoptosis induced by the toll-like receptor adaptor TRIF is dependent on its receptor interacting protein homotypic interaction motif. *J Immunol* 174, 4942-4952.
- Kaiser, W.J., Upton, J.W., Long, A.B., Livingston-Rosanoff, D., Daley-Bauer, L.P., Hakem, R., Caspary, T., and Mocarski, E.S. (2011). RIP3 mediates the embryonic lethality of caspase-8-deficient mice. *Nature* 471, 368-372.
- Kajino-Sakamoto, R., Inagaki, M., Lippert, E., Akira, S., Robine, S., Matsumoto, K., Jobin, C., and Ninomiya-Tsuji, J. (2008). Enterocyte-derived TAK1 signaling prevents epithelium apoptosis and the development of ileitis and colitis. *J Immunol* 181, 1143-1152.
- Kaser, A., Lee, A.H., Franke, A., Glickman, J.N., Zeissig, S., Tilg, H., Nieuwenhuis, E.E., Higgins, D.E., Schreiber, S., Glimcher, L.H., *et al.* (2008). XBP1 links ER stress to intestinal inflammation and confers genetic risk for human inflammatory bowel disease. *Cell* 134, 743-756.
- Kawahara, A., Ohsawa, Y., Matsumura, H., Uchiyama, Y., and Nagata, S. (1998). Caspase-independent cell killing by Fas-associated protein with death domain. *J Cell Biol* 143, 1353-1360.
- Kenny, E.F., and O'Neill, L.A. (2008). Signalling adaptors used by Toll-like receptors: an update. *Cytokine* 43, 342-349.
- Khan, M.A., Ma, C., Knodler, L.A., Valdez, Y., Rosenberger, C.M., Deng, W., Finlay, B.B., and Vallance, B.A. (2006). Toll-like receptor 4 contributes to colitis development but not to host defense during *Citrobacter rodentium* infection in mice. *Infect Immun* 74, 2522-2536.
- Kono, H., Chen, C.J., Ontiveros, F., and Rock, K.L. (2010). Uric acid promotes an acute inflammatory response to sterile cell death in mice. *J Clin Invest* 120, 1939-1949.

- Kontoyiannis, D., Pasparakis, M., Pizarro, T.T., Cominelli, F., and Kollias, G. (1999). Impaired on/off regulation of TNF biosynthesis in mice lacking TNF AU-rich elements: implications for joint and gut-associated immunopathologies. *Immunity* 10, 387-398.
- Kuang, A.A., Diehl, G.E., Zhang, J., and Winoto, A. (2000). FADD is required for DR4- and DR5-mediated apoptosis: lack of trail-induced apoptosis in FADD-deficient mouse embryonic fibroblasts. *J Biol Chem* 275, 25065-25068.
- Lamkanfi, M., and Dixit, V.M. (2010). Manipulation of host cell death pathways during microbial infections. *Cell Host Microbe* 8, 44-54.
- Laster, S.M., Wood, J.G., and Gooding, L.R. (1988). Tumor necrosis factor can induce both apoptotic and necrotic forms of cell lysis. *J Immunol* 141, 2629-2634.
- Lavrik, I.N., Mock, T., Golks, A., Hoffmann, J.C., Baumann, S., and Krammer, P.H. (2008). CD95 stimulation results in the formation of a novel death effector domain protein-containing complex. *J Biol Chem* 283, 26401-26408.
- Leaphart, C.L., Cavallo, J., Gribar, S.C., Cetin, S., Li, J., Branca, M.F., Dubowski, T.D., Sodhi, C.P., and Hackam, D.J. (2007). A critical role for TLR4 in the pathogenesis of necrotizing enterocolitis by modulating intestinal injury and repair. *J Immunol* 179, 4808-4820.
- Lee, K.H., Feig, C., Tchikov, V., Schickel, R., Hallas, C., Schutze, S., Peter, M.E., and Chan, A.C. (2006). The role of receptor internalization in CD95 signaling. *Embo J* 25, 1009-1023.
- Li, M., and Beg, A.A. (2000). Induction of necrotic-like cell death by tumor necrosis factor alpha and caspase inhibitors: novel mechanism for killing virus-infected cells. *J Virol* 74, 7470-7477.
- Liedtke, C., Bangen, J.M., Freimuth, J., Beraza, N., Lambertz, D., Cubero, F.J., Hatting, M., Karlmark, K.R., Streetz, K.L., Krombach, G.A., *et al.* (2011). Loss of Caspase-8 Protects Mice Against Inflammation-Related Hepatocarcinogenesis but Induces Non-Apoptotic Liver Injury. *Gastroenterology*.
- Locksley, R.M., Killeen, N., and Lenardo, M.J. (2001). The TNF and TNF receptor superfamilies: integrating mammalian biology. *Cell* 104, 487-501.
- Lu, J.V., Weist, B.M., van Raam, B.J., Marro, B.S., Nguyen, L.V., Srinivas, P., Bell, B.D., Luhrs, K.A., Lane, T.E., Salvesen, G.S., *et al.* (2011). Complementary roles of Fas-associated death domain (FADD) and receptor interacting protein kinase-3 (RIPK3) in T-cell homeostasis and antiviral immunity. *Proc Natl Acad Sci U S A* 108, 15312-15317.
- Ma, Y., Temkin, V., Liu, H., and Pope, R.M. (2005). NF-kappaB protects macrophages from lipopolysaccharide-induced cell death: the role of caspase 8 and receptor-interacting protein. *J Biol Chem* 280, 41827-41834.

- MacDonald, T.T., Hutchings, P., Choy, M.Y., Murch, S., and Cooke, A. (1990). Tumour necrosis factor-alpha and interferon-gamma production measured at the single cell level in normal and inflamed human intestine. *Clin Exp Immunol* *81*, 301-305.
- Madara, J.L. (1990). Maintenance of the macromolecular barrier at cell extrusion sites in intestinal epithelium: physiological rearrangement of tight junctions. *J Membr Biol* *116*, 177-184.
- Madison, B.B., Dunbar, L., Qiao, X.T., Braunstein, K., Braunstein, E., and Gumucio, D.L. (2002). Cis elements of the villin gene control expression in restricted domains of the vertical (crypt) and horizontal (duodenum, cecum) axes of the intestine. *J Biol Chem* *277*, 33275-33283.
- Marchiando, A.M., Shen, L., Graham, W.V., Edelblum, K.L., Duckworth, C.A., Guan, Y., Montrose, M.H., Turner, J.R., and Watson, A.J. (2011). The epithelial barrier is maintained by in vivo tight junction expansion during pathologic intestinal epithelial shedding. *Gastroenterology* *140*, 1208-1218 e1201-1202.
- Matsumura, Y., Shimada, K., Tanaka, N., Fujimoto, K., Hirao, Y., and Konishi, N. (2009). Phosphorylation status of Fas-associated death domain-containing protein regulates telomerase activity and strongly correlates with prostate cancer outcomes. *Pathobiology* *76*, 293-302.
- Mc Guire, C., Volckaert, T., Wolke, U., Sze, M., de Rycke, R., Waisman, A., Prinz, M., Beyaert, R., Pasparakis, M., and van Loo, G. (2010). Oligodendrocyte-specific FADD deletion protects mice from autoimmune-mediated demyelination. *J Immunol* *185*, 7646-7653.
- McGuckin, M.A., Eri, R., Simms, L.A., Florin, T.H., and Radford-Smith, G. (2009). Intestinal barrier dysfunction in inflammatory bowel diseases. *Inflamm Bowel Dis* *15*, 100-113.
- Medema, J.P., Scaffidi, C., Kischkel, F.C., Shevchenko, A., Mann, M., Krammer, P.H., and Peter, M.E. (1997). FLICE is activated by association with the CD95 death-inducing signaling complex (DISC). *Embo J* *16*, 2794-2804.
- Micheau, O., and Tschopp, J. (2003). Induction of TNF receptor I-mediated apoptosis via two sequential signaling complexes. *Cell* *114*, 181-190.
- Moussion, C., Ortega, N., and Girard, J.P. (2008). The IL-1-like cytokine IL-33 is constitutively expressed in the nucleus of endothelial cells and epithelial cells in vivo: a novel 'alarmin'? *PLoS One* *3*, e3331.
- Muzio, M., Chinnaiyan, A.M., Kischkel, F.C., O'Rourke, K., Shevchenko, A., Ni, J., Scaffidi, C., Bretz, J.D., Zhang, M., Gentz, R., *et al.* (1996). FLICE, a novel FADD-homologous ICE/CED-3-like protease, is recruited to the CD95 (Fas/APO-1) death-inducing signaling complex. *Cell* *85*, 817-827.
- Nenci, A., Becker, C., Wullaert, A., Gareus, R., van Loo, G., Danese, S., Huth, M., Nikolaev, A., Neufert, C., Madison, B., *et al.* (2007). Epithelial NEMO links innate immunity to chronic intestinal inflammation. *Nature* *446*, 557-561.

- Newton, K., Harris, A.W., Bath, M.L., Smith, K.G., and Strasser, A. (1998). A dominant interfering mutant of FADD/MORT1 enhances deletion of autoreactive thymocytes and inhibits proliferation of mature T lymphocytes. *Embo J* 17, 706-718.
- Newton, K., Sun, X., and Dixit, V.M. (2004). Kinase RIP3 is dispensable for normal NF-kappa Bs, signaling by the B-cell and T-cell receptors, tumor necrosis factor receptor 1, and Toll-like receptors 2 and 4. *Mol Cell Biol* 24, 1464-1469.
- O'Donnell, M.A., Perez-Jimenez, E., Oberst, A., Ng, A., Massoumi, R., Xavier, R., Green, D.R., and Ting, A.T. (2011). Caspase 8 inhibits programmed necrosis by processing CYLD. *Nat Cell Biol*.
- Oberst, A., Dillon, C.P., Weinlich, R., McCormick, L.L., Fitzgerald, P., Pop, C., Hakem, R., Salvesen, G.S., and Green, D.R. (2011). Catalytic activity of the caspase-8-FLIP(L) complex inhibits RIPK3-dependent necrosis. *Nature* 471, 363-367.
- Park, J.M., Ng, V.H., Maeda, S., Rest, R.F., and Karin, M. (2004). Anthrolysin O and other gram-positive cytolysins are toll-like receptor 4 agonists. *J Exp Med* 200, 1647-1655.
- Pasparakis, M., Alexopoulou, L., Episkopou, V., and Kollias, G. (1996). Immune and inflammatory responses in TNF alpha-deficient mice: a critical requirement for TNF alpha in the formation of primary B cell follicles, follicular dendritic cell networks and germinal centers, and in the maturation of the humoral immune response. *J Exp Med* 184, 1397-1411.
- Peyrin-Biroulet, L. (2010). Anti-TNF therapy in inflammatory bowel diseases: a huge review. *Minerva Gastroenterol Dietol* 56, 233-243.
- Pop, C., Oberst, A., Drag, M., Van Raam, B.J., Riedl, S.J., Green, D.R., and Salvesen, G.S. (2011). FLIP(L) induces caspase 8 activity in the absence of interdomain caspase 8 cleavage and alters substrate specificity. *Biochem J* 433, 447-457.
- Pyo, J.O., Jang, M.H., Kwon, Y.K., Lee, H.J., Jun, J.I., Woo, H.N., Cho, D.H., Choi, B., Lee, H., Kim, J.H., *et al.* (2005). Essential roles of Atg5 and FADD in autophagic cell death: dissection of autophagic cell death into vacuole formation and cell death. *J Biol Chem* 280, 20722-20729.
- Quintana, F.J., and Cohen, I.R. (2005). Heat shock proteins as endogenous adjuvants in sterile and septic inflammation. *J Immunol* 175, 2777-2782.
- Radtke, F., and Clevers, H. (2005). Self-renewal and cancer of the gut: two sides of a coin. *Science* 307, 1904-1909.
- Rajewsky, K., Gu, H., Kuhn, R., Betz, U.A., Muller, W., Roes, J., and Schwenk, F. (1996). Conditional gene targeting. *J Clin Invest* 98, 600-603.
- Rakoff-Nahoum, S., Hao, L., and Medzhitov, R. (2006). Role of toll-like receptors in spontaneous commensal-dependent colitis. *Immunity* 25, 319-329.

- Rakoff-Nahoum, S., Paglino, J., Eslami-Varzaneh, F., Edberg, S., and Medzhitov, R. (2004). Recognition of commensal microflora by toll-like receptors is required for intestinal homeostasis. *Cell* 118, 229-241.
- Rebe, C., Cathelin, S., Launay, S., Filomenko, R., Prevotat, L., L'Ollivier, C., Gyan, E., Micheau, O., Grant, S., Dubart-Kupperschmitt, A., *et al.* (2007). Caspase-8 prevents sustained activation of NF-kappaB in monocytes undergoing macrophagic differentiation. *Blood* 109, 1442-1450.
- Roda, G., Sartini, A., Zambon, E., Calafiore, A., Marocchi, M., Caponi, A., Belluzzi, A., and Roda, E. (2010). Intestinal epithelial cells in inflammatory bowel diseases. *World J Gastroenterol* 16, 4264-4271.
- Rosenblatt, J., Raff, M.C., and Cramer, L.P. (2001). An epithelial cell destined for apoptosis signals its neighbors to extrude it by an actin- and myosin-dependent mechanism. *Curr Biol* 11, 1847-1857.
- Roulis, M., Armaka, M., Manoloukos, M., Apostolaki, M., and Kollias, G. (2011). Intestinal epithelial cells as producers but not targets of chronic TNF suffice to cause murine Crohn-like pathology. *Proc Natl Acad Sci U S A* 108, 5396-5401.
- Ruckdeschel, K., Pfaffinger, G., Haase, R., Sing, A., Weighardt, H., Hacker, G., Holzmann, B., and Heesemann, J. (2004). Signaling of apoptosis through TLRs critically involves toll/IL-1 receptor domain-containing adapter inducing IFN-beta, but not MyD88, in bacteria-infected murine macrophages. *J Immunol* 173, 3320-3328.
- Sato, A., Iizuka, M., Nakagomi, O., Suzuki, M., Horie, Y., Konno, S., Hirasawa, F., Sasaki, K., Shindo, K., and Watanabe, S. (2006). Rotavirus double-stranded RNA induces apoptosis and diminishes wound repair in rat intestinal epithelial cells. *J Gastroenterol Hepatol* 21, 521-530.
- Sauer, B., and Henderson, N. (1988). Site-specific DNA recombination in mammalian cells by the Cre recombinase of bacteriophage P1. *Proc Natl Acad Sci U S A* 85, 5166-5170.
- Scaffidi, P., Misteli, T., and Bianchi, M.E. (2002). Release of chromatin protein HMGB1 by necrotic cells triggers inflammation. *Nature* 418, 191-195.
- Schneider, P., Thome, M., Burns, K., Bodmer, J.L., Hofmann, K., Kataoka, T., Holler, N., and Tschopp, J. (1997). TRAIL receptors 1 (DR4) and 2 (DR5) signal FADD-dependent apoptosis and activate NF-kappaB. *Immunity* 7, 831-836.
- Schutze, S., Tchikov, V., and Schneider-Brachert, W. (2008). Regulation of TNFR1 and CD95 signalling by receptor compartmentalization. *Nat Rev Mol Cell Biol* 9, 655-662.
- Screaton, R.A., Kiessling, S., Sansom, O.J., Millar, C.B., Maddison, K., Bird, A., Clarke, A.R., and Frisch, S.M. (2003). Fas-associated death domain protein interacts with methyl-CpG binding domain protein 4: a potential link between genome surveillance and apoptosis. *Proc Natl Acad Sci U S A* 100, 5211-5216.

- Shimada, K., Matsuyoshi, S., Nakamura, M., Ishida, E., and Konishi, N. (2005). Phosphorylation status of Fas-associated death domain-containing protein (FADD) is associated with prostate cancer progression. *J Pathol* 206, 423-432.
- Shu, H.B., Takeuchi, M., and Goeddel, D.V. (1996). The tumor necrosis factor receptor 2 signal transducers TRAF2 and c-IAP1 are components of the tumor necrosis factor receptor 1 signaling complex. *Proc Natl Acad Sci U S A* 93, 13973-13978.
- Soung, Y.H., Lee, J.W., Kim, S.Y., Nam, S.W., Park, W.S., Kim, S.H., Lee, J.Y., Yoo, N.J., and Lee, S.H. (2004). Mutation of FADD gene is rare in human colon and stomach cancers. *Apmis* 112, 595-597.
- Stevceva, L., Pavli, P., Buffinton, G., Wozniak, A., and Doe, W.F. (1999). Dextran sodium sulphate-induced colitis activity varies with mouse strain but develops in lipopolysaccharide-unresponsive mice. *J Gastroenterol Hepatol* 14, 54-60.
- Strasser, A., Jost, P.J., and Nagata, S. (2009). The many roles of FAS receptor signaling in the immune system. *Immunity* 30, 180-192.
- Strater, J., and Moller, P. (2000). Expression and function of death receptors and their natural ligands in the intestine. *Ann N Y Acad Sci* 915, 162-170.
- Strater, J., Walczak, H., Pukrop, T., Von Muller, L., Hasel, C., Kornmann, M., Mertens, T., and Moller, P. (2002). TRAIL and its receptors in the colonic epithelium: a putative role in the defense of viral infections. *Gastroenterology* 122, 659-666.
- Tabas, I., and Ron, D. (2011). Integrating the mechanisms of apoptosis induced by endoplasmic reticulum stress. *Nat Cell Biol* 13, 184-190.
- Tada, K., Okazaki, T., Sakon, S., Kobayashi, T., Kurosawa, K., Yamaoka, S., Hashimoto, H., Mak, T.W., Yagita, H., Okumura, K., *et al.* (2001). Critical roles of TRAF2 and TRAF5 in tumor necrosis factor-induced NF-kappa B activation and protection from cell death. *J Biol Chem* 276, 36530-36534.
- Takeuchi, O., and Akira, S. (2010). Pattern recognition receptors and inflammation. *Cell* 140, 805-820.
- Tejedor Cerdena, M.A., Velasco Guardado, A., Fernandez Prodomingo, A., Concepcion Pinero Perez, M.C., Calderon, R., Prieto Bermejo, A.B., Sanchez Garrido, A., Martinez Moreno, J., Geijo Martinez, F., Blanco Munez, O.J., *et al.* (2011). Cytomegalovirus ileitis in an immunocompetent patient. *Rev Esp Enferm Dig* 103, 154-156.
- Tenev, T., Bianchi, K., Darding, M., Broemer, M., Langlais, C., Wallberg, F., Zachariou, A., Lopez, J., MacFarlane, M., Cain, K., *et al.* (2011). The Ripoptosome, a signaling platform that assembles in response to genotoxic stress and loss of IAPs. *Mol Cell* 43, 432-448.
- Tokunaga, F., Nakagawa, T., Nakahara, M., Saeki, Y., Taniguchi, M., Sakata, S., Tanaka, K., Nakano, H., and Iwai, K. (2011). SHARPIN is a component of the NF-kappaB-activating linear ubiquitin chain assembly complex. *Nature* 471, 633-636.

- Tokunaga, F., Sakata, S., Saeki, Y., Satomi, Y., Kirisako, T., Kamei, K., Nakagawa, T., Kato, M., Murata, S., Yamaoka, S., *et al.* (2009). Involvement of linear polyubiquitylation of NEMO in NF-kappaB activation. *Nat Cell Biol* 11, 123-132.
- Tourneur, L., Delluc, S., Levy, V., Valensi, F., Radford-Weiss, I., Legrand, O., Vargaftig, J., Boix, C., Macintyre, E.A., Varet, B., *et al.* (2004). Absence or low expression of fas-associated protein with death domain in acute myeloid leukemia cells predicts resistance to chemotherapy and poor outcome. *Cancer Res* 64, 8101-8108.
- Tourneur, L., Mistou, S., Michiels, F.M., Devauchelle, V., Renia, L., Feunteun, J., and Chiocchia, G. (2003). Loss of FADD protein expression results in a biased Fas-signaling pathway and correlates with the development of tumoral status in thyroid follicular cells. *Oncogene* 22, 2795-2804.
- Tourneur, L., Mistou, S., Schmitt, A., and Chiocchia, G. (2008). Adenosine receptors control a new pathway of Fas-associated death domain protein expression regulation by secretion. *J Biol Chem* 283, 17929-17938.
- Trichonas, G., Murakami, Y., Thanos, A., Morizane, Y., Kayama, M., Debouck, C.M., Hisatomi, T., Miller, J.W., and Vavvas, D.G. (2010). Receptor interacting protein kinases mediate retinal detachment-induced photoreceptor necrosis and compensate for inhibition of apoptosis. *Proc Natl Acad Sci U S A* 107, 21695-21700.
- Ukena, S.N., Singh, A., Dringenberg, U., Engelhardt, R., Seidler, U., Hansen, W., Bleich, A., Bruder, D., Franzke, A., Rogler, G., *et al.* (2007). Probiotic *Escherichia coli* Nissle 1917 inhibits leaky gut by enhancing mucosal integrity. *PLoS One* 2, e1308.
- Upton, J.W., Kaiser, W.J., and Mocarski, E.S. (2008). Cytomegalovirus M45 cell death suppression requires receptor-interacting protein (RIP) homotypic interaction motif (RHIM)-dependent interaction with RIP1. *J Biol Chem* 283, 16966-16970.
- Upton, J.W., Kaiser, W.J., and Mocarski, E.S. (2010). Virus inhibition of RIP3-dependent necrosis. *Cell Host Microbe* 7, 302-313.
- van der Flier, L.G., and Clevers, H. (2009). Stem cells, self-renewal, and differentiation in the intestinal epithelium. *Annu Rev Physiol* 71, 241-260.
- Vanden Berghe, T., van Loo, G., Saelens, X., Van Gurp, M., Brouckaert, G., Kalai, M., Declercq, W., and Vandenabeele, P. (2004). Differential signaling to apoptotic and necrotic cell death by Fas-associated death domain protein FADD. *J Biol Chem* 279, 7925-7933.
- Varfolomeev, E., Maecker, H., Sharp, D., Lawrence, D., Renz, M., Vucic, D., and Ashkenazi, A. (2005). Molecular determinants of kinase pathway activation by Apo2 ligand/tumor necrosis factor-related apoptosis-inducing ligand. *J Biol Chem* 280, 40599-40608.
- Varfolomeev, E.E., Schuchmann, M., Luria, V., Chiannikulchai, N., Beckmann, J.S., Mett, I.L., Rebrikov, D., Brodianski, V.M., Kemper, O.C., Kollet, O., *et al.* (1998). Targeted disruption of the mouse Caspase 8 gene ablates cell death induction by the TNF receptors, Fas/Apo1, and DR3 and is lethal prenatally. *Immunity* 9, 267-276.

- Vazquez-Torres, A., Vallance, B.A., Bergman, M.A., Finlay, B.B., Cookson, B.T., Jones-Carson, J., and Fang, F.C. (2004). Toll-like receptor 4 dependence of innate and adaptive immunity to Salmonella: importance of the Kupffer cell network. *J Immunol* 172, 6202-6208.
- Vercammen, D., Beyaert, R., Denecker, G., Goossens, V., Van Loo, G., Declercq, W., Grooten, J., Fiers, W., and Vandenaabeele, P. (1998). Inhibition of caspases increases the sensitivity of L929 cells to necrosis mediated by tumor necrosis factor. *J Exp Med* 187, 1477-1485.
- Vereecke, L., Beyaert, R., and van Loo, G. (2011). Enterocyte death and intestinal barrier maintenance in homeostasis and disease. *Trends Mol Med* 17, 584-593.
- Walczak, H. (2011). TNF and ubiquitin at the crossroads of gene activation, cell death, inflammation, and cancer. *Immunol Rev* 244, 9-28.
- Wang, L., Du, F., and Wang, X. (2008). TNF-alpha induces two distinct caspase-8 activation pathways. *Cell* 133, 693-703.
- Watson, A.J., Chu, S., Sieck, L., Gerasimenko, O., Bullen, T., Campbell, F., McKenna, M., Rose, T., and Montrose, M.H. (2005). Epithelial barrier function in vivo is sustained despite gaps in epithelial layers. *Gastroenterology* 129, 902-912.
- Weiss, D.S., Raupach, B., Takeda, K., Akira, S., and Zychlinsky, A. (2004). Toll-like receptors are temporally involved in host defense. *J Immunol* 172, 4463-4469.
- Wells, J.M., Rossi, O., Meijerink, M., and van Baarlen, P. (2011). Epithelial crosstalk at the microbiota-mucosal interface. *Proc Natl Acad Sci U S A* 108 Suppl 1, 4607-4614.
- Wertz, I.E., O'Rourke, K.M., Zhou, H., Eby, M., Aravind, L., Seshagiri, S., Wu, P., Wiesmann, C., Baker, R., Boone, D.L., *et al.* (2004). De-ubiquitination and ubiquitin ligase domains of A20 downregulate NF-kappaB signalling. *Nature* 430, 694-699.
- Wiley, S.R., Schooley, K., Smolak, P.J., Din, W.S., Huang, C.P., Nicholl, J.K., Sutherland, G.R., Smith, T.D., Rauch, C., Smith, C.A., *et al.* (1995). Identification and characterization of a new member of the TNF family that induces apoptosis. *Immunity* 3, 673-682.
- Wilson, N.S., Dixit, V., and Ashkenazi, A. (2009). Death receptor signal transducers: nodes of coordination in immune signaling networks. *Nat Immunol* 10, 348-355.
- Wright, A., Reiley, W.W., Chang, M., Jin, W., Lee, A.J., Zhang, M., and Sun, S.C. (2007). Regulation of early wave of germ cell apoptosis and spermatogenesis by deubiquitinating enzyme CYLD. *Dev Cell* 13, 705-716.
- Yeh, W.C., Pompa, J.L., McCurrach, M.E., Shu, H.B., Elia, A.J., Shahinian, A., Ng, M., Wakeham, A., Khoo, W., Mitchell, K., *et al.* (1998). FADD: essential for embryo development and signaling from some, but not all, inducers of apoptosis. *Science* 279, 1954-1958.

- Zhande, R., Dauphinee, S.M., Thomas, J.A., Yamamoto, M., Akira, S., and Karsan, A. (2007). FADD negatively regulates lipopolysaccharide signaling by impairing interleukin-1 receptor-associated kinase 1-MyD88 interaction. *Mol Cell Biol* 27, 7394-7404.
- Zhang, D.W., Shao, J., Lin, J., Zhang, N., Lu, B.J., Lin, S.C., Dong, M.Q., and Han, J. (2009). RIP3, an energy metabolism regulator that switches TNF-induced cell death from apoptosis to necrosis. *Science* 325, 332-336.
- Zhang, H., Zhou, X., McQuade, T., Li, J., Chan, F.K., and Zhang, J. (2011). Functional complementation between FADD and RIP1 in embryos and lymphocytes. *Nature* 471, 373-376.
- Zhang, J., Cado, D., Chen, A., Kabra, N.H., and Winoto, A. (1998). Fas-mediated apoptosis and activation-induced T-cell proliferation are defective in mice lacking FADD/Mort1. *Nature* 392, 296-300.
- Zhang, J., Kabra, N.H., Cado, D., Kang, C., and Winoto, A. (2001). FADD-deficient T cells exhibit a disaccord in regulation of the cell cycle machinery. *J Biol Chem* 276, 29815-29818.
- Zhou, R., Wei, H., Sun, R., and Tian, Z. (2007). Recognition of double-stranded RNA by TLR3 induces severe small intestinal injury in mice. *J Immunol* 178, 4548-4556.

Acknowledgements

I would like to thank Prof. Manolis Pasparakis for offering me the chance to work in his Lab and for his support throughout the whole PHD thesis. I very much appreciate his scientific guidance and his never declining interest in my work.

I am deeply grateful for the help offered by Andy Wullaert and Katerina Vlantis, who never became tired of supervising and helping me, whenever help was needed. I specially want to thank Andy for his commitment during the revision and his overall contribution to our publication, as well as for his comments for this manuscript. I would like to thank Vanesa Fernández-Majada for many encouraging and helpful discussions, her comments to this manuscript and her support inside and outside the lab.

I want to express my appreciation for the great help provided by the team of our technical assistants Daniela Baier, Jennifer Buchholz, Brigitte Hülser, Patrick Jankowski, Elza Mahlberg, Claudia Uthoff-Hachenberg, Julia von Rhein, and Bianca Wolff. I would like to thank Martin Hafner, Silke Röpke and Johannes Winkler for their efforts in handling the bureaucratic and administrative issues that had to be dealt with during my thesis. I also like to thank Chun Kim for numerous inspiring discussions, Ralph Gareus and all the other former and current members of the Pasparakis lab, who were always willing to help and made the time in- and outside the lab a valuable experience. I would like to express my gratitude to all co-operators that contributed to this work, especially Geert van Loo with whom it was a great pleasure to discuss current results and for sharing his ideas. I deeply appreciate the friendly support offered by Prof. Carien Niessen during the rotation period and throughout my whole PHD thesis as a member of my PHD committee. Finally, I would like to thank the International Graduate School in Genetics and Functional Genomics for funding the first part of my PHD thesis and Isabell Witt for her dedication to the organisation of the various classes and events that were offered by the Graduate School.

Diese Doktorarbeit wäre nicht ohne die Unterstützung meiner Familie und Freunde möglich gewesen. Ich möchte mich vielmals für die Hilfe in einfachen und schwierigen Zeiten bedanken.

Teile dieser Doktorarbeit wurden in folgender Publikation veröffentlicht:

Welz, P.S., Wullaert, A., Vlantis, K., Kondylis, V., Fernandez-Majada, V., Ermolaeva, M., Kirsch, P., Sterner-Kock, A., van Loo, G., and Pasparakis, M. (2011). FADD prevents RIP3-mediated epithelial cell necrosis and chronic intestinal inflammation. *Nature* 477, 330-334.

FADD prevents RIP3-mediated epithelial cell necrosis and chronic intestinal inflammation

Patrick-Simon Welz¹, Andy Wullaert¹, Katerina Vlantis¹, Vangelis Kondylis¹, Vanesa Fernández-Majada¹, Maria Ermolaeva¹, Petra Kirsch², Anja Sterner-Kock³, Geert van Loo⁴ & Manolis Pasparakis¹

Intestinal immune homeostasis depends on a tightly regulated cross talk between commensal bacteria, mucosal immune cells and intestinal epithelial cells (IECs)^{1–4}. Epithelial barrier disruption is considered to be a potential cause of inflammatory bowel disease; however, the mechanisms regulating intestinal epithelial integrity are poorly understood^{1,5}. Here we show that mice with IEC-specific knockout of FADD (FADD^{IEC-KO}), an adaptor protein required for death-receptor-induced apoptosis⁶, spontaneously developed epithelial cell necrosis, loss of Paneth cells, enteritis and severe erosive colitis. Genetic deficiency in RIP3, a critical regulator of programmed necrosis^{7–9}, prevented the development of spontaneous pathology in both the small intestine and colon of FADD^{IEC-KO} mice, demonstrating that intestinal inflammation is triggered by RIP3-dependent death of FADD-deficient IECs. Epithelial-specific inhibition of CYLD, a deubiquitinase that regulates cellular necrosis¹⁰, prevented colitis development in FADD^{IEC-KO} but not in NEMO^{IEC-KO} mice¹¹, showing that different mechanisms mediated death of colonic epithelial cells in these two models. In FADD^{IEC-KO} mice, TNF deficiency ameliorated colon inflammation, whereas MYD88 deficiency and also elimination of the microbiota prevented colon inflammation, indicating that bacteria-mediated Toll-like-receptor signalling drives colitis by inducing the expression of TNF and other cytokines. However, neither CYLD, TNF or MYD88 deficiency nor elimination of the microbiota could prevent Paneth cell loss and enteritis in FADD^{IEC-KO} mice, showing that different mechanisms drive RIP3-dependent necrosis of FADD-deficient IECs in the small and large bowel. Therefore, by inhibiting RIP3-mediated IEC necrosis, FADD preserves epithelial barrier integrity and antibacterial defence, maintains homeostasis and prevents chronic intestinal inflammation. Collectively, these results show that mechanisms preventing RIP3-mediated epithelial cell death are critical for the maintenance of intestinal homeostasis and indicate that programmed necrosis of IECs might be implicated in the pathogenesis of inflammatory bowel disease, in which Paneth cell and barrier defects are thought to contribute to intestinal inflammation.

To study the role of FADD in the intestinal epithelium we crossed mice carrying loxP-flanked *Fadd* alleles (FADD^{FL}) with villin-Cre transgenics (Fig. 1a, b). FADD^{IEC-KO} mice were born normally but developed a spontaneous phenotype resulting in the death of about 50% of these animals before weaning. Surviving FADD^{IEC-KO} mice showed reduced body weight and diarrhoea, indicating that they suffered from intestinal disease. High-resolution mini-endoscopy revealed mucosal thickening, ulceration and altered vascularisation in the colon of FADD^{IEC-KO} mice (Fig. 1c). Macroscopically, colons from FADD^{IEC-KO} mice were shorter and thicker compared to controls (Fig. 1d). Histological analysis of colon sections from 10-week-old FADD^{IEC-KO} mice revealed severe transmural inflammation affecting the entire colon with large areas of

epithelial erosion accompanied by crypt abscesses (Fig. 1e, f). Whereas FADD^{IEC-KO} mice developed spontaneous colitis with 100% penetrance, none of their FADD^{FL} littermates housed in the same cages showed any signs of colon inflammation, showing that colitis development was determined by FADD deficiency in IECs and was not transferable horizontally to co-housed wild-type littermates. Dying epithelial cells and early signs of inflammation were detectable in 2-week-old FADD^{IEC-KO} mice, and crypt abscesses together with increased immune cell infiltration and epithelial hyperproliferation were observed in 3-week-old animals (Fig. 1e). Increased cytokine and chemokine expression (Fig. 1g) and infiltration of F4/80⁺ and Gr-1⁺ myeloid cells initially, but also T and B lymphocytes in older animals, were detected in the colons of FADD^{IEC-KO} mice (Supplementary Fig. 1). However, FADD^{IEC-KO}/*Rag1*^{-/-} mice developed colitis, showing that T and B cells are not essential for colon inflammation in this model (data not shown). Thus, epithelial-specific FADD ablation caused the spontaneous development of severe colon inflammation driven primarily by an innate immune response. Immunostaining for Ki67 and cyclin D1 mRNA expression analysis revealed ongoing epithelial regeneration with increased epithelial cell proliferation in the colon of FADD^{IEC-KO} mice (Supplementary Fig. 2). In some cases, dysplastic crypts were detected in colons from 10-week-old FADD^{IEC-KO} mice, indicating that the chronic inflammatory and regenerative lesions occasionally resulted in epithelial dysplasia (data not shown).

Histological analysis of colon sections from FADD^{IEC-KO} mice revealed increased death of crypt epithelial cells in 2- to 3-week-old mice (Fig. 1e), indicating that epithelial cell death occurs early on during lesion development. Consistent with the well-established role of FADD as a mediator of apoptosis^{6,12,13}, many of the dead cells observed in crypt abscesses and early dying cells in the crypt epithelium did not stain with antibodies recognizing active caspase 3 (Fig. 2a), indicating that these cells did not die by apoptosis. Electron microscopy revealed epithelial cells showing signs of cellular necrosis such as disruption of the plasma membrane, swollen organelles, lack of chromatin condensation in the nucleus and a cytoplasm with lower electron density (Fig. 2b and Supplementary Fig. 3), indicating that FADD-deficient IECs mainly undergo necrotic cell death. Caspase inhibition and lack of FADD or caspase 8 were previously shown to sensitize certain cell types to a particular type of necrotic death, termed programmed necrosis or necroptosis, which is induced by death receptors such as TNFR1 and requires the kinases RIP1 and RIP3 (refs 7–9, 14–16). We therefore reasoned that programmed necrosis of FADD-deficient IECs could be a critical early event triggering colitis in FADD^{IEC-KO} mice. Primary IECs lacking FADD expressed increased levels of RIP3, an essential mediator of programmed necrosis^{7–9,14,17}, indicating that FADD deficiency might sensitize colonic epithelial cells to RIP3-dependent necrosis (Fig. 2c, d). To assess unambiguously the role of RIP3 in epithelial cell death

¹Institute for Genetics, Centre for Molecular Medicine (CMMC), and Cologne Excellence Cluster on Cellular Stress Responses in Aging-Associated Diseases (CECAD), University of Cologne, Zùlpicher Str. 47a, 50674 Cologne, Germany. ²Tierforschungszentrum, University of Ulm, Albert-Einstein-Allee 11, D-89081 Ulm, Germany. ³Center for Experimental Medicine, Uniklinik Köln, University of Cologne, Robert-Kochstr. 10, 50931 Cologne, Germany. ⁴Department for Molecular Biomedical Research, VIB, and Department of Biomedical Molecular Biology, Ghent University, Technologiepark 927, 9052 Ghent, Belgium.

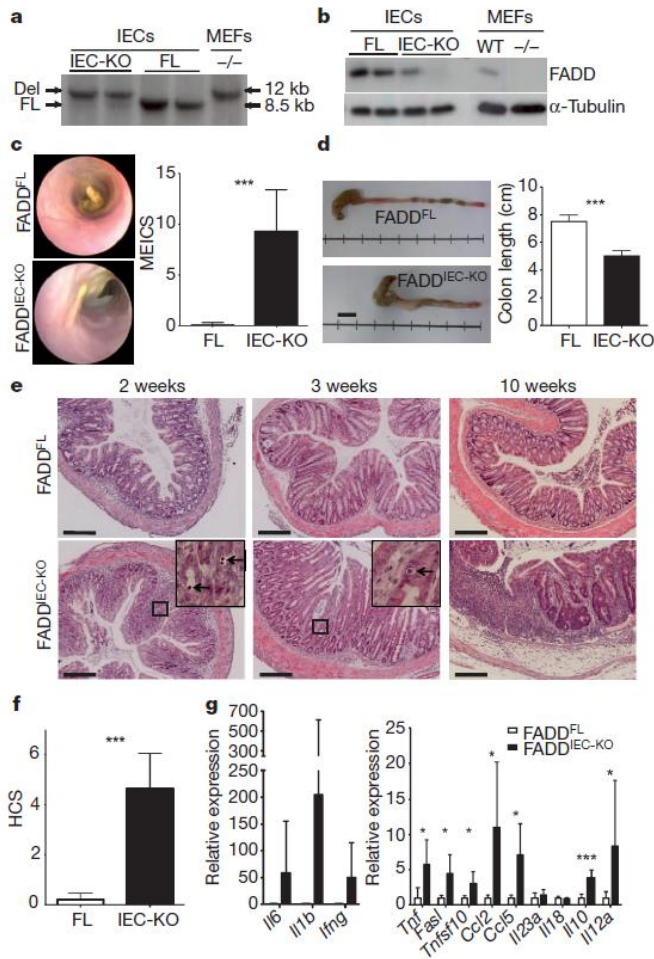


Figure 1 | Mice with IEC-specific ablation of FADD spontaneously develop severe colitis. **a**, **b**, Southern blot of EcoRV-digested genomic DNA (**a**) and immunoblot of protein extracts (**b**) from colonic IECs from FADD^{FL} and FADD^{IEC-KO} mice and from wild-type (WT) and *Fadd*^{-/-} (-/-) MEFs. Del, deleted; FL, loxP flanked. α -Tubulin serves as loading control. **c**, Representative endoscopic images and quantification of murine endoscopic index of colitis severity (MEICS) in FADD^{IEC-KO} (*n* = 31) and FADD^{FL} littermates (*n* = 37). **d**, Representative colon pictures and quantification of colon length in FADD^{IEC-KO} (*n* = 4) and FADD^{FL} littermates (*n* = 5). Scale bar, 1 cm. **e**, Representative histological images from haematoxylin & eosin stained colon sections from FADD^{FL} and FADD^{IEC-KO} mice. Arrows in insets indicate dying epithelial cells in 2- and 3-week-old mice. Scale bars, 100 μ m. **f**, Histological colitis score (HCS) measuring severity of inflammation and tissue damage in colons from FADD^{FL} (*n* = 7) and FADD^{IEC-KO} (*n* = 7) mice. **g**, Quantitative polymerase chain reaction with reverse transcription (qRT-PCR) analysis of cytokine and chemokine expression in colons from 10-week-old FADD^{IEC-KO} and FADD^{FL} littermates (*n* = 5–8 for each genotype). All graphs show mean values \pm standard deviation (s.d.). **P* \leq 0.05; ****P* \leq 0.005.

and colitis development, we crossed FADD^{IEC-KO} mice with RIP3-deficient mice¹⁸. FADD^{IEC-KO}/*Ripk3*^{-/-} mice developed normally and did not show macroscopic signs of disease and the early lethality associated with epithelial FADD deficiency. Moreover, colon sections from double-deficient FADD^{IEC-KO}/*Ripk3*^{-/-} mice showed a normal histology without signs of epithelial cell death or inflammation (Fig. 2e), demonstrating that RIP3 is essential for the spontaneous death of epithelial cells and the development of colitis in FADD^{IEC-KO} mice.

The deubiquitinating enzyme CYLD was identified as an important mediator of TNFR1-induced necrosis, presumably acting by deubiquitinating RIP1 to facilitate the formation of the RIP1/RIP3-containing ‘necrosome’ complex^{10,14}. To assess whether CYLD catalytic activity

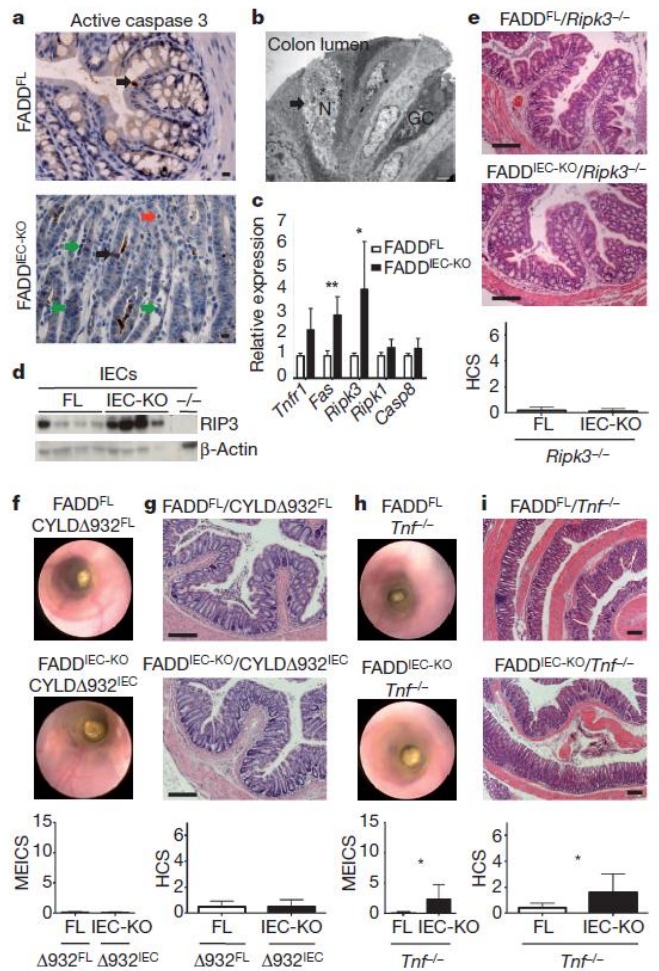


Figure 2 | RIP3- and CYLD-dependent necrosis of IECs triggers colitis in FADD^{IEC-KO} mice. **a**, Colon sections from FADD^{IEC-KO} and FADD^{FL} mice were immunostained for active caspase 3 (brown) and counterstained with haematoxylin (blue). Black arrow indicates apoptotic, red arrow shows early resident necrotic and green arrows show late detached necrotic epithelial cells. **b**, Representative electron microscopy picture showing a necrotic epithelial cell (arrow) in the proximal colon of a FADD^{IEC-KO} mouse. GC, goblet cell; N, nucleus. Scale bar, 2 μ m. **c**, qRT-PCR showed increased *Tnfr1*, *Fas* and *Ripk3* messenger RNA expression in colonic IECs from FADD^{IEC-KO} (*n* = 3) compared to FADD^{FL} (*n* = 4) mice. **d**, Immunoblotting for RIP3 and β -actin (loading control) in colonic IECs from FADD^{IEC-KO} (IEC-KO), FADD^{FL} (FL) and *Ripk3*^{-/-} (-/-) mice. Lanes represent IECs from individual mice. **e**, Representative histological images and quantification of HCS in colon sections from FADD^{IEC-KO}/*Ripk3*^{-/-} (*n* = 5) and FADD^{FL}/*Ripk3*^{-/-} (*n* = 3) littermates. **f**, Representative endoscopic images and quantification of MEICS in colons from FADD^{IEC-KO}/*CYLD* Δ 932^{IEC} (*n* = 11) and FADD^{FL}/*CYLD* Δ 932^{FL} (*n* = 7) littermates. **g**, Representative histological images and quantification of HCS in colon sections from FADD^{IEC-KO}/*CYLD* Δ 932^{IEC} (*n* = 10) and FADD^{FL}/*CYLD* Δ 932^{FL} (*n* = 6) littermates. **h**, Representative endoscopic images and quantification of MEICS in colons from FADD^{IEC-KO}/*Tnf*^{-/-} (*n* = 6) and FADD^{FL}/*Tnf*^{-/-} (*n* = 6) littermates. **i**, Representative histological images and quantification of HCS in colon sections from FADD^{IEC-KO}/*Tnf*^{-/-} (*n* = 5) and FADD^{FL}/*Tnf*^{-/-} (*n* = 6) littermates. All graphs show mean values \pm s.d. **P* \leq 0.05; ***P* \leq 0.01. Scale bars: **a**, 10 μ m; **b**, 2 μ m, **e**, **g** and **i**, 100 μ m.

was required for spontaneous programmed necrosis of FADD-deficient IECs, we crossed FADD^{IEC-KO} mice with mice carrying conditional *CYLD* Δ 932^{FL} alleles, which upon Cre recombination produce truncated *CYLD* Δ 932 protein lacking the last 20 amino acids that are essential for its deubiquitinase activity¹⁹ (Supplementary Fig. 4a). Mouse embryonic fibroblasts (MEFs) homozygously expressing

truncated CYLD Δ 932 were protected from TNF-induced death in the presence of the pan-caspase inhibitor zVAD-fmk, demonstrating that CYLD deubiquitinase activity is important for necroptosis (Supplementary Fig. 4d). FADD^{IEC-KO}/CYLD Δ 932^{IEC} mice, which lack FADD and at the same time express catalytically inactive CYLD Δ 932 specifically in IECs (Supplementary Fig. 4b, c), did not show any macroscopic signs of disease such as reduced weight or diarrhoea. In addition, endoscopic (Fig. 2f) and histological analysis (Fig. 2g) did not reveal signs of inflammation or epithelial destruction in the colons of FADD^{IEC-KO}/CYLD Δ 932^{IEC} mice. Therefore, CYLD catalytic activity is required for colonocyte death and colitis development in FADD^{IEC-KO} mice. CYLD was also shown to contribute to TNF-induced apoptosis in the presence of Smac-mimetic compounds inducing the degradation of cIAP1/2 (ref. 20). We therefore investigated whether CYLD catalytic activity is also required for epithelial cell death and colitis development in NEMO^{IEC-KO} mice, which show increased IEC apoptosis and spontaneously develop severe chronic colon inflammation¹¹. In contrast to FADD^{IEC-KO}/CYLD Δ 932^{IEC} mice, NEMO^{IEC-KO}/CYLD Δ 932^{IEC} animals developed severe colitis similarly to single NEMO^{IEC-KO} mice as assessed by endoscopic and histological analysis (Supplementary Fig. 5). Therefore, inhibition of CYLD catalytic activity prevented epithelial cell death and colitis development in FADD^{IEC-KO} but not in NEMO^{IEC-KO} mice, indicating that the IECs in these two models die by different mechanisms.

TNF is a potent inducer of necroptosis and has an important pathogenic role in the development of intestinal inflammation in both humans and animal models^{21,22}. We therefore crossed FADD^{IEC-KO} mice with TNF-deficient mice to investigate whether TNF is implicated in colitis development in this model. Endoscopic and histological analysis of FADD^{IEC-KO}/Tnf^{-/-} mice showed areas of mild focal epithelial lesions in the colonic mucosa characterized by crypt elongation and the presence of inflammatory infiltrates (Fig. 2h, i). However, endoscopic and histological inflammation scores in FADD^{IEC-KO}/Tnf^{-/-} mice were significantly lower compared to FADD^{IEC-KO} animals, showing that TNF deficiency strongly ameliorated but could not completely prevent colon inflammation. Thus, TNF has an important role but TNF-independent mechanisms also contribute to the pathogenesis of colitis in FADD^{IEC-KO} mice.

Epithelial cell death could trigger colitis by disrupting the epithelial barrier thus allowing commensal bacteria to invade the mucosa, where they could induce inflammation by activating Toll-like-receptor (TLR) signalling on mucosal immune cells. To address the potential role of TLR signalling in colitis development, we crossed FADD^{IEC-KO} mice with mice lacking MYD88, an essential adaptor molecule for signalling downstream of most TLRs. FADD^{IEC-KO}/Myd88^{-/-} mice did not show macroscopic, endoscopic or histological signs of colon inflammation (Fig. 3a, b) demonstrating that MYD88-dependent signalling is essential for colitis development and suggesting that inflammation could be driven by commensal bacteria. Indeed, treatment with broad-spectrum antibiotics strongly attenuated colon inflammation in FADD^{IEC-KO} mice (Supplementary Fig. 6). Furthermore, FADD^{IEC-KO} mice raised in germ-free conditions did not show any endoscopic or histological signs of colon inflammation (Fig. 3c, d). When young adult germ-free FADD^{IEC-KO} mice were conventionalized by exposure to the microbiota of SPF mice they rapidly developed severe intestinal disease leading to the death of 4 out of 12 animals within 7 days (Supplementary Table 1). Endoscopic and histological analysis of colons from conventionalized FADD^{IEC-KO} mice 7 days after co-housing revealed severe colitis with mucosal thickening, epithelial erosion and transmural inflammation (Fig. 3c, d). Collectively, these results show that commensal bacteria induce colitis in FADD^{IEC-KO} mice by activating MYD88-dependent TLR signalling. Although the cellular targets of bacteria-induced TLR signalling in this model remain unclear at present, it is likely that the microbiota induces colitis development by activating the expression of TNF and other proinflammatory cytokines in mucosal immune cells. Indeed, conventionalization induced

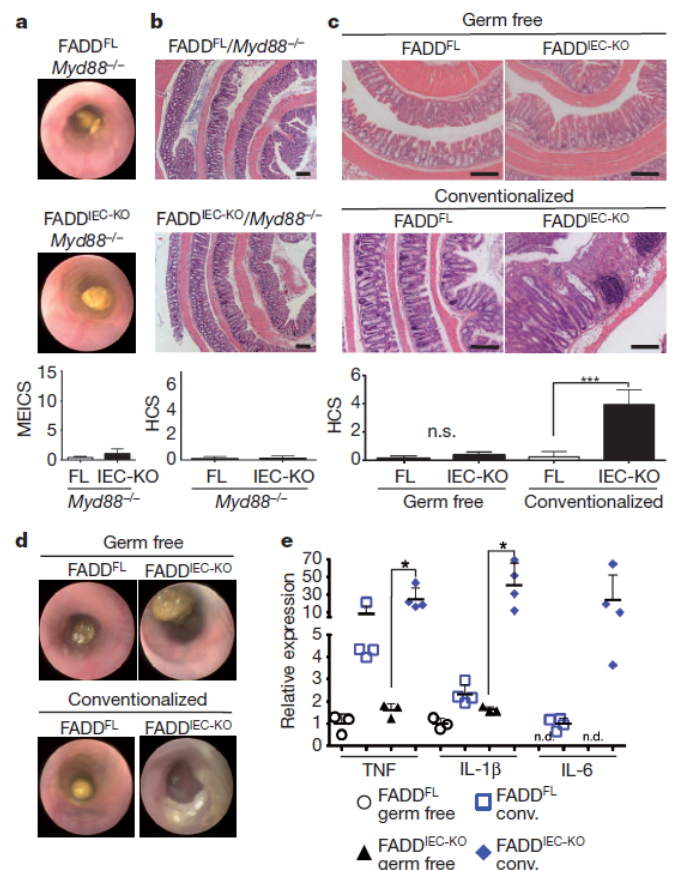


Figure 3 | Spontaneous colitis development in FADD^{IEC-KO} mice requires MYD88-dependent signalling and the presence of the microbiota. **a**, Representative endoscopic images and quantification of MEICS in colons from FADD^{IEC-KO}/Myd88^{-/-} ($n = 9$) and FADD^{FL}/Myd88^{-/-} ($n = 6$) littermates. **b**, Representative histological images and quantification of HCS in colon sections from FADD^{IEC-KO}/Myd88^{-/-} ($n = 9$) and FADD^{FL}/Myd88^{-/-} ($n = 6$) littermates. **c**, Representative histological images and quantification of HCS in colon sections from germ-free FADD^{FL} ($n = 5$), germ-free FADD^{IEC-KO} ($n = 7$), conventionalized FADD^{FL} ($n = 8$) and conventionalized FADD^{IEC-KO} ($n = 8$) mice. n.s., not significant. **d**, Representative endoscopic colon images of germ-free and conventionalized FADD^{FL} and FADD^{IEC-KO} mice. **e**, qRT-PCR analysis of TNF, IL-1 β and IL-6 expression in colons of conventionalized (conv.) FADD^{FL} and FADD^{IEC-KO} mice compared to germ-free animals. n.d., not detectable. Graphs show mean values \pm s.d. * $P \leq 0.05$; ** $P \leq 0.01$; *** $P \leq 0.005$. Scale bars, 100 μ m.

increased expression of TNF, IL-1 β and IL-6 in the colons of both control FADD^{FL} and FADD^{IEC-KO} mice (Fig. 3e), supporting the notion that bacteria trigger colitis by inducing cytokine expression in the colonic mucosa.

In addition to colitis, FADD^{IEC-KO} mice also developed enteritis characterized by altered intestinal architecture with blunted and fused villi, mucosal oedema and increased cellularity of the lamina propria (Fig. 4a). Consistent with inflammatory changes, increased numbers of granulocytes and increased epithelial cell proliferation were detected in the small intestine of FADD^{IEC-KO} mice (Supplementary Fig. 7). In addition, small intestinal crypts in FADD^{IEC-KO} mice contained strongly reduced numbers of Paneth cells, as identified by their characteristic morphology with a large cytoplasm filled with eosinophilic granules (Fig. 4a). Immunostaining for lysozyme, an early marker of Paneth cells, confirmed the strongly reduced Paneth cell numbers in FADD^{IEC-KO} mice (Fig. 4b). Paneth cells are believed to contribute to the intestinal antibacterial defence by releasing antimicrobial factors stored in cytoplasmic granules. Consistent with the reduced Paneth cell numbers, we detected impaired expression of antimicrobial factors

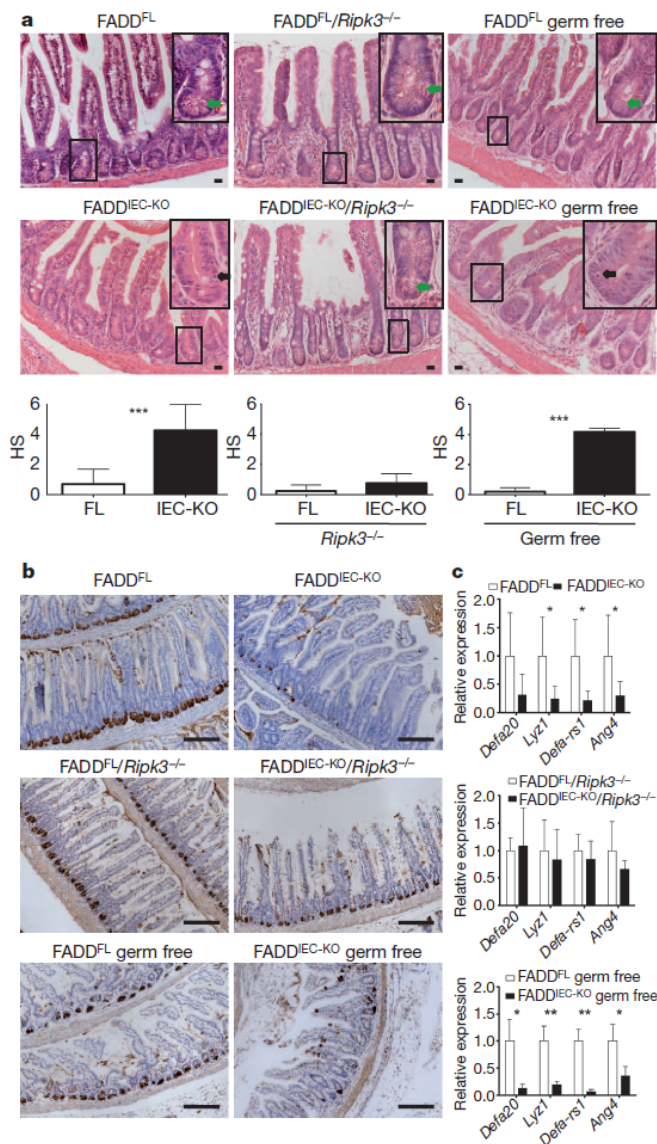


Figure 4 | Spontaneous development of enteritis and loss of Paneth cells in FADD^{IEC-KO} mice requires RIP3-mediated necrosis of IECs but does not depend on the microbiota. **a**, Representative histological images and quantification of histological score (HS) in small intestinal sections from mice with the indicated genotypes. FADD^{IEC-KO} mice show death of small intestinal IECs, enteritis and loss of Paneth cells. This pathology was prevented by RIP3 deficiency but persisted in germ-free FADD^{IEC-KO} mice. Green arrows indicate Paneth cells, black arrows indicate dying crypt epithelial cells in insets. FADD^{FL} ($n = 11$), FADD^{IEC-KO} ($n = 8$), FADD^{FL}/*Ripk3*^{-/-} ($n = 6$), FADD^{IEC-KO}/*Ripk3*^{-/-} ($n = 4$), germ-free FADD^{FL} ($n = 5$), germ-free FADD^{IEC-KO} ($n = 7$). **b**, Small intestinal sections were immunostained for lysozyme (brown) and counterstained with haematoxylin (blue). Paneth cell loss was prevented by RIP3 deficiency but persisted in germ-free FADD^{IEC-KO} mice. **c**, Expression of the Paneth-cell-specific genes *Defa20*, *Lyz1*, *Defa-rs1* and *Ang4* was measured by qRT-PCR in small intestinal mRNA samples from mice with the indicated genotypes. FADD^{FL} ($n = 6$), FADD^{IEC-KO} ($n = 6$), FADD^{FL}/*Ripk3*^{-/-} ($n = 3$), FADD^{IEC-KO}/*Ripk3*^{-/-} ($n = 5$), germ-free FADD^{FL} ($n = 3$), germ-free FADD^{IEC-KO} ($n = 3$). Graphs show mean values \pm s.d. * $P \leq 0.05$; ** $P \leq 0.01$. Scale bars: **a**, 10 μ m; **b**, 100 μ m.

including lysozyme (*Lyz1*), α -defensin 20 (*Defa20*), α -defensin-related sequence 1 (*Defa-rs1*) and angiogenin 4 (*Ang4*) in the ileum of FADD^{IEC-KO} mice (Fig. 4c). Increased numbers of dying epithelial cells that did not stain with antibodies recognizing active caspase 3 were detected in small intestinal crypts from FADD^{IEC-KO} mice

(Supplementary Fig. 8), suggesting that caspase-independent death of FADD-deficient IECs could contribute to the development of enteritis. Indeed, RIP3 deficiency prevented epithelial cell death, Paneth cell loss and enteritis in FADD^{IEC-KO} mice (Fig. 4 and Supplementary Fig. 8), demonstrating that, similarly to the colitis, the small intestinal lesions are caused by RIP3-dependent programmed necrosis of FADD-deficient IECs. However, in contrast to our findings in the colon, neither the absence of the microbiota nor genetic deficiency in MYD88, TNF or CYLD could prevent Paneth cell loss and enteritis in FADD^{IEC-KO} mice (Fig. 4 and Supplementary Figs 7–9). These results indicate that different, perhaps cell-intrinsic mechanisms induce RIP3-dependent programmed necrosis of small intestinal IECs. Interestingly, mice with epithelial-specific ablation of the transcription factor XBP1, a critical regulator of the endoplasmic reticulum stress response, developed spontaneous enteritis and Paneth cell loss²³, and mutations affecting autophagy also caused Paneth cell abnormalities²⁴. These findings indicated that owing to their highly secretory activity Paneth cells are particularly sensitive to endoplasmic reticulum stress and autophagy defects¹. Although the mechanisms inducing RIP3-dependent necrosis of small intestinal IECs in FADD^{IEC-KO} mice remain unclear at present, it is tempting to speculate that pathways linked to endoplasmic reticulum stress or autophagy might be implicated in triggering programmed necrosis of epithelial cells, Paneth cell loss and enteritis in these animals. Paneth cell loss might also be important for the development of colitis in FADD^{IEC-KO} mice, as reduced expression of Paneth-cell-derived antimicrobial factors could induce alterations in the microbiota, which might contribute to the bacteria-driven mechanisms triggering programmed necrosis of colonic epithelial cells and inflammation.

Our *in vivo* genetic mouse model studies indicate that mechanisms regulating programmed necrosis in IECs might be relevant for the pathogenesis of chronic intestinal inflammation in humans. Paneth cell defects leading to impaired antimicrobial peptide expression have been suggested to contribute to the pathogenesis of inflammatory bowel disease¹. Interestingly, epithelial patchy necrosis has been detected in the colon of Crohn's disease patients, indicating that necrotic death of IECs might be implicated in human colon inflammation²⁵. In this context, the potential capacity of enteropathogenic bacteria or viruses to induce TNF expression in the intestinal mucosa and at the same time to modulate epithelial responses to TNF signalling, for example by expressing inhibitors of apoptosis or programmed necrosis¹⁷, might be critical for triggering acute episodes of intestinal inflammation or precipitating chronic inflammatory bowel disease in genetically susceptible individuals. Moreover, our results indicate that anti-TNF therapy, shown to be highly effective in a subset of inflammatory bowel disease patients²², might in part function by preventing TNF-mediated necrosis of epithelial cells. Taken together, our findings revealed a previously unrecognized essential physiological function of FADD in protecting epithelial cells from RIP3-dependent necrosis and preventing intestinal inflammation *in vivo*. This function of FADD seems to be cell specific, as conditional FADD ablation did not sensitize hepatocytes²⁶ or oligodendrocytes²⁷ to spontaneous programmed necrosis but on the contrary protected these cells from TNF- or autoimmune-inflammation-induced cytotoxicity, respectively. In addition to recent studies showing that regulation of RIP-kinase-mediated necrosis is important for embryonic development^{28–30}, our findings provide a paradigm demonstrating that sensitization of epithelial cells to programmed necrosis triggers chronic inflammation *in vivo*, highlighting the significance of the mechanisms regulating programmed necrosis for the maintenance of physiological immune homeostasis and the prevention of inflammation in epithelial surfaces.

METHODS SUMMARY

Mice were maintained at the SPF animal facility of the Institute for Genetics, University of Cologne. Mice were either generated using gene targeting in C57BL/6 embryonic stem cells (Bruce4) or backcrossed for at least 10 generations

into the C57BL/6 genetic background. Germ-free mice were produced at the gnotobiotic facility of the University of Ulm and were conventionalized as described in detail in Supplementary Table 1. Endoscopic analysis was performed using a high-resolution mini-endoscope, Coloview (Karl-Storz). IECs were isolated by sequential incubation of intestinal tissue in 1 mM dithiothreitol (DTT) and 1.5 mM EDTA solutions. RNA preparation and RT-PCR analysis, protein extraction and immunoblotting, tissue preparation and immunohistological analysis were performed using standard protocols. Haematoxylin & eosin stained sections were scored in a blinded fashion for the amount of inflammation and tissue damage on separate scales from 0 to 3, which were added to a total score of 0 to 6.

Full Methods and any associated references are available in the online version of the paper at www.nature.com/nature.

Received 1 December 2010; accepted 6 June 2011.

Published online 31 July 2011.

- Kaser, A., Zeissig, S. & Blumberg, R. S. Inflammatory bowel disease. *Annu. Rev. Immunol.* **28**, 573–621 (2010).
- Strober, W., Fuss, I. & Mannon, P. The fundamental basis of inflammatory bowel disease. *J. Clin. Invest.* **117**, 514–521 (2007).
- MacDonald, T. T. & Monteleone, G. Immunity, inflammation, and allergy in the gut. *Science* **307**, 1920–1925 (2005).
- Xavier, R. J. & Podolsky, D. K. Unravelling the pathogenesis of inflammatory bowel disease. *Nature* **448**, 427–434 (2007).
- Turner, J. R. Intestinal mucosal barrier function in health and disease. *Nature Rev. Immunol.* **9**, 799–809 (2009).
- Wilson, N. S., Dixit, V. & Ashkenazi, A. Death receptor signal transducers: nodes of coordination in immune signaling networks. *Nature Immunol.* **10**, 348–355 (2009).
- Cho, Y. S. *et al.* Phosphorylation-driven assembly of the RIP1–RIP3 complex regulates programmed necrosis and virus-induced inflammation. *Cell* **137**, 1112–1123 (2009).
- He, S. *et al.* Receptor interacting protein kinase-3 determines cellular necrotic response to TNF- α . *Cell* **137**, 1100–1111 (2009).
- Zhang, D. W. *et al.* RIP3, an energy metabolism regulator that switches TNF-induced cell death from apoptosis to necrosis. *Science* **325**, 332–336 (2009).
- Hitomi, J. *et al.* Identification of a molecular signaling network that regulates a cellular necrotic cell death pathway. *Cell* **135**, 1311–1323 (2008).
- Nenci, A. *et al.* Epithelial NEMO links innate immunity to chronic intestinal inflammation. *Nature* **446**, 557–561 (2007).
- Zhang, J., Cado, D., Chen, A., Kabra, N. H. & Winoto, A. Fas-mediated apoptosis and activation-induced T-cell proliferation are defective in mice lacking FADD/Mort1. *Nature* **392**, 296–300 (1998).
- Yeh, W. C. *et al.* FADD: essential for embryo development and signaling from some, but not all, inducers of apoptosis. *Science* **279**, 1954–1958 (1998).
- Vandenabeele, P., Galluzzi, L., Vanden Berghe, T. & Kroemer, G. Molecular mechanisms of necroptosis: an ordered cellular explosion. *Nature Rev. Mol. Cell Biol.* **11**, 700–714 (2010).
- Holler, N. *et al.* Fas triggers an alternative, caspase-8-independent cell death pathway using the kinase RIP as effector molecule. *Nature Immunol.* **1**, 489–495 (2000).
- Osborn, S. L. *et al.* Fas-associated death domain (FADD) is a negative regulator of T-cell receptor-mediated necroptosis. *Proc. Natl Acad. Sci. USA* **107**, 13034–13039 (2010).
- Upton, J. W., Kaiser, W. J. & Mocarski, E. S. Virus inhibition of RIP3-dependent necrosis. *Cell Host Microbe* **7**, 302–313 (2010).
- Newton, K., Sun, X. & Dixit, V. M. Kinase RIP3 is dispensable for normal NF- κ Bs, signaling by the B-cell and T-cell receptors, tumor necrosis factor receptor 1, and Toll-like receptors 2 and 4. *Mol. Cell. Biol.* **24**, 1464–1469 (2004).
- Kovalenko, A. *et al.* The tumour suppressor CYLD negatively regulates NF- κ B signalling by deubiquitination. *Nature* **424**, 801–805 (2003).
- Wang, L., Du, F. & Wang, X. TNF- α induces two distinct caspase-8 activation pathways. *Cell* **133**, 693–703 (2008).
- Kollias, G. TNF pathophysiology in murine models of chronic inflammation and autoimmunity. *Semin. Arthritis Rheum.* **34**, 3–6 (2005).
- Peyrin-Biroulet, L. Anti-TNF therapy in inflammatory bowel diseases: a huge review. *Minerva Gastroenterol. Dietol.* **56**, 233–243 (2010).
- Kaser, A. *et al.* XBP1 links ER stress to intestinal inflammation and confers genetic risk for human inflammatory bowel disease. *Cell* **134**, 743–756 (2008).
- Cadwell, K. *et al.* A key role for autophagy and the autophagy gene *Atg16l1* in mouse and human intestinal Paneth cells. *Nature* **456**, 259–263 (2008).
- Dourmashin, R. R. *et al.* Epithelial patchy necrosis in Crohn's disease. *Hum. Pathol.* **14**, 643–648 (1983).
- Luedde, T. *et al.* Deletion of NEMO/IKK γ in liver parenchymal cells causes steatohepatitis and hepatocellular carcinoma. *Cancer Cell* **11**, 119–132 (2007).
- Mc Guire, C. *et al.* Oligodendrocyte-specific FADD deletion protects mice from autoimmune-mediated demyelination. *J. Immunol.* **185**, 7646–7653 (2010).
- Zhang, H. *et al.* Functional complementation between FADD and RIP1 in embryos and lymphocytes. *Nature* **471**, 373–376 (2011).
- Oberst, A. *et al.* Catalytic activity of the caspase-8-FLIP_L complex inhibits RIPK3-dependent necrosis. *Nature* **471**, 363–367 (2011).
- Kaiser, W. J. *et al.* RIP3 mediates the embryonic lethality of caspase-8-deficient mice. *Nature* **471**, 368–372 (2011).

Supplementary Information is linked to the online version of the paper at www.nature.com/nature.

Acknowledgements We thank C. Uthoff-Hachenberg, J. Pfeiffer, E. Mahlberg, D. Beier, J. Buchholz, B. Huelser, B. Wolff, E. Merkel and S. Schmidt for technical support. We also thank V. Dixit and K. Newton for providing *Ripk3*^{-/-} mice and R. Massoumi for providing anti-CYLD antibody. This work was funded by grants from the Deutsche Forschungsgemeinschaft (SFB 670, SFB 829, CECAD) and European Commission FP7 program grants 'INFLA-CARE' and 'Masterswitch' (EC contract numbers 223151 and 223404 respectively) to M.P. V. F.-M. was supported by a long-term EMBO fellowship, G.v.L. was supported by 'Group-ID MRP' of Ghent University and P.-S.W. was supported by a fellowship from the International Graduate School in Genetics and Functional Genomics at the University of Cologne.

Author Contributions P.-S.W., A.W., K.V., V.K., V.F.-M., M.E., P.K. and G.v.L. performed the research. P.-S.W., A.W., K.V., V.K., V.F.-M. and A.S.-K. analysed the data and contributed to writing the manuscript. M.P. provided ideas, co-ordinated the project and wrote the manuscript.

Author Information Reprints and permissions information is available at www.nature.com/reprints. The authors declare no competing financial interests. Readers are welcome to comment on the online version of this article at www.nature.com/nature. Correspondence and requests for materials should be addressed to M.P. (P.asparakis@uni-koeln.de).

METHODS

Mice. FADD^{FL} mice were generated as described previously²⁷ and the CYLDΔ932^{FL} mice were generated as described in Supplementary Fig. 4, using gene targeting in C57BL/6 embryonic stem cells (Bruce 4). Villin-Cre (ref. 31); *Tnf*^{-/-} (ref. 32), *Myd88*^{-/-} (ref. 33) and *Ripk3*^{-/-} (ref. 18) mice were backcrossed for at least 10 generations into the C57BL/6 genetic background. Mice were maintained at the SPF animal facility of the Institute for Genetics, University of Cologne, kept under a 12 h light cycle, and given a regular chow diet (Harlan, diet no. 2918) *ad libitum*. All animal procedures were conducted in accordance with European, national and institutional guidelines and protocols and were approved by local government authorities. For antibiotic treatment 1 g l⁻¹ ampicillin (ICN Biomedicals), 1 g l⁻¹ neomycin (Sigma), 0.5 g l⁻¹ meronem (AstraZeneca) and 0.5 g l⁻¹ ciprofloxacin (Fluka) were added to the drinking water starting from the second day after birth. At weaning, ciprofloxacin was substituted by 0.5 g l⁻¹ vancomycin (Eberth). Germ-free mice were produced at the gnotobiotic facility of the University of Ulm. Germ-free mice were conventionalized as described in detail in Supplementary Table 1. Sex-matched littermates not carrying the villin-Cre transgene were used as controls in all experiments. Unless otherwise indicated, mice were analysed between 6–12 weeks of age.

High-resolution mini-endoscopy. Mice were anaesthetized using intraperitoneal injection of ketamine (Ratiopharm)/rompun (Bayer) and a high-resolution mini-endoscope, Coloview (Karl-Storz), was used to determine the murine endoscopic index of colitis severity (MEICS), as described previously³⁴.

IEC isolation and immunoblotting. IECs were isolated by sequential incubation of intestinal tissue in 1 mM dithiothreitol (DTT) and 1.5 mM EDTA solutions as described previously³⁵. Protein extracts were prepared from IECs as described³⁶. Protease and phosphatase inhibitor tablets (Roche) were added to the lysis buffer. Protein extracts were separated by 10% SDS-PAGE gels and transferred to Immobilon-P PVDF membranes (Millipore). Membranes were probed with primary antibodies anti-FADD, anti- α -tubulin (Sigma), anti- β -actin (Santa Cruz), anti-mouse RIP3 (Enzo), anti-CYLD (provided by R. Masoumi). Membranes were incubated with secondary HRP-coupled antibodies (GE Healthcare and Jackson ImmuneResearch) and developed with chemiluminescent detection substrate (GE Healthcare and Thermo Scientific).

Histology. Tissues were fixed overnight in 4% paraformaldehyde, embedded in paraffin and cut in 4- μ m sections. Paraffin sections were rehydrated and heat-induced antigen retrieval was performed either in 10 mM sodium citrate, 0.05% Tween-20 pH 6 or in TEX (50 mM Tris, 1 mM EDTA, 0.5% Triton X-100; pH 8) with 20 μ g ml⁻¹ protease K. Primary antibodies used for IHC were anti-Ki67 (Dako), anti-Gr-1 (PharMingen), anti-F4/80, anti-B220 (homemade), anti-CD3 (Abcam), anti-active caspase 3 (R&D systems), anti-human lysozyme (Dako). Biotinylated secondary antibodies were purchased from Perkin Elmer and Dako. Stainings were visualized with ABC Kit Vectastain Elite (Vector) and DAB substrate (DAKO). Incubation times with the DAB substrate were equal for all samples. Haematoxylin & eosin stained sections were scored in a blinded fashion for the amount of inflammation and tissue damage on separate scales from 0 to 3, which were added to obtain a total histological colitis score of 0 to 6. For inflammation the scoring was defined as follows: 0, no inflammatory infiltrate in the lamina propria; 1, increased presence of inflammatory cells in the mucosa; 2, inflammatory infiltrate extending into the submucosa; 3, transmural extension of inflammatory infiltrate. For tissue damage, the scoring was defined as follows: 0, no mucosal damage; 1, discrete epithelial lesions; 2, extended epithelial damage associated with areas containing elongated crypts, crypt abscesses or focal

ulceration; 3, extensive ulceration of the bowel wall. For scoring the amount of inflammation and tissue damage in the small intestine similar scales from 0 to 3 were used, which were added to obtain a total histological score of 0 to 6. For small intestinal inflammation the scoring was defined as follows: 0, no inflammatory infiltrate in the lamina propria; 1, increased presence of inflammatory cells between the crypts; 2, inflammatory infiltrate extending into the villi; 3, extension of inflammatory infiltrate throughout the lamina propria. For tissue damage, the scoring was based on the percentage of small intestinal crypts affected by IEC death and Paneth cell loss as follows: 0, 0–10% of crypts affected; 1, 10–40% of crypts affected; 2, 40–70% of crypts affected; 3, more than 70% of crypts affected. For electron microscopy 3-mm-long samples from distal, medial and proximal colon were excised from FADD^{FL} and FADD^{IEC-KO} mice and immediately fixed in 2.5% glutaraldehyde/2% paraformaldehyde in phosphate buffer pH 7.4 for 3 h at room temperature (20 °C). The tissues were post-fixed in 1% OsO₄ and embedded in Epon resin. 70–90-nm sections were cut, stained with uranyl acetate and lead citrate and viewed under a Philips CM-10 transmission electron microscope. Representative pictures were captured using an Orius SC200 CCD camera (Gatan GmbH). Evaluation of cell death on histological sections was performed by an experienced pathologist (A.S.-K.).

Cell death assays. Primary MEFs were isolated from wild-type and homozygous CYLDΔ932 mice. For the induction of necroptosis, cells were pre-treated for one hour with 1 μ g ml⁻¹ cycloheximide (CHX; Sigma) and 20 μ M α VAD-fmk (ENZO) and subsequently stimulated with 1, 10 or 30 ng ml⁻¹ murine TNF for 12 h. Cell survival was determined by spectrophotometric measurement of crystal violet incorporation. Values are presented as per cent survival of triplicates compared to untreated cells.

Quantitative RT-PCR. Total RNA was extracted with Trizol Reagent (Invitrogen) and RNeasy Columns (Qiagen) and cDNA was prepared with Superscript III cDNA-synthesis Kit (Invitrogen). RT-PCR was performed with SyBrGreen or TaqMan analysis (Applied Biosystems). TATA-box-binding protein was used as a reference gene.

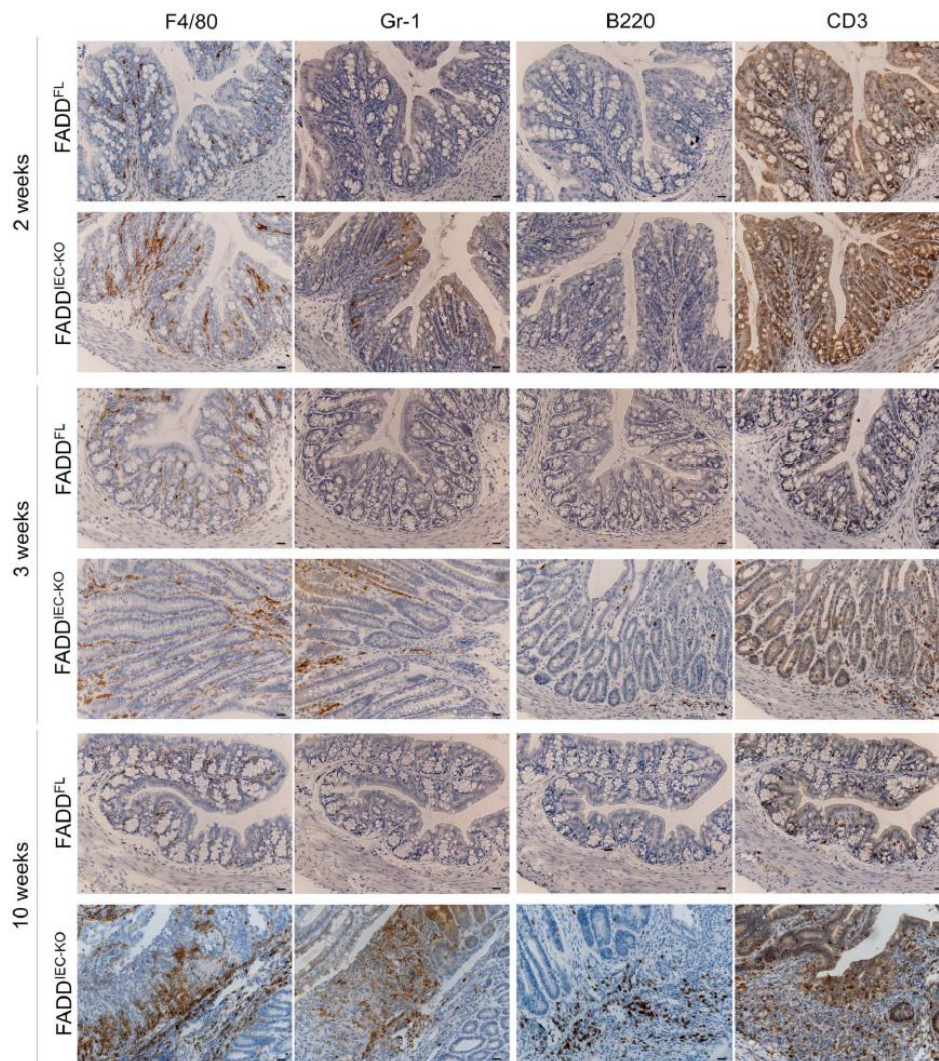
Southern blotting. Genomic DNA extraction, digestion and Southern blotting were performed according to standard protocols. The probe used for Southern blot analysis of the *Fadd* locus was amplified using primers: sense 5'-CGTGAGGA GCAGGCAAGCAG-3' and antisense 5'-TGGTGAAGCCCTCCAGCCTGT-3'.

Statistics. All data shown represent the mean \pm s.d. Statistical analyses were performed with unpaired Student's *t*-tests with unequal variance. **P* \leq 0.05; ***P* \leq 0.01; ****P* \leq 0.005.

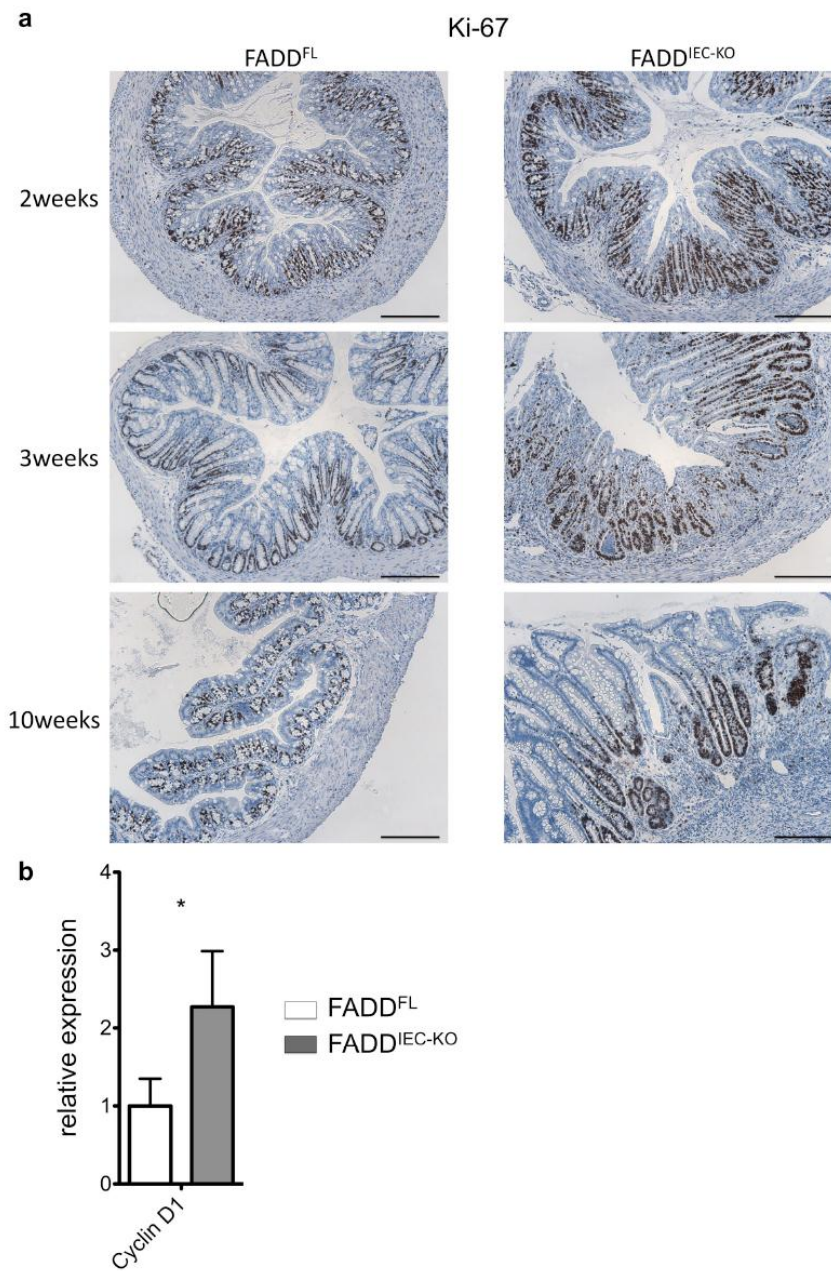
31. Madison, B. B. *et al.* cis elements of the villin gene control expression in restricted domains of the vertical (crypt) and horizontal (duodenum, cecum) axes of the intestine. *J. Biol. Chem.* **277**, 33275–33283 (2002).
32. Pasparakis, M., Alexopoulou, L., Episkopou, V. & Kollias, G. Immune and inflammatory responses in TNF α -deficient mice: a critical requirement for TNF α in the formation of primary B cell follicles, follicular dendritic cell networks and germinal centers, and in the maturation of the humoral immune response. *J. Exp. Med.* **184**, 1397–1411 (1996).
33. Adachi, O. *et al.* Targeted disruption of the *Myd88* gene results in loss of IL-1- and IL-18-mediated function. *Immunity* **9**, 143–150 (1998).
34. Becker, C. *et al.* *In vivo* imaging of colitis and colon cancer development in mice using high resolution chromoendoscopy. *Gut* **54**, 950–954 (2005).
35. Ukena, S. N. *et al.* Probiotic *Escherichia coli* Nissle 1917 inhibits leaky gut by enhancing mucosal integrity. *PLoS ONE* **2**, e1308 (2007).
36. Schmidt-Suppran, M. *et al.* NEMO/IKK γ -deficient mice model incontinentia pigmenti. *Mol. Cell* **5**, 981–992 (2000).

Supplementary table I. Detailed description of the mice used for the conventionalization experiment in figure 4e-h. Germ free mice were transferred from the gnotobiotic facility of the University of Ulm to the animal facility of the Institute for Genetics in Cologne in special containers ensuring maintenance of germ free status. For conventionalisation, 8-12 week old germ free mice were exposed to the microbiota of FADD^{FL}, FADD^{IEC-KO}/CYLDA932^{IEC} or FADD^{IEC-KO}/*Ripk3*^{-/-} mice as described in detail in the table below. In the case of female mice, they were co-housed in the same cage with the designated mouse, while male mice were exposed to bedding from a cage housing the designated mouse. All mice described in this experiment were conventionalised at the same time (March 1, 2011) and were followed for one week. Due to the fact that all conventionalized FADD^{IEC-KO} mice showed signs of severe colitis and 4 out of 12 died within a week (date of death indicated in the table), all surviving mice were sacrificed for sample collection and histological analysis 7 days after the conventionalization. The histological colitis scores for each individual mouse are shown in the right column. The bar graph in figure 4g includes the histological colitis scores from all surviving FADD^{IEC-KO} mice (n=8) and all FADD^{FL} mice (n=8). The cytokine expression analysis shown in Figure 3e was performed on RNA isolated from 4 FADD^{FL} (F23, F25, F36, M37) and 4 FADD^{IEC-KO} mice (F41, F26, F35, F43).

Germ free mouse number/genotype	Mouse used for conventionalization (number/genotype)	Death	HCS
F24, FADD ^{FL}	Co-housed with mouse 828322 FADD ^{IEC-KO} /CYLDA932 ^{IEC}	-	0
F33, FADD ^{IEC-KO}		-	4,5
F34, FADD ^{IEC-KO}		day 4	-
F40, FADD ^{IEC-KO}		-	3,5
F23, FADD ^{FL}	Co-housed with mouse 795717 FADD ^{FL}	-	0
F36, FADD ^{FL}		-	0
F41, FADD ^{IEC-KO}		-	4
F42, FADD ^{IEC-KO}		day 7	-
F25, FADD ^{FL}	Co-housed with mouse 795719 FADD ^{FL}	-	0,5
F26, FADD ^{IEC-KO}		-	3
F35, FADD ^{IEC-KO}		-	4
F43, FADD ^{IEC-KO}		-	4
M28, FADD ^{IEC-KO}	Exposed to bedding from a cage housing mouse 848098 FADD ^{IEC-KO} / <i>Ripk3</i> ^{-/-}	day 7	-
M29, FADD ^{FL}		-	0
M30, FADD ^{FL}		-	0
M31, FADD ^{FL}		-	0,5
M32, FADD ^{IEC-KO}		day 7	-
M37, FADD ^{FL}	Exposed to bedding from a cage housing mouse 848098 FADD ^{IEC-KO} / <i>Ripk3</i> ^{-/-}	-	1
M38, FADD ^{IEC-KO}		-	6
M39, FADD ^{IEC-KO}		-	2,5

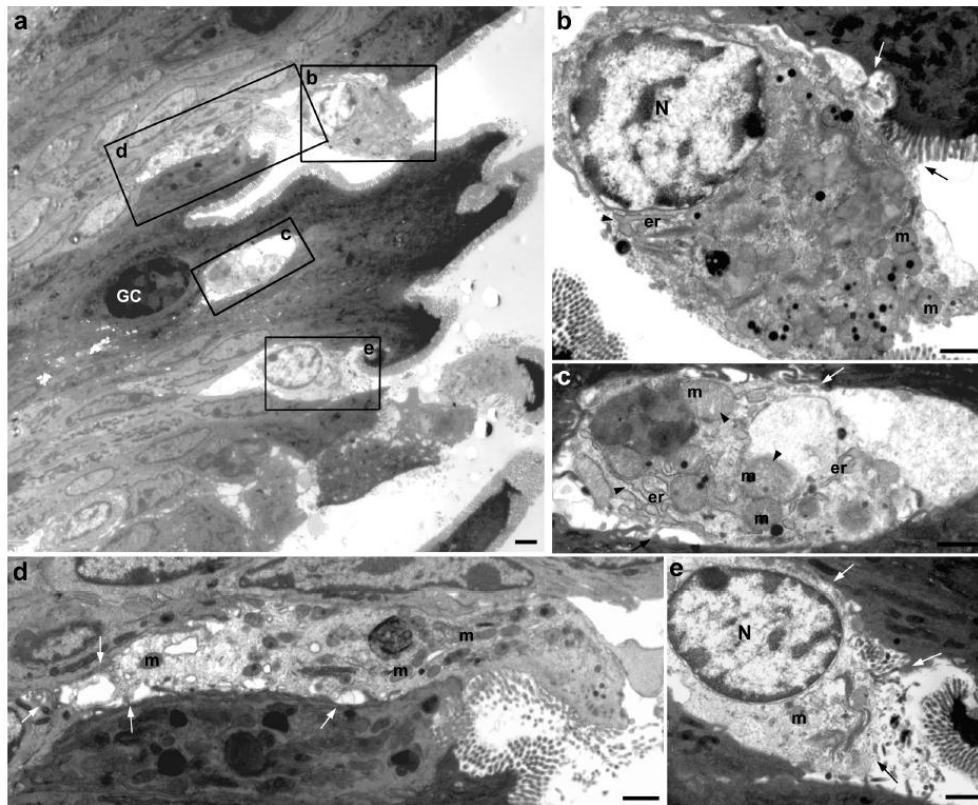


Supplementary Figure 1. Inflammatory infiltrates in the colon of FADD^{IEC-KO} mice. Colonic cross-sections from FADD^{IEC-KO} and FADD^{FL} mice were immunostained for F4/80, Gr-1, B220, CD3 (brown) and counterstained with haematoxylin (blue). Macrophage (F4/80+) and granulocyte (Gr-1+) infiltration into the colonic mucosa was detectable already in 2- and 3-week-old FADD^{IEC-KO} mice, while large inflammatory infiltrates were detected at 10 weeks of age. Increased B- (B220+) and T-cell (CD3+) infiltration was detectable in the mucosa of 10-week-old FADD^{IEC-KO} mice, while small numbers of lymphocytes were observed in 2- and 3-week old animals. Scale bars, 10µm.



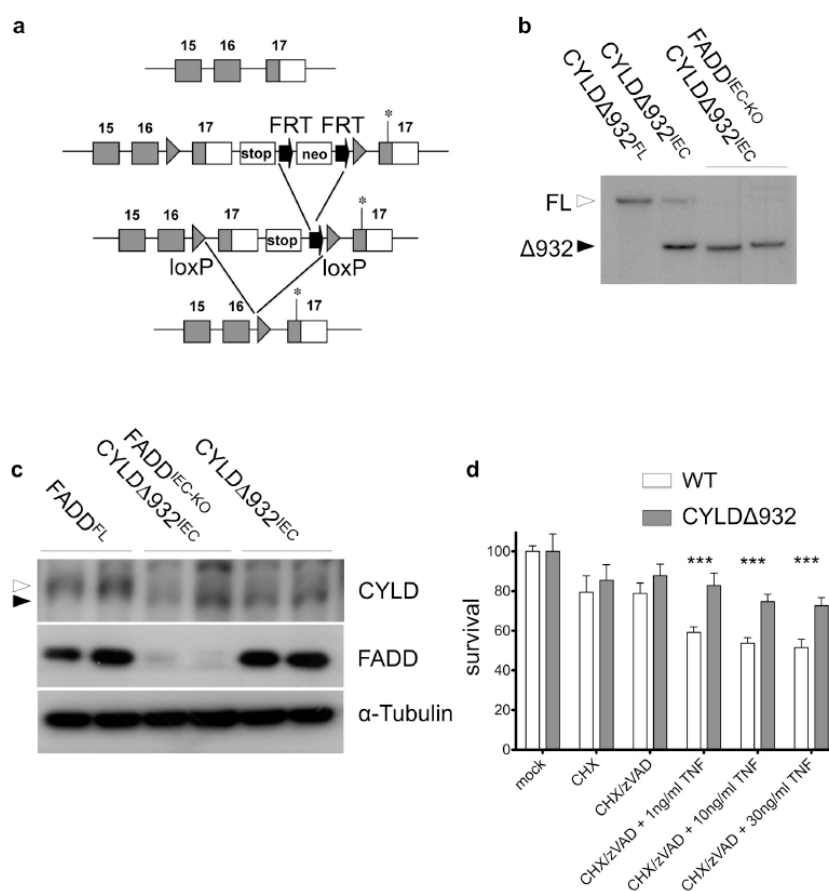
Supplementary Figure 2. Increased proliferation of epithelial cells in the colon of FADD^{IEC-KO} mice.

a. Representative pictures from colonic cross-sections from 2-, 3- and 10-week-old FADD^{IEC-KO} and FADD^{FL} mice immunostained with antibodies recognising Ki-67 (brown) and counterstained with haematoxylin (blue). Elevated epithelial proliferation was detectable in FADD^{IEC-KO} mice already at 2 weeks of age, which was further increased at 3 and 10 weeks. Scale bars, 100µm. **b.** Quantitative RT-PCR analysis on mRNA isolated from primary colonic IECs showed increased Cyclin D1 expression in FADD^{IEC-KO} compared to FADD^{FL} animals (n=4).



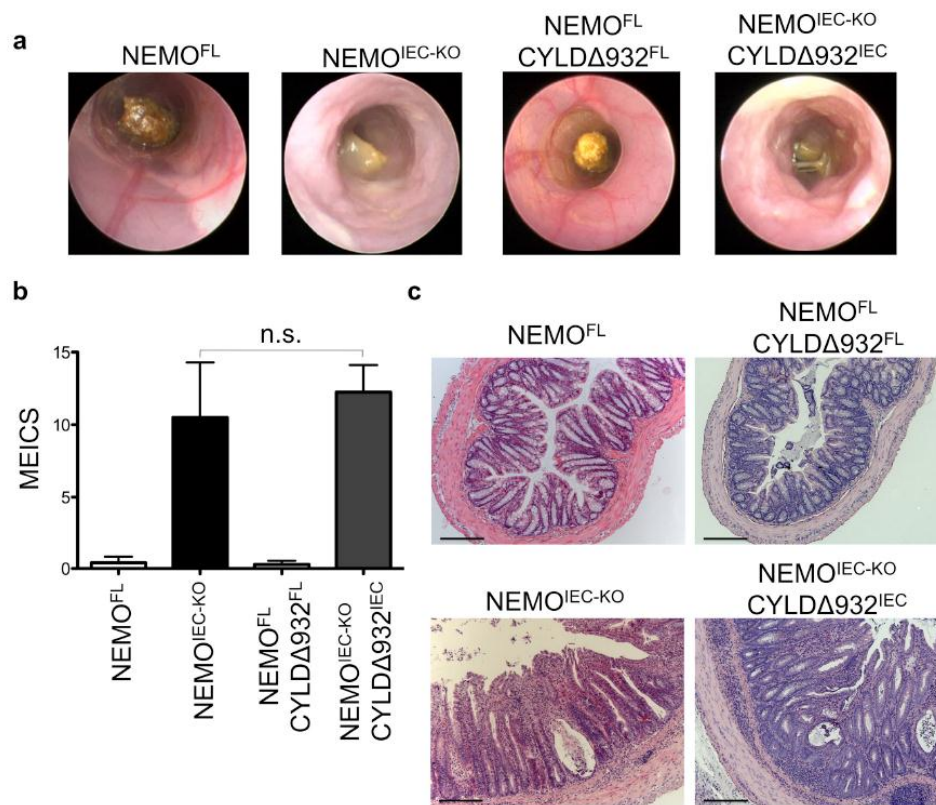
Supplementary Figure 3. Electron microscopy reveals dying epithelial cells in the colon of $FADD^{IEC-KO}$ mice showing signs of necrosis.

a. Low magnification of an area of distal colon from a $FADD^{IEC-KO}$ mouse. Note the disruption of the intestinal epithelium at several points. **b-e.** Higher magnification of IECs displaying necrotic features. These IECs show reduced cytoplasmic electron density compared to neighboring cells, swollen endoplasmic reticulum and mitochondria (arrowheads in **b, c**), as well as extensive disruption of the plasma membrane (including the apical brush border; **b, e**) and their cell-cell contacts (arrows). No apoptotic bodies or chromatin condensation in their nuclei (**N**) (**b, e**) are obvious in these cells. er, endoplasmic reticulum; m, mitochondria; GC, Goblet cell. Bars: (a) 2 μ m, (b-e) 1 μ m.



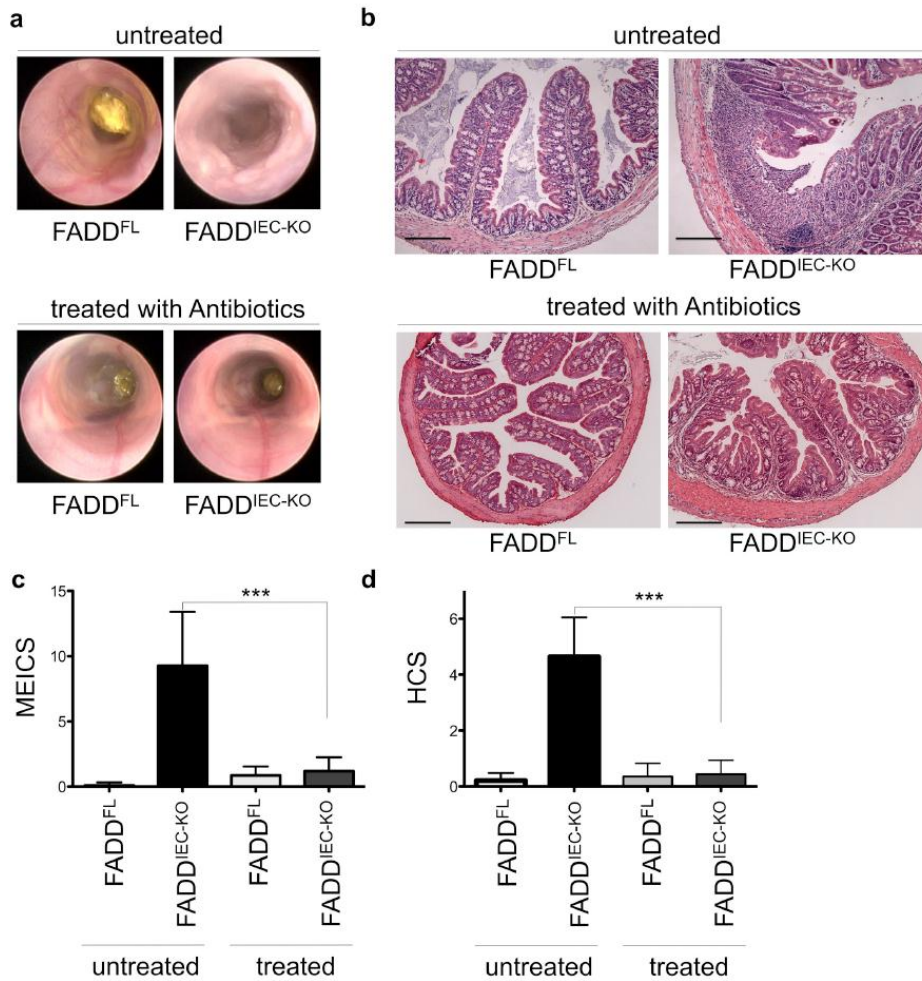
Supplementary Figure 4. Generation of $CYLDA932^{FL}$ mice allowing conditional expression of truncated catalytically inactive $CYLDA932$ protein.

a. Schematic depiction of the targeting strategy used for the generation of the $CYLDA932^{FL}$ mice. A stop cassette as well as a neomycin resistance (neo) cassette flanked with FRT sites were introduced after the last exon (exon 17) of the *CylD* gene. Exon 17, the stop cassette and the neo cassette are flanked with loxP sites. At the 3' of the loxP flanked region we introduced a mutated exon 17 containing a nonsense mutation at position 932. This mutation introduces a premature termination codon at position 932 truncating the last 20 amino acids of the protein, which include subdomain III of the His box that is essential for catalytic activity. In $CYLDA932^{FL}$ mice the neo cassette has been removed by FLP-mediated recombination, while the stop cassette prevents potential transcriptional read-through and expression of the mutated Exon 17. Cre-mediated recombination excises the loxP-flanked fragment containing the wild type exon 17 and the stop cassette, facilitating the replacement of wild type exon 17 with the mutated exon 17, resulting in expression of the catalytically inactive truncated $CYLDA932$ protein. **b.** Southern blot analysis of genomic DNA isolated from primary IECs from $CYLDA932^{FL}$, $CYLDA932^{IEC}$ and $FADD^{IECKO}/CYLDA932^{IEC}$ mice showing efficient deletion of the loxP-flanked genomic *CylD* fragment. DNA was digested with SpeI and the probe used was amplified using primers: sense: 5'TCA TGG CCA GCA GTC TCG AAG3'; anti-sense: 5'TTT CTG TGG GCC TAC ATA CGG3'. FL, loxP-flanked allele; $\Delta 932$, deleted allele. **c.** Western blot analysis of protein extracts from primary IECs of $CYLDA932^{FL}$, $CYLDA932^{IEC}$ and $FADD^{IECKO}/CYLDA932^{IEC}$ mice showing the expression of the lower molecular weight truncated $CYLDA932$ protein (filled black arrowhead) as well as efficient FADD deletion in the double mutant IECs. White arrowhead indicates the wild type full length CYLD protein. **d.** $CYLDA932^{IEC}$ MEFs were protected from necrotic cell death induced by the combined treatment with cycloheximide, z-VAD and TNF α . (mean values of triplicates \pm SD shown)



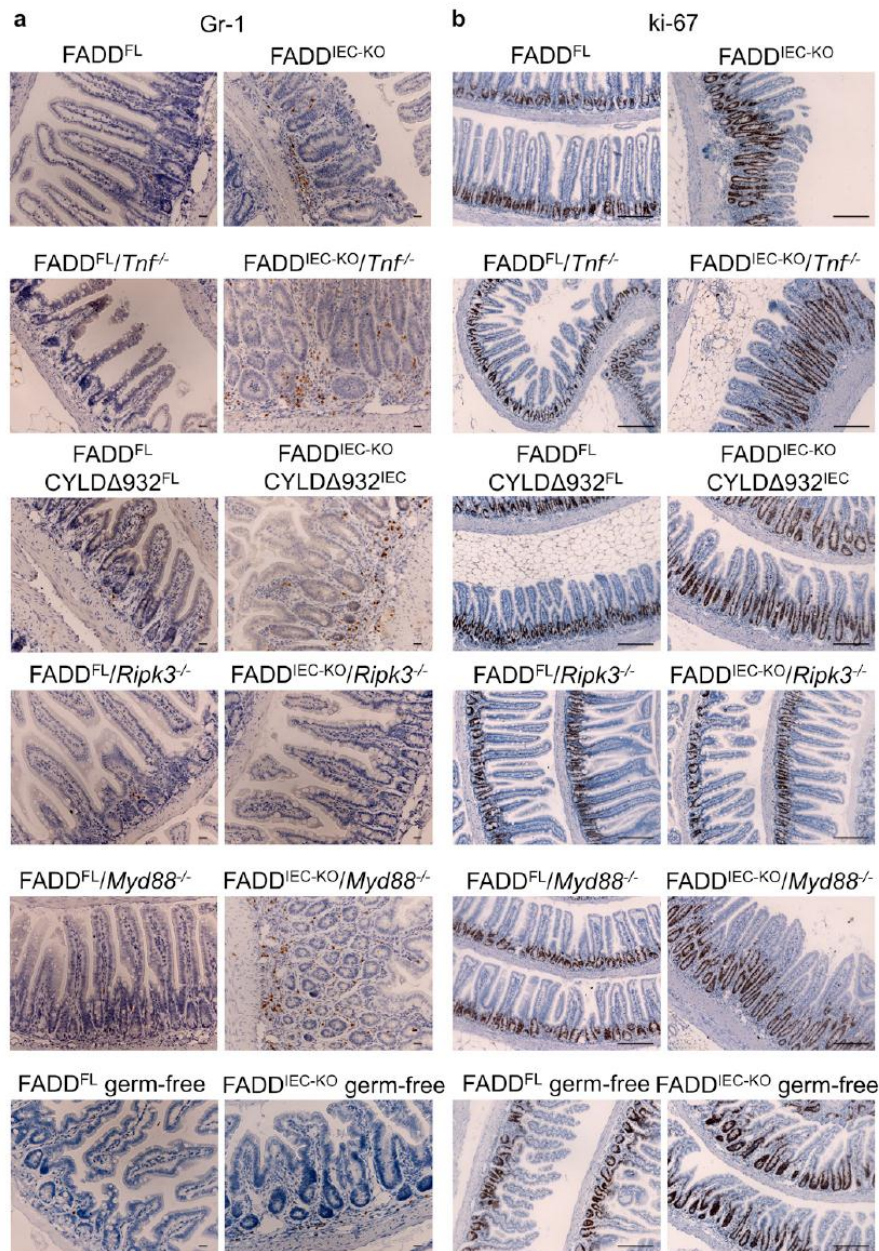
Supplementary Figure 5: Colitis in NEMO^{IEC-KO} mice develops independently of CYLD catalytic activity in IECs.

a, b. Representative endoscopic images (**a**) and quantification of MEICS (**b**) show that double NEMO^{IEC-KO}/CYLDΔ932^{IEC} mice develop severe colitis similarly to NEMO^{IEC-KO} animals. NEMO^{FL} (n=5), NEMO^{IEC-KO} (n=5), NEMO^{FL}/CYLDΔ932^{FL} (n=9), NEMO^{IEC-KO}/CYLDΔ932^{IEC} (n=4). Mean values ± SD shown. **c.** Representative histological images of colonic cross sections show severe colitis with crypt abscesses and strong inflammation in double NEMO^{IEC-KO}/CYLDΔ932^{IEC} mice similarly to NEMO^{IEC-KO} animals. Scale bar, 100μm.



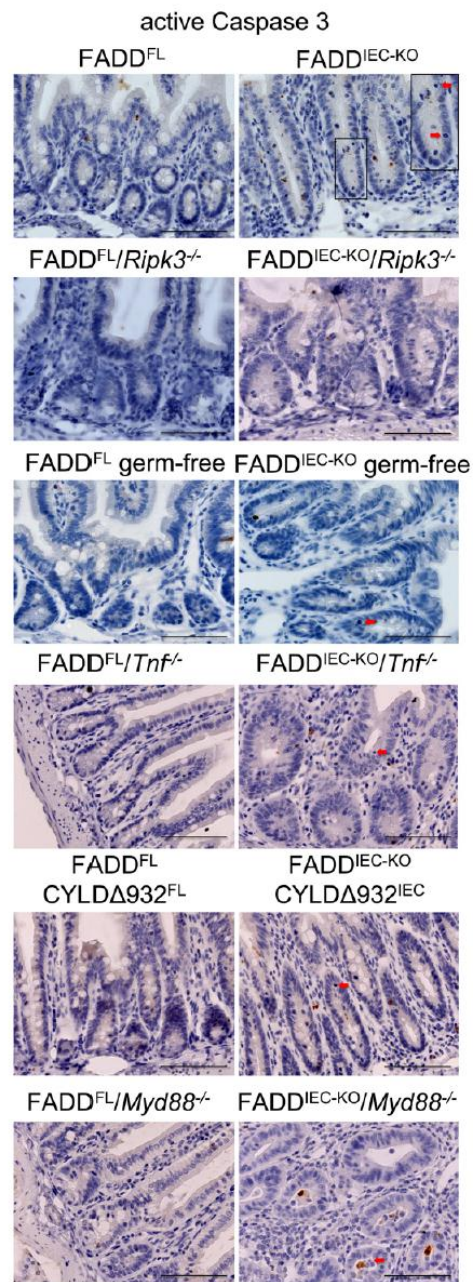
Supplementary Figure 6. Antibiotic treatment ameliorates colitis in FADD^{IEC-KO} mice

a, b. Representative endoscopic images (**a**) and quantification of MEICS (**b**) showing that antibiotic treated FADD^{IEC-KO} mice have a largely normal colonic mucosa compared to the severe colitis seen in untreated animals. FADD^{FL} untreated, n=37; FADD^{IEC-KO} untreated, n=31; FADD^{FL} treated, n=7; FADD^{IEC-KO} treated, n=8. Mean values ± SD shown. **c.** Representative histological images of colonic sections showing that antibiotic treated FADD^{IEC-KO} mice have a largely normal colonic mucosa comparable to FADD^{FL} control mice, in contrast to the severe inflammatory lesions seen in the colon of untreated FADD^{IEC-KO} animals. Scale bar, 100µm. **d.** Histological colitis score (HCS) measuring severity of inflammation and tissue damage in untreated FADD^{FL} (n=7) and FADD^{IEC-KO} (n=7), and in antibiotic treated FADD^{FL} (n=7) and FADD^{IEC-KO} (n=8) mice. Mean values ± SD shown.



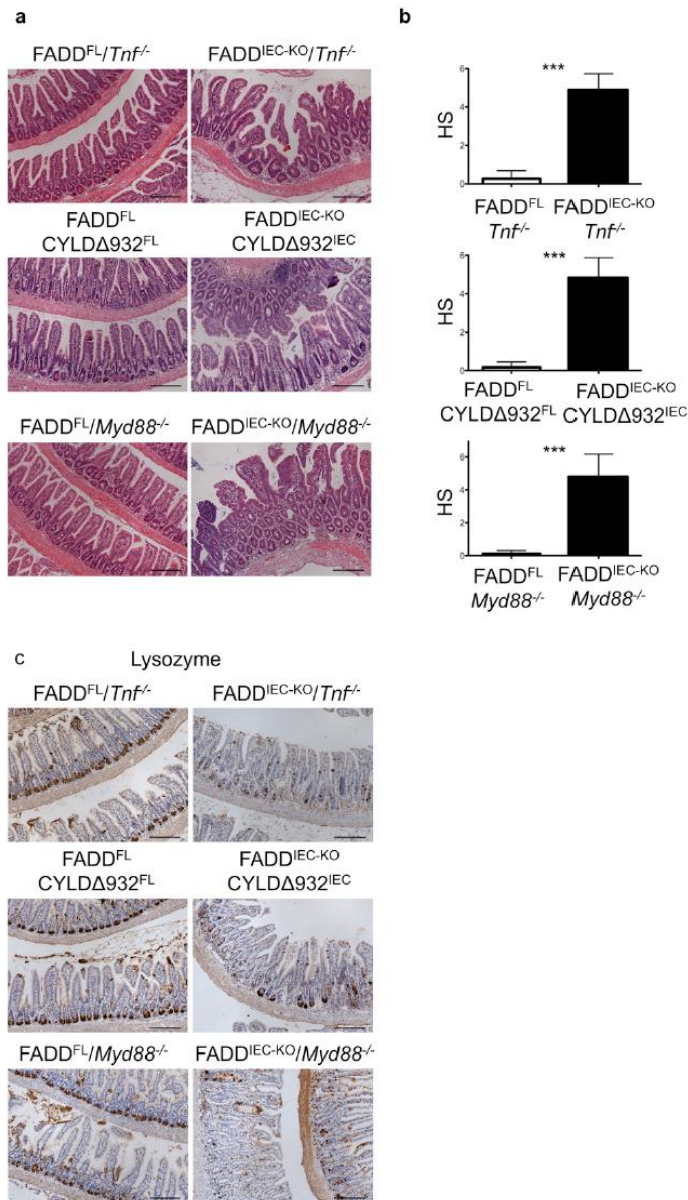
Supplementary Figure 7. Increased inflammation and epithelial cell proliferation in the small intestine of $FADD^{IEC-KO}$ mice depends on RIP3 but is independent of CYLD catalytic activity, TNF, Myd88 or the presence of the microbiota.

a. Small intestinal sections were immunostained with anti-Gr-1 antibodies (brown) and were counterstained with haematoxylin (blue). Representative images from mice with the indicated genotypes are shown. Scale bars, 10 μ m. **b.** Small intestinal sections were immunostained with anti-Ki-67 antibodies (brown) and were counterstained with haematoxylin (blue). Representative images from mice with the indicated genotypes are shown. Scale bars, 100 μ m.



Supplementary Figure 8. Caspase-independent death of small intestinal IECs in FADD^{IEC-KO} mice.

Small intestinal sections from mice with the indicated genotypes were immunostained with antibodies recognising active caspase-3 (brown) and counterstained with haematoxylin. Dying epithelial cells that did not stain for active caspase-3 were detected in crypts from FADD^{IEC-KO} but not in FADD^{FL} littermate controls. RIP3 deficiency prevented epithelial cell death in FADD^{IEC-KO}/Ripk3^{-/-} animals. However, deficiency in TNF, MyD88, CYLD or the absence of the microbiota did not prevent epithelial cell death in FADD^{IEC-KO} mice. Red arrows indicate caspase-3 negative dying enterocytes. Scale bars, 100µm



Supplementary Figure 9. Enteritis, loss of Paneth cells and death of IECs in the small intestine of FADD^{IEC-KO} mice occurs independently of TNF, Myd88 or CYLD catalytic activity.

a. Representative histological images of small intestinal sections showing strongly decreased numbers of Paneth cells, dying enterocytes as well as infiltrating immune cells into the mucosa of FADD^{IEC-KO}/Tnf^{-/-}, FADD^{IEC-KO}/CYLDA932^{IEC} as well as FADD^{IEC-KO}/Myd88^{-/-} mice compared to their respective littermate controls lacking the villinCre transgene. Scale bars, 100µm. **b.** Histological score (HS) measuring severity of inflammation and tissue damage in small intestines of mice with the indicated genotypes. FADD^{FL}/Tnf^{-/-} (n=6), FADD^{IEC-KO}/Tnf^{-/-} (n=4), FADD^{FL}/CYLDA932^{FL} (n=3), FADD^{IEC-KO}/CYLDA932^{IEC} (n=3), FADD^{FL}/Myd88^{-/-} (n=5), FADD^{IEC-KO}/Myd88^{-/-} (n=7). Mean values ± SD shown. **c.** Immunostaining of small intestinal sections with antibodies recognising Lysozyme revealed strongly decreased Paneth cell numbers in FADD^{IEC-KO}/Tnf^{-/-}, FADD^{IEC-KO}/CYLDA932^{IEC} and also in FADD^{IEC-KO}/Myd88^{-/-} mice compared to their respective VillinCre negative littermate controls. Scale bars, 100µm

Erklärung:

Ich versichere, dass ich die von mir vorgelegte Dissertation selbständig angefertigt, die benutzten Quellen und Hilfsmittel vollständig angegeben und die Stellen der Arbeit – einschließlich Tabellen, Karten und Abbildungen –, die anderen Werken im Wortlaut oder dem Sinn nach entnommen sind, in jedem Einzelfall als Entlehnung kenntlich gemacht habe; dass diese Dissertation noch keiner anderen Fakultät oder Universität zur Prüfung vorgelegen hat; dass sie – abgesehen von unten angegebenen Teilpublikationen – noch nicht veröffentlicht worden ist sowie, dass ich eine solche Veröffentlichung vor Abschluss des Promotionsverfahrens nicht vornehmen werde. Die Bestimmungen der Promotionsordnung sind mir bekannt. Die von mir vorgelegte Dissertation ist von Prof. Dr. Manolis Pasparakis betreut worden.

Datum

Patrick-Simon Welz

Curriculum Vitae

Personal data

Name: Patrick-Simon

Surname: Welz

Date of birth: 16 February 1981

Place of birth: Lübeck

Nationality: german

Business adress: University of Cologne
Institute for Genetics
AG Pasparakis
Zülpicher Str. 47a
50674 Cologne

Education

2007 Graduation from the University Bielefeld, Bielefeld, Germany

2006-2007 external Diploma thesis on “Die Rolle der Intermediärfilamente Neurofilament und Vimentin in der Pathologie der Wobbler-Maus” at the University of Aarhus, Aarhus, Denmark,
Supervisor: Prof. Thomas Schmitt-John

2001-2007 Studies in Biology at the University Bielefeld, Bielefeld, Germany

2000-2001 alternative service at “Marli Werkstätten GmbH”, helping mentally ill people at work, Lübeck, Germany

2000 Graduation (Abitur) from Johanneum zu Lübeck, Lübeck, Germany

Research career

- 2011 awarded the “best publication prize” by the Graduate School for Biological Sciences
- since 2008 PHD thesis “*In vivo* analysis of the role of FADD in the regulation of intestinal epithelial homeostasis”, Institute for Genetics, University of Cologne, Cologne, Germany,
Supervisor: Prof. Manolis Pasparakis
- 2007-2008 Rotational period of the “International Graduate School in Genetics and Functional Genomics”, University of Cologne, Cologne, Germany
- 2007 Graduate student at the University of Cologne, awarded a research fellowship by the “International Graduate School in Genetics and Functional Genomics”

Publications

Welz, P.S., Wullaert, A., Vlantis, K., Kondylis, V., Fernandez-Majada, V., Ermolaeva, M., Kirsch, P., Sterner-Kock, A., van Loo, G., and Pasparakis, M. (2011). FADD prevents RIP3-mediated epithelial cell necrosis and chronic intestinal inflammation. *Nature* 477, 330-334.

Bonnet, M.C., Preukschat, D., **Welz, P.S.**, van Loo, G., Ermolaeva, M.A., Bloch, W., Haase, I., and Pasparakis, M. (2011). The Adaptor Protein FADD Protects Epidermal Keratinocytes from Necroptosis In Vivo and Prevents Skin Inflammation. *Immunity* 35, 572-582.

Conferences

- 2011 „19th Euroconference on Apoptosis “Metabolism, Epigenetics and Cell Death”“, poster-presentation, Stockholm, Sweden, awarded a CECAD Travel grant for the expenses of this meeting
- 2010 „18th Euroconference on Apoptosis“, Ghent, Belgium
- 2009 UEGF Workshop „Cell signalling and the gut“, lecture, Cambridge, England
- 2009 4th ENII-MUGEN SUMMER SCHOOL, poster-presentation, Capo Caccia, Italy

